GEOLOGICAL SURVEY OF FINLAND
Report of Investigation 204
2013

Petrology and provenance of the Mesoproterozoic Satakunta formation, SW Finland

Jussi Pokki, Jarmo Kohonen, Raimo Lahtinen, O. Tapani Rämö and Tom Andersen

GTK

GEOLOGIAN TUTKIMUSKESKUS **GEOLOGICAL SURVEY OF FINLAND**

Tutkimusraportti 204 Report of Investigation 204

Jussi Pokki, Jarmo Kohonen, Raimo Lahtinen, O. Tapani Rämö and
Tom Andersen

Petrology and provenance of the Mesoproterozoic Satakunta formation, SW Finland

Front cover: Close-up of slightly conglomeratic sandstone from the Satakunta formation showing lamella rich in quartz (black to white grains) alternating with compositionally more immature fine-grained lamella.
Photo: Jari Väätäinen, GTK.

Layout: Elvi Turtiainen Oy

Espoo 2013

Pokki, J., Kohonen, J., Lahtinen, R., Rämö, O. T. & Andersen, T. 2013. Petrology and provenance of the Mesoproterozoic Satakunta formation, SW Finland. *Geological Survey of Finland, Report of Investigation 204*, 47 pages, 26 figures, 8 tables and 7 appendices.

The Satakunta formation (traditionally referred to as the Satakunta sandstone) is a Mesoproterozoic sequence in a fault-bounded basin within the Palaeoproterozoic Svecofennian Domain, resembling typical red beds with ferric oxides. Compositional variations of the sandstones and associated sediments were studied to consider the subdivision that could represent different basin stages of the formation. In addition, the provenance and especially the presence of rapakivi detritus were scrutinized. We propose a basin evolution model starting from c. 1.60 Ga and ending at 1.27 Ga.

The SW margin of the formation, a 591-m-thick 'type section' and the NE margin constitute three distinct lithological assemblages, but a basin-wide stratigraphy cannot be determined. The southwestern margin sequence consists of conglomerates with very well rounded vein-quartz pebbles in a subarkosic matrix. The most voluminous component of the formation is a monotonous medium-grained arkosic arenite with laumontite locally common in the cement. Coarse-grained conglomeratic sandstones are typical rocks in the NE margin of the formation.

The source of the southwestern margin sequence had been weathered with a notable loss of Na and Ca and enrichment of detrital heavy minerals. It is geochemically dominated by microcline granites, whereas the source rocks of the northeastern margin sequence had been dominated by a granodioritic composition. The Th/Sc ratio of the sediments indicates that the source is felsic throughout. The 138 detrital zircons analysed for U-Pb geochronology imply an exclusively Svecofennian provenance peaking at 1.88 Ga and recording the erosion of 1.83–1.81 Ga late orogenic granites.

The mature SW margin sequence is partly derived from reworked post-Svecofennian platform cover and was deposited during the early stage of the extension related to the anorogenic rapakivi magmatism. The monotonous 'type section' is understood to be a result of a large fluvial braidplain or coastal plain representing a tectonically inactive late stage of the large extensional basin system some 1.50 Ga ago. The immature, conglomeratic sandstones of the NE margin of the formation represent the early stage of a new rifting event before the intrusion of the 1.27 Ga diabase dykes. The Laitila rapakivi granite was plausibly exposed only after the sedimentation of the preserved part of the Satakunta formation.

Keywords (GeoRef Thesaurus, AGI): sandstone, conglomerate, laumontite, zircon, provenance, granites, rapakivi, Fennoscandian Shield, Mesoproterozoic, Satakunta, Finland

Jussi Pokki
Geological Survey of Finland
P.O. Box 96
FI-02151 ESPOO
FINLAND

E-mail: jussi.pokki@gtk.fi

ISBN 978-952-217-264-8 (pdf)
ISSN 0781-4240

Pokki, J., Kohonen, J., Lahtinen, R., Rämö, O. T. & Andersen, T. 2013. Petrology and provenance of the Mesoproterozoic Satakunta formation, SW Finland. Tiivistelmä: Lounais-Suomen keskiproterotsooisen Satakunnan muodostuman petrologia ja lähdealue. *Geologian tutkimuskeskus, Tutkimusraportti 204*, 47 sivua, 26 kuvaa, 8 taulukkoa ja 7 liitettä.

Satakunnan muodostuma (perinteisesti Satakunnan hiekkakivi) on keskiproterotsooinen, tyypillisiä *red-bed*-kerrostumia muistuttava siirrosten rajaama muodostuma. Se sijaitsee hautavajoamassa Lounais-Suomen varhaisproterotsooisella svekofennisellä pääalueella. Tässä tutkimuksessa tutkittiin muodostuman koostumuksellisia vaihteluita tavoitteena jäsentää se sellaisiin yksiköihin, jotka voisivat edustaa eri allasvaiheita muodostuman kerrostumishistoriassa. Myös muodostuman lähdealue ja rapakivigraniittien mahdollinen osuus siinä olivat tutkimuksen kohteina. Esitämme altaan kehityksestä mallin, joka kuvaa ajanjaksoa 1,60–1,27 miljardia vuotta sitten.

Satakunnan muodostuman lounaisreuna, 591 m paksu ”tyyppileikkaus” ja muodostuman koillisreuna muodostavat kolme erilaista kivilajiseuruetta, mutta koko muodostuman kattavaa kerrosjärjestystä ei pystytä määrittelemään. Muodostuman lounaisreunalla tavataan konglomeraatteja, joissa on erittäin hyvin pyöristyneitä juonikvartsikappaleita subarkoosisessa välimassassa. Satakunnan muodostuman yleisin kivilaji on ”tyyppileikkausta” leimaava keskirakeinen arkoosinen areniitti, jossa on paikoitellen runsaasti laumontiitti-iskosta. Muodostuman koillisreunassa tyypillisiä ovat koostumuksellisesti epäkypsät konglomeraattiset hiekkakivet.

Altaan lounaisosan sedimenttikivien detritus on peräisin rapautuneista kivilajeista koostuvalta lähdealueelta, jota luonnehtivat natriumin ja kalsiumin vaje ja detritaalisten raskasmineraalien rikastuminen. Geokemiallisesti sitä luonnehtii mikrokliinigraniiteihin viittaava koostumus, kun taas koillisreunaa luonnehtii granodioriitteihin viittaava koostumus. Th/Sc-suhteen perusteella muodostuman lähdealue on kauttaaltaan felsinen. 138 analysoitua detritaalizirkonia viittaavat yksinomaan svekofenniseen lähdealueeseen, jota hallitsevat 1,88 Ga:n ikäiset kivilajit ja josta erottuvat myös 1,83–1,81 Ga:n myöhäisorogeeniset graniitit.

Satakunnan muodostuman lounaisosan tulkitaan osittain muodostuneen uudelleen kerrostuneista svekofennisiä kiviä nuoremmista sedimenttikivistä anorogeenisten rapakivigraniittien syntymiseen liittyvän maankuoren venymisen alkuvaiheessa. ”Tyyppileikkauksen” kerrostumisympäristönä oli suuri palmikoiva fluviaalinen tasanko tai rantatasanko, ja se edustaa suuren altaan tektonisesti ei-aktiivista myöhäisvaihetta 1,50 miljardia vuotta sitten. Koostumukseltaan epäkypsät konglomeraattiset hiekkakivet muodostuman koillisreunalla edustavat maankuoren uuden repeytymisen alkuvaihetta ennen 1,27 Ga:n ikäisten diabaasijuonten tunkeutumista. Laitilan rapakivigraniitti paljastui vasta sen jälkeen, kun Satakunnan muodostuma nykyisessä laajuudessaan oli jo kerrostunut.

Asiasanat (Geosanasto, GTK): hiekkakivi, konglomeraatti, laumontiitti, zirkoni, lähtöalue, graniitit, rapakivi, Fennoskandian kilpi, mesoproterotsooinen, Satakunta, Suomi

Jussi Pokki
Geologian tutkimuskeskus
PL 96
02151 ESPOO

Sähköposti: jussi.pokki@gtk.fi

CONTENTS

1 INTRODUCTION

The Satakunta formation is a Mesoproterozoic sequence of siliciclastic sandstones and conglomerates in a fault-bounded basin within the Palaeoproterozoic Svecofennian Domain. The sedimentary rocks in the formation resemble typical red beds with ferric oxides. The formation has traditionally been referred to as the Satakunta sandstone, but in this study we prefer the term Satakunta formation, according to the national stratigraphic database compiled in collaboration with the Stratigraphic Commission of Finland (Strand et al. 2010).

The geological record of the Mesoproterozoic Era in southwestern Finland is represented by rapa-kivi granites, sandstones and olivine diabases. The Laitila rapakivi batholith (c. 1570 Ma; Vaasjoki 1977) is situated immediately south of the

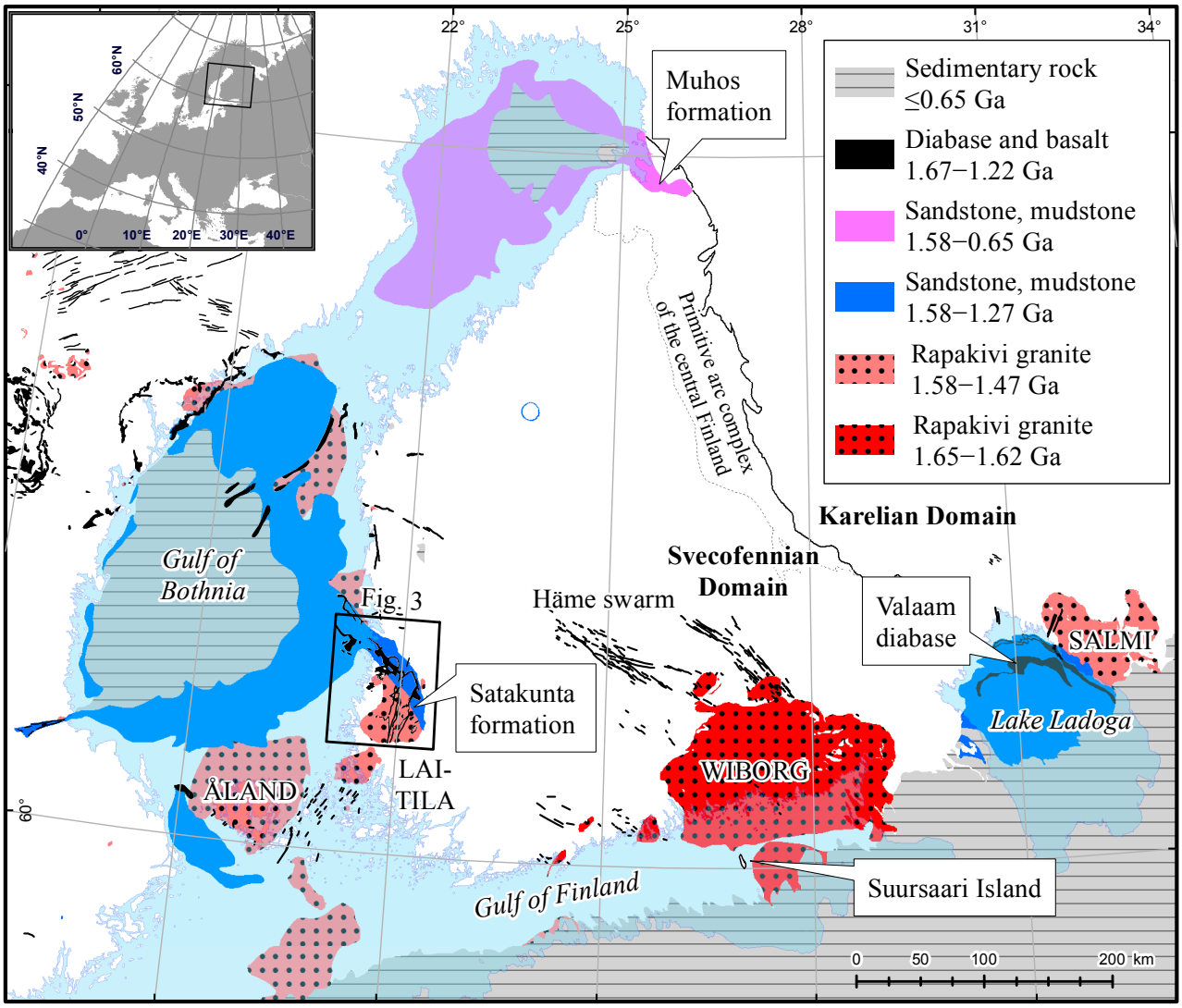

Fig. 1. The regional context of the Satakunta formation and extent of the Mesoproterozoic rocks within the eastern part of the Fennoscandian Shield. The spatial connection between the sedimentary rocks (Satakunta and Ladoga regions and the Suursaari Island) and the rapakivi granites and associated mafic dykes is to be noted. The map and lithological units are according to Koistinen et al. (2001).

Satakunta formation, and two coeval rapakivi stocks are present near the northeastern margin of the formation (Haapala 1977). The mafic dykes are informally divided into the older 'Subjotnian' swarm (c. 1650 Ma; Pihlaja 1987) and the younger 'Post-Jotnian' swarm (1260 ± 10 Ma; Suominen 1991).

The Satakunta formation covers a NW–SE elongated area of 85 km by 20 km, extending from the Gulf of Bothnia to the Finnish mainland (Fig. 1). The formation is arkosic arenite to subarkose in composition, and continental deposition has been suggested by most authors (e.g. Simonen & Kouvo 1955, Marttila 1969). The observed sedimentary structures include cross-bedding, ripple marks, mud cracks and raindrop imprints. All the reported primary features and facies associations are in accordance with fluvial depositional models (Kohonen et al. 1993). Drilling results demonstrate that the minimum thickness of the formation is 591 m and, according to gravimetric surveys, the maximum thickness may be more than 1500 m (Elo 1976). The Satakunta formation is intruded by numerous mafic dykes ('Post-Jotnian' diabases), and the most accurate age determination of 1256.2 ± 1.4 Ma (Söderlund et al. 2004) gives the minimum depositional age for it.

The Satakunta formation has been studied for more than one hundred years, but a geologically meaningful maximum age of deposition or timing for the onset of the rifting and related basin formation is still lacking. The Satakunta area is rather poorly exposed and, despite some drilling ventures, a primary contact between the sandstone and rapakivi granite, either depositional or intrusive, is yet to be found.

In previous research, an important focus has been the relationship between the sandstone detritus and the Laitila rapakivi batholith presently bordering the Satakunta formation in the SW (Fig. 1). Pioneers such as Eskola (1907, 1925), Sauramo (1916) and Laitakari (1925, 1932) all assumed that the sandstone contains detritus from the adjacent Laitila batholith. However, Simonen and Kouvo (1955) and Marttila (1969) studied the petrography of the sandstone more thoroughly and concluded that most of the detritus comes from the Svecofennian basement. Vaasjoki and Sakko (1987) reached the same conclusion based on isotopic data from detrital zircons and monazites.

Most of the previous petrological research on the Satakunta formation has focused on the present erosional level, but here we describe the mineralogical and geochemical composition of the sandstone, both in vertical (core M52-PO-60-001 reaching to 620 metres below ground level; mbgl) and lateral dimensions. We also present a review of detrital heavy mineral studies and new detrital zircon age results from two samples (one from the depth of 615 m and the other from an outcrop). Finally, we discuss the source, compositional variations and possible subdivision of the sandstone and speculate on its relationship with rapakivi granites.

2 GEOLOGICAL SETTING

2.1 Extensional reactivation of the Svecofennian crust

The complex and multiphase Svecofennian orogeny (c. 1900–1800 Ma) resulted in an accretionary collage of microplates (Lahtinen et al. 2005). The Svecofennian crust forms the crystalline basement for the Satakunta formation and other nonconformable, unfolded and unmetamorphic (or very low grade metamorphic) supracrustal rocks (Fig. 1). The Svecofennian bedrock is mainly composed of felsic plutonic and highly metamorphic to migmatitic supracrustal rocks. Synorogenic granodiorites (in places porphyric with microcline megacrysts), tonalites (sometimes garnetiferous) and quartz diorites are dominant. The associated supracrustals mainly consist of medium- to high-grade metamorphic schists and migmatitic mica gneisses. Besides the folding, major shear and fault zones divide the bedrock into blocks showing diverse rock types and metamorphic grades. The dominant direction of Svecofennian ductile shear zones is NW–SE.

The collisional thickening is interpreted to have been followed by orogenic collapse at 1.79–1.77 Ga, and finally the stabilization of the continental crust in the cratonic stage (Lahtinen et al. 2005). The late Palaeoproterozoic geological record is scarce in Finland, and little is known of the time

period (c. 1750–1650) following the cratonization but predating the intrusion of the first anorogenic rapakivi intrusions (Pokki et al. 2013).

A new extensional tectonic episode was commenced at ~1650 Ma and resulted in A-type granites, mafic dykes and associated sedimentary rocks. Whatever the ultimate tectonic explanation (e.g. Rämö & Haapala 2005) of the anorogenic rapakivi magmatism, the characteristic features include major tectonothermal activity with mantle upwelling, mafic underplating and the emplacement of rapakivi granites. This is associated with local crustal thinning and the formation of intracratonic basins. A layer with a high seismic velocity in the lower crust has been interpreted to be thinned in an E–W-oriented zone in the Gulf of Finland and the Ladoga area (Korja et al. 1993).

2.2 Igneous rocks (1650–1250 Ma): a review

Rapakivi granites and related more mafic rocks (leucogabbroids, diabases) were formed during a period of more than 100 My in an anorogenic province reaching from central Sweden and the Baltic countries to Russia (Fig. 1). The age of rapakivi plutons in southeastern Finland (Wiborg, Suomenniemi, Ahvenisto, Onas, Bodom and Obbnäs) is 1650–1620 Ma, whereas that of rapakivi plutons in southwestern Finland (e.g., Åland, Laitila and Vehmaa plutons; Peipohja, Eurajoki and Reposaari stocks) is 1590–1540 Ma. The youngest is the Salmi batholith located in the vicinity of Lake Ladoga (1550–1530 Ma).

Rapakivi magma was formed in the lower crust as a result of partial melting caused by heat from mafic magma. The felsic melt ascended along shear zones and faults. Alkalic feldspar is the most common mineral in rapakivi granites, and typical accessory minerals include fluorite, zircon, apatite, ilmenite, magnetite, anatase and allanite (e.g. Rämö & Haapala 2005). The mafic magma filled in places the crustal-scale fractures and formed swarms of sub-parallel diabase dykes. The most noticeable is the Häme swarm consisting of 1665 Ma and 1645 Ma dykes northwest of the Wiborg batholith (Fig. 1). In southeastern Fennoscandia, mafic and felsic volcanic rocks are found as small remnants in Ruoholampi and Taalikkala (Simonen 1987) megaxenoliths in the Wiborg batholith and on the Island of Suursaari, Gulf of Finland. For further details of Mesoproterozoic igneous rocks, see Rämö and Haapala (2005) and Kohonen and Rämö (2005).

2.3 Sedimentary rocks (1650–1250 Ma): a review

Mesoproterozoic sedimentary rocks in the Fennoscandian Shield are known in the Gulf of Bothnia with mainland extensions in Finland (Satakunta) and Sweden (Gävle, Nordingrå), in Lake Ladoga and in the Baltic Sea southwest of the Åland Islands (Fig. 1). In addition, further occurrences are met in central Sweden and central Norway (Dala, Svartälven, Mälaren), southern Sweden (Almesåkra) and in a depression north of Gotland. Potentially Mesoproterozoic sedimentary rocks are also found in the northern Gulf of Bothnia with mainland extension in Finland (Muhos formation), in the Lappajärvi impact structure, in southern Sweden (Almesåkra) and in the Arctic Ocean around the Kola Peninsula (Koistinen et al. 2001). In the geological past, the Mesoproterozoic sedimentary rocks may have been much more widespread, and the pattern of current occurrences is understood to more closely reflect selective preservation than the extent of the original depositories (e.g. Kohonen et al. 1993; Kohonen & Rämö 2005).

In many reviews (e.g., Simonen 1980), the depositional age of the Satakunta sequences has been estimated at around 1300–1400 Ma. Nevertheless, the rapakivi granites and the 'Jotnian' red-bed sequences appear to be spatially related, which suggests a causal relationship. Kohonen et al. (1993) tentatively proposed that the oldest part of the Satakunta sequence may have been deposited at the onset of the rifting related to the emplacement of the rapakivi granites (~1650 Ma) or even earlier. New data indicate that in the regional context, the 'Jotnian' sedimentation began earlier than so far believed: the upper parts of the Ladoga basin sedimentary sequence are intruded by the 1460 Ma Valaam diabase (Rämö et al. 2001). The depositional history of the Satakunta formation may also be long and complex. In fact, the Satakunta formation and Pasha graben sequence in Lake Ladoga

(Amantov et al. 1996) may be analogous, and the present Satakunta basin may represent a deep section remnant of a larger graben corresponding to the Ladoga basin both in dimensions and age.

Simonen and Kouvo (1955) loosely correlated the Muhos formation with the Satakunta formation, because both contain sedimentary rocks on a down-faulted crystalline block. This preliminary 'correlation' definitely does not mean that the two basins are necessarily coeval. The depositional age of the Muhos formation is very poorly constrained. Based on microfossil data, Tynni and Uutela (1984) tentatively estimated the age of the Muhos formation to be around 1200 Ma, and the reliability of the old ^{40}K-^{40}Ar age determinations (Satakunta c. 1300 Ma; Muhos 1280 and 1310 Ma; Simonen 1960) may also be questioned. In fact, the Muhos and Satakunta sequences are not very similar: the sedimentary rocks in the Muhos formation are much more fine-grained and more immature. Red and green siltstones and shales with less than 10% sandstones and conglomerates are typical (Simonen & Kouvo 1955). Contrary to the Satakunta and the Ladoga basins, the Muhos basin is not known to be associated with rapakivi granites.

The quartz arenitic conglomerate that is older than an adjoining 1633 ± 2 Ma quartz-feldspar porphyry (Rämö et al. 2007) on the Island of Suursaari, Russia (see Fig. 1), is interpreted to represent a remnant of a previously unrecognized ultramature mid-Proterozoic sedimentary cover preceding the rift-related 'Jotnian-type' deposition (Pokki et al. 2013). Especially interesting is the potential existence of pre-rift deposits in Satakunta and in other Mesoproterozoic basins.

3 DESCRIPTION OF THE SATAKUNTA FORMATION

3.1 Dimensions of the Satakunta formation

A strong negative gravimetric anomaly occupies the Satakunta area (Fig. 2), at least partly due to the low densities of the sandstone and the rapakivi granite. The contact between the Satakunta formation and its basement is nowhere exposed. At its northeastern margin, the formation is framed

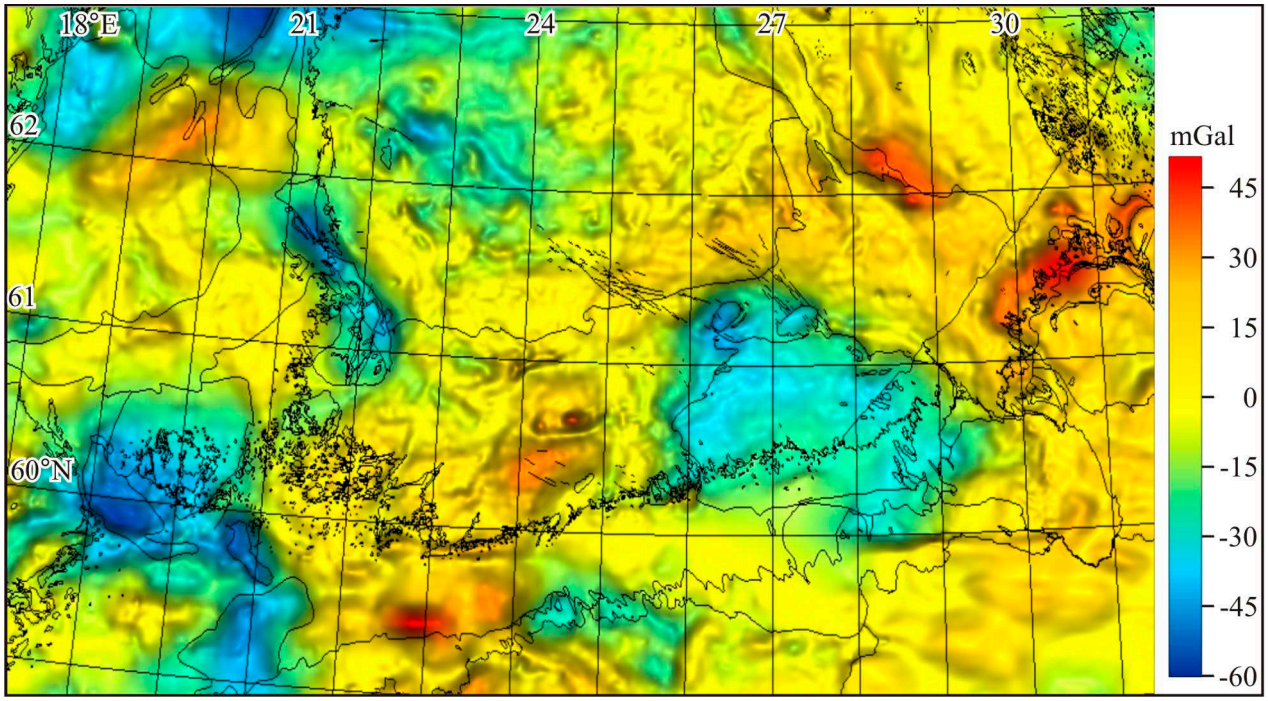

Fig. 2. Rapakivi granite batholiths and sedimentary rock basins are associated with negative gravimetric anomalies. In the Satakunta area, the anomaly is most significant along the rift and its extension near the Finnish mainland. Lithological units outlined are the same as in Fig. 1 (Koistinen et al. 2001). The gravimetric map, compiled at GTK, is based on the Bouguer anomaly network in Fennoscandia (Korhonen et al. 2002).

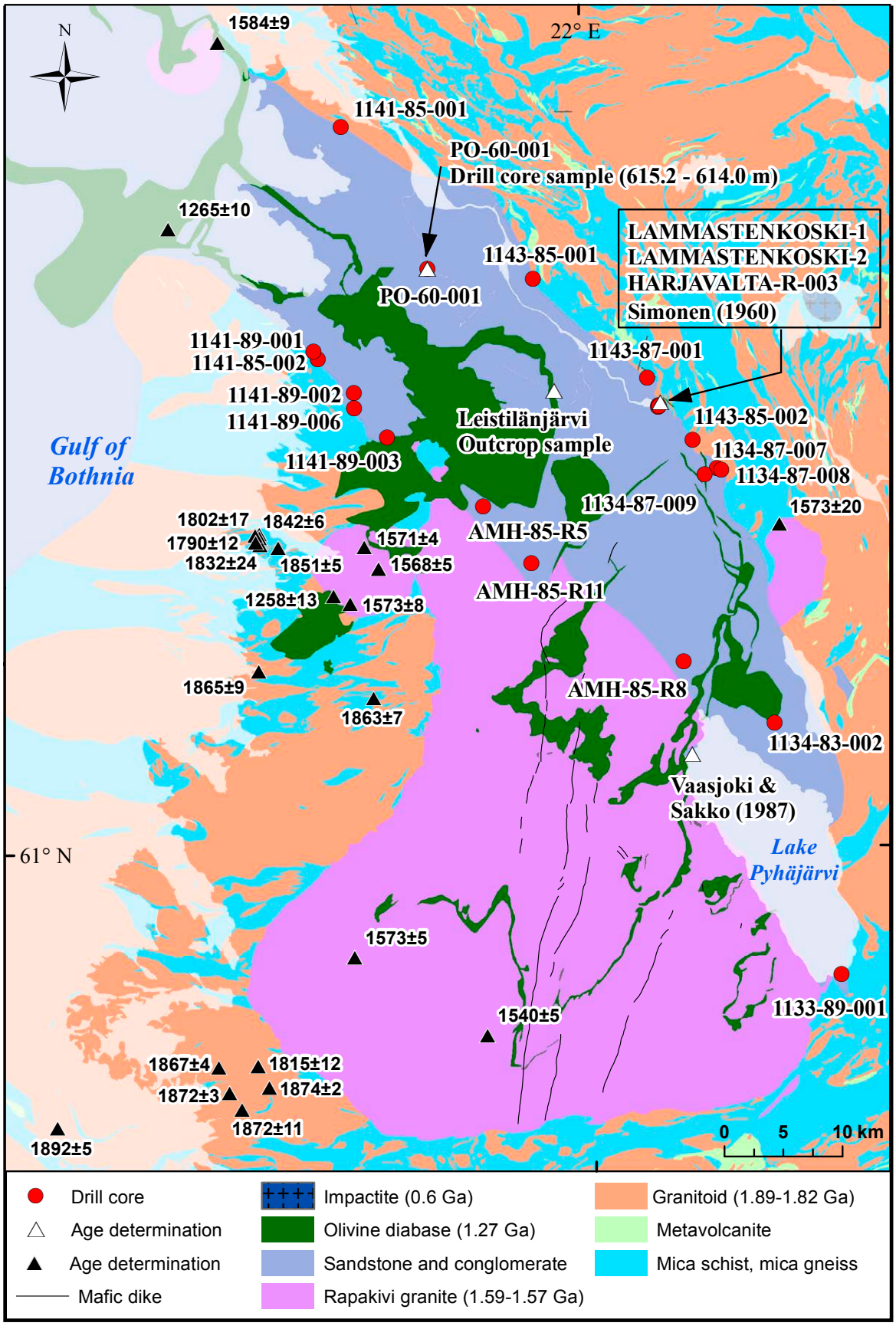

Fig. 3. Geology of the Satakunta area. Results (2σ error margins) (compiled by Hannu Huhma, GTK) and/or sampling sites of age determinations in the area are indicated in the image, as well as drilling sites in the Satakunta formation. Visit GTK Active Map Explorer (http://geomaps2.gtk.fi/activemap/) for further information on the age determinations. Geology based on the GTK bedrock map database (Bedrock of Finland – DigiKP). Contains data from the National Land Survey of Finland Topographic Database 03/2013 © NLS and HALTIK.

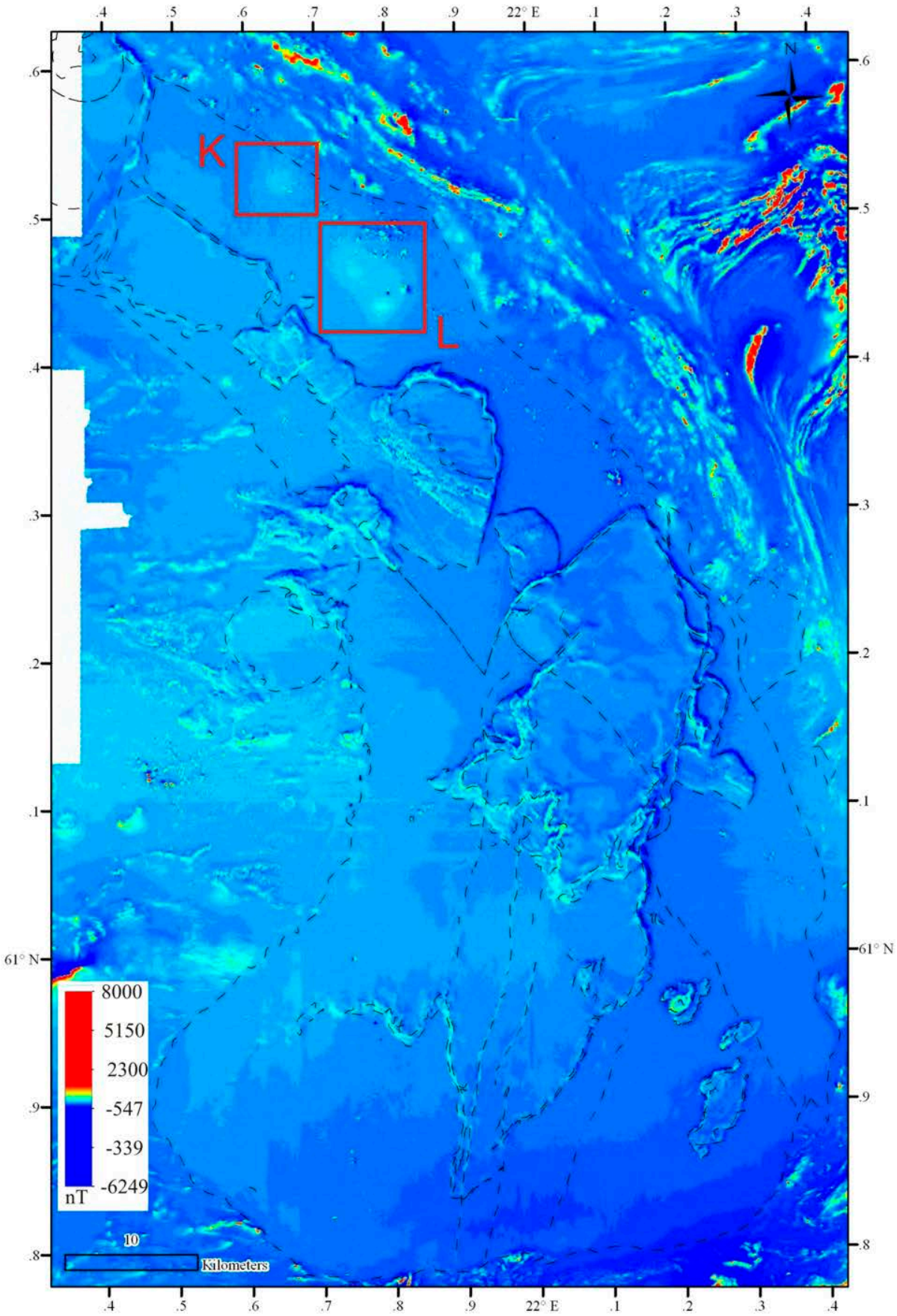

Fig. 4. The borders of the Satakunta formation cannot be distinguished from the aeromagnetic map, but diabase is clearly visible. Also indicated are Kylänsaari (K) and Lattomeri (L) anomalies (Puranen 1963), which may be caused by diabase dykes not penetrating the formation all the way to the top. Sandstone and conglomerate, olivine diabase, rapakivi granite and mafic dykes have been indicated with a dashed line.

by 1.89–1.87 Ga felsic to intermediate magmatic rocks, metasedimentary rocks and the small Peipohja rapakivi granite pluton (Fig. 3). Its southwestern margin is mostly framed by the Laitila rapakivi granite batholith. The Satakunta formation cannot be accurately differentiated from rapakivi granite and Svecofennian rocks on an aeromagnetic map, even though there are highly magnetic schists further to the northeast (Fig. 4).

According to several gravimetric studies, the Satakunta formation is underlain by rapakivi granite (Puranen 1963, Elo 1976, Elo 1982). The Laitila rapakivi extends unexposed, roofed by Svecofennian rocks, north of the Satakunta formation and northwest of the Väkkärä granite (3 in Fig. 5) (Elo 1982).

The Satakunta formation is thinner at the southwestern margin than at the northeastern margin, and forms a half-graben-like geometry (Laurén 1970). The sedimentary succession also thickens to the northwest (Fig. 5), and its average thickness is estimated at 1.3 ± 0.3 km, with the maximum thickness being 1.8 ± 0.4 km (Elo 1976). See also the gravimetric models in Elo and Pirttijärvi (2010).

The Satakunta formation is probably fault bounded in most if not in all places, because even its surface is generally at a lower elevation than the

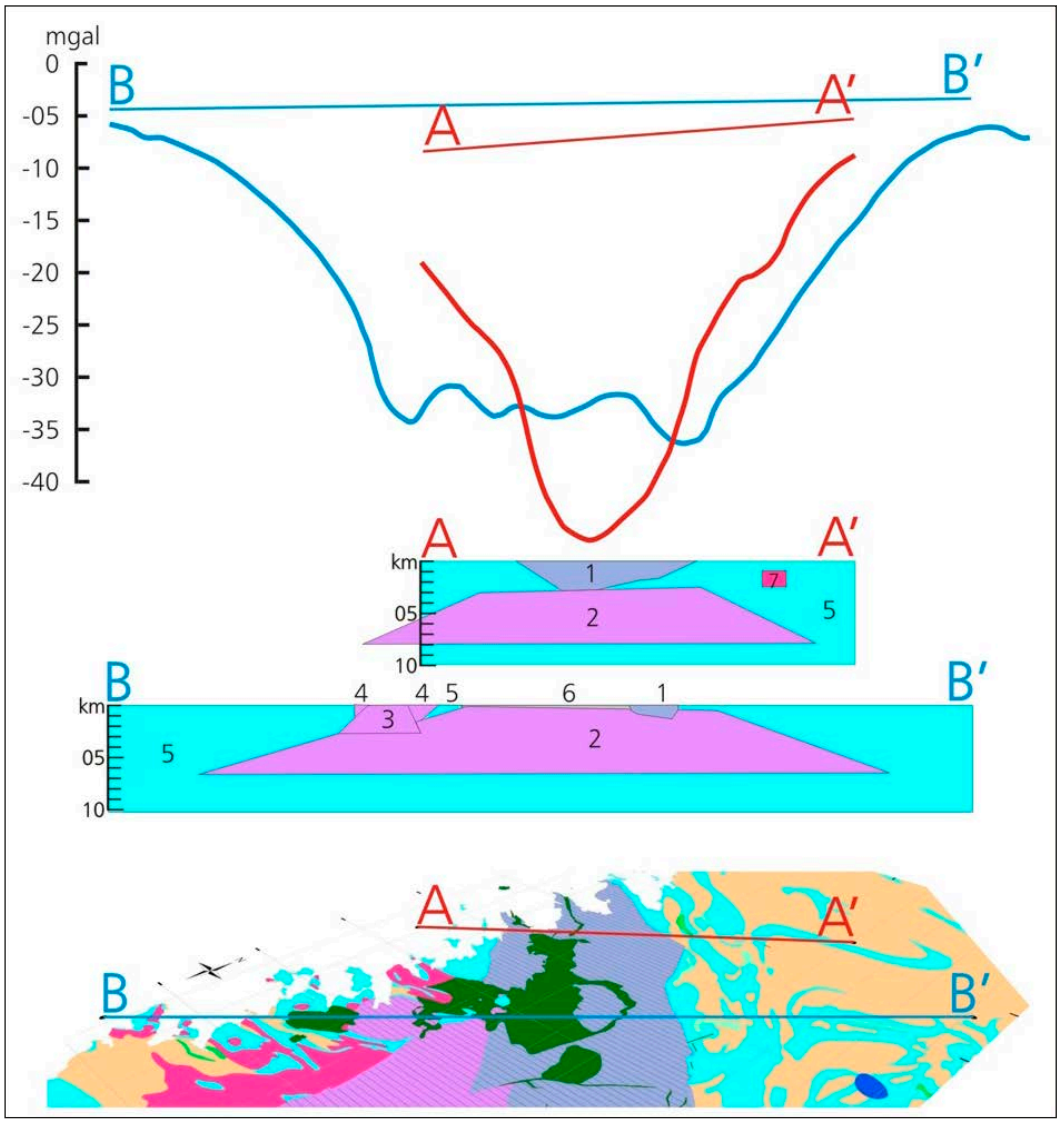

Fig. 5. According to the gravimetric profiles of Elo (1982), the Laitila rapakivi extends unexposed, roofed by Svecofennian rocks, north of the Satakunta formation and northwest of the Väkkärä granite. The gravimetric models above cause calculated anomalies shown with the red and blue curves, which equal the observed anomalies. The straight lines are the base levels for the calculated anomalies. 1 = sandstone, 2 = rapakivi granite, 3 = Väkkärä granite, 4 = Tarkki granite, 5 = Svecofennian bedrock, 6 = sandstone+diabase+rapakivi, 7 = granite.

surface of the surrounding bedrock. At the Harjavalta outcrop, the strata have been postdepositionally inclined by 40° (Fig. 6) (Hämäläinen 1985). A faulted contact is also topographically implied by the sudden deepening of water at the southwestern margin of Lake Pyhäjärvi (see App. 3 in Pokki 2007).

Fig. 6. Lammaistenkoski at the northeastern margin of the rift basin is the largest outcrop of the Satakunta formation. The sedimentary strata dip 40° due to postdepositional faulting. Photo: Jussi Pokki, GTK (P = 6810310, I = 238725; ETRS89-TM35FIN).

3.2 Drill core logging: methods

Twenty drill cores stored at the national drill core centre of Geological Survey of Finland (GTK) were logged (WinLoG 4.37) in July and August 2006. The logging included systematic recording of grain sizes, lithofacies, structures, textures and sampling. In addition, observations were made from core 1133-89-001. The detailed logging was carried out at a rate of about 6 m/hour.

Core M52-PO-60-001 is the longest (618.55 m), consisting of 591 m sandstone with minor mudstone interlayers. The drilling site is at the centre of the short axis of the formation, whereas most drill cores are from the marginal parts (Fig. 3). Eight cores penetrate sedimentary rocks more than 30 m (the lengths of the cores below overburden), six cores less than 10 m. Three cores reach the Svecofennian basement, all of which are from the southwestern margin of the formation, near the coast of the Bothnian Sea. The drill core logs are available in Pokki (2007).

Grain size was logged using the Udden-Wentworth classification by comparing the grain size in the cores with standard-sized sieved grains glued onto plexiglass. The grain size in the conglomerate family (next section) was estimated according to the largest clast. The class of coarse gravel (diameter of clasts 64–256 mm) was abandoned, because the diameter of the drill cores was less than 64 mm. Therefore, all grains with a diameter larger than 4 mm were classified as medium gravel. The grain size in the sandstone family was estimated according to the class that covered the largest area in the surface of the core. Gravel in slightly conglomeratic sandstone or conglomeratic sandstone was neglected, as these contain <30% gravel by definition.

3.3 Division into lithofacies

Lithofacies analysis is a standard method in the modern sedimentological approach. The analysis is based on lithofacies associations and their significance in recognising the ancient depositional environments. A lithofacies is a rock unit that differs from other lithofacies in lithology, structures or textures, which usually reflect the condition of its origin or depositional process.

The drill cores were divided into lithofacies based on the relative amounts of gravel, sand and mud (Folk 1954). The conglomerate family contains more than 30% clasts larger than 2 mm. If they are not this frequent, the rock belongs to the sandstone or mudstone family (Fig. 7). In the sandstone family, grains larger than 0.0625 mm predominate, while in the mudstone family the opposite prevails. In the classification of Folk (1954), sandstone and mudstone *sensu stricto* contain <0.01% gravel, but we used 1% as the limit.

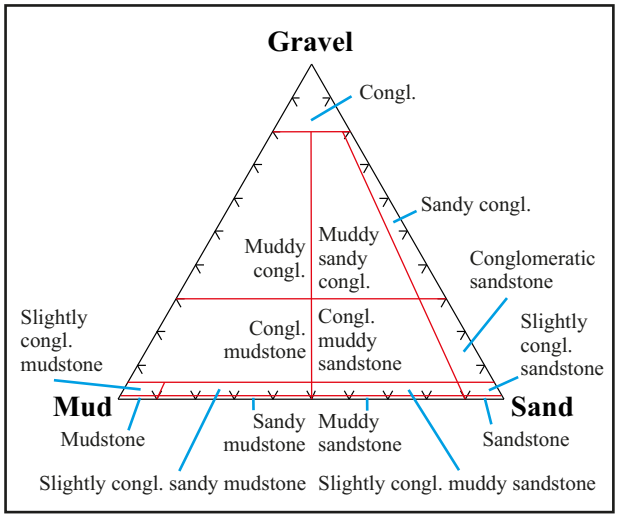

Fig. 7. The lithofacies classification used in this study is based on the relative quantities of grain sizes corresponding to gravel, sand and mud (modified after Folk 1954).

In core M52-PO-60-001, mudstone, muddy sandstone and sandstone were divided into two groups each (Table 1). Fm (fine grained, massive) is massive at the macroscopic scale and Fl (fine grained, laminated) clearly shows lamination. Muddy sandstone is sandstone containing lamellae of mud deposited from suspension: Sl (sand, laminated) is parallel laminated, whereas Sr is cross-laminated. Of the sandstone facies, St1 is cross-bedded and consists of relatively well-sorted medium sand. Cross-bedding manifests itself by frequent alterations in grain size. The grain size in St2 is smaller, typically that of fine sand. St2 is very well sorted and appears massive.

Table 1. Lithofacies classification used in the logging of the drill cores.

Lithofacies	Abbreviation	Mud / sand (%)	Gravel / sand (%)	Other
Mudstone	M	>90	<1	
Fm		>90	<1	massive
Fl		>90	<1	laminated
Sandy mudstone	SM	90–50	<1	
Muddy sandstone	MS	50–10	<1	
Sr		50–10	<1	cross-laminated
Sl		50–10	<1	parallel laminated
Sandstone	SS	<10	<1	
St1		<10	<1	cross-bedded
St2		<10	<1	massive
Slightly conglomeratic sandstone	SCS	<10	1–5	
Conglomeratic sandstone	CS	<10	5–30	
Sandy conglomerate	SC	<10	30–80	
Conglomerate	C	0–100	>80	

3.4 Drill core descriptions

3.4.1 M52-PO-60-001 (591 m; the 'type section')

Core M52-PO-60-001 consists almost entirely of sandstone or more fine-grained lithofacies. It can be divided into lower, middle and upper parts. The lower part (618–410 m) mostly consists of St1, and below 464 m it is very monotonous with coarse sand being the typical grain size. Mudstone interlayers are only few centimetres thick. The middle part of the core (410–130 m) predominantly consists of St2 with fine sand as the typical grain size. It also contains Sr and Sl, and the mudstone interlayers are thicker (the thickest at 387.40–386.55 m) than in other parts of the core. The upper part (130–27 m) mostly consists of St1 with grain sizes of fine sand at 100–43 m, medium sand at 43–27 m and both at 130–100 m.

The drill core is at its coarsest with slightly conglomeratic sandstone (at 561.75–561.65 m), and the maximum grain size in the core is 6 mm (at 561.7 m and 74.8 m). Thin mudstone interlayers and mudstone intraclasts appear throughout, but these intraclasts are rare at 588–572 m. The contacts with mudstone are usually sharp; in places, the lower contacts of mudstone layers are gradational and upper contacts are sharp.

Some parts of the core appear very light in colour, as if they were very rich in quartz. However, fresh clastic feldspar is very abundant in places throughout the core (e.g., at 472 m, 483 m, 500 m, 567 m, 592 m and 616 m). Below 412 m, grains are very well rounded in places; white cement is common and the core may be easily crushed. At 506.2–505.7 m and 525.8–525.4 m the core appears ground, as if weathered, probably due to the dissolution of carbonate cement. The upper and lower parts of the drill core show a strong epigenetic red colour. In the middle part, epigenetic colouring is sparse. Reddish stripes of oxidation can follow the foresets of cross-bedding, but in some places the stripes are not related to primary structures; e.g., at 101.30–101.00 m the stripes are perpendicular to the bedding, and plausibly record the vertical flow of epigenetic pore fluids. Light coloured spots with a diameter less than 2 cm are common in parts that bear epigenetic colour. Some cracks are filled with carbonate.

3.4.2 Drill cores reaching the Svecofennian basement

Cores 1141-89-001 (depth 31.5 m), 1141-85-002 (23.0 m) and 1141-89-006 (40.7 m) from the southwestern margin of the Satakunta formation reach the Svecofennian basement (Fig. 3). They contain conglomerate and are the most coarse-grained drill cores from the basin. Their coarsest parts are not systematically at their lowermost

level, e.g., there is a 10 cm layer of sandstone below conglomerate in core 1141-89-006. The largest clasts are very well-rounded vein quartz, with the longest dimension from a few centimetres up to more than the diameter of the cores. Angular clastic feldspar is common in the matrix. Parts showing a reddish and greenish tint in the matrix follow one after another.

The non-conformity in core 1141-89-001 contains 1.7 m core loss (between 23.50 and 21.38 m). The basement is chlorite schist, fresh below 27 m. Core 1141-85-002 contains coarse-grained granite below 10.47 m, and due to weathering the granite shows a reddish colour that is strong in places. Some of the quartz grains in the granite are round and resemble the drop quartz of rapakivi granites.

3.4.3 Other drill cores

Of the other cores, only 1141-89-002 (50.5 m) and 1133-89-001 (101.1 m) contain conglomerate, the former less than 30 cm. The largest clasts in core 1133-89-001 are predominantly vein quartz and microcline granite. Most of this core consists of conglomeratic sandstone or sandy conglomerate, and conglomerate is not present at the bottom in this core, either.

Slightly conglomeratic sandstone is the most typical lithofacies in the cores from the southwestern margin of the Satakunta formation that do not reach the basement. Core 1134-83-002, transversally from the central part of the basin, contains mudstone interlayers. Sandstone is the most typical lithofacies in the drill cores from the northeastern margin sequence; however, layers of sandy conglomerate occur in the top parts of drill cores from the Harjavalta outcrop. Mudstone interlayers occur in three drill cores from the northeastern margin sequence. Cores 1143-85-001 and 1141-85-001 are more fine-grained than other drill cores from the northeastern margin. The former is exceptionally red in colour, whereas the latter is exceptionally light.

3.4.4 Summary

The long drill core (M52-PO-60-001) consists of a surprisingly monotonous assemblage of sandstone lithofacies. The abundant cross-bedding and scarcity of fine sediments together with common mud chip intraclasts strongly point to a poorly channelled fluvial depositional environment. Even the observed massive sandstones (typical for the St2 facies) may be understood as intersecting channel fills in a fluvial environment. An aeolian contribution is possible due to the very well-rounded nature of some parts of the core. Detailed depositional models cannot be constructed, but considering the thickness of the sampled succession (591 m), several fluvial sub-environments are plausibly represented.

The three drill cores reaching the Svecofennian basement at the southwestern margin of the Satakunta formation and the southernmost core 1133-89-001 are the most coarse-grained drill cores. The most fine-grained cores come from the central part of the formation (M52-PO-60-001) and from the northwest (1143-85-001). Mudstone intraclasts are common only in the most fine-grained cores (although they are met in 1134-87-007, 1134-87-009 and in the cores from the Harjavalta outcrop). In core M52-PO-60-001, mudstone intraclasts occur almost throughout. Core 1143-85-001 from the northeastern margin resembles M52-PO-60-001 more than it resembles other drill cores. Core 1141-85-001 is exceptionally light in colour and – apart from M52-PO-60-001 – it is the only core that could contain quartz arenitic parts in macroscopic observation. The coarse-grained drill cores in the marginal parts are composed of arkose arenite or subarkose. Fresh detrital feldspar is common in places, even in the lowermost parts of core M52-PO-60-001.

The observed lithofacies assemblages of the short drill cores do not allow detailed interpretation, but a rather proximal high energy fluvial environment (braided river; Miall 1977) seems most plausible. At the SW margin, the source material is a mixture of mature quartz pebble detritus mixed with poorly rounded material rich in feldspar.

4 MINERALOGICAL COMPOSITION

4.1 Method

The samples for mineralogical study were selected to represent different lithological types and to verify the composition of parts that appeared to be rich in quartz. The total number of studied samples was 24. The modes of the samples were determined using a Mineral Liberation Analyzer (MLA), a combined scanning electron microscope (SEM) and an energy dispersive spectrum (EDS) analyser at the Outokumpu Mineral Technology Laboratory of GTK. In XMOD (X-ray modal) analysis, minerals are identified according to the spectrum produced by X-rays. The procedure is rapid and reliable, and it takes 10 to 15 minutes to gain 6000 spectra from one thin section.

4.2 Main and accessory minerals

4.2.1 Overview

The Satakunta formation consists of arkosic arenite and subarkose at the present erosion level (Simonen & Kouvo 1955, Marttila 1969) (Fig. 8A). The most mature sample of Simonen and Kouvo (1955) was obtained from from Yläne, and it may be from a glacial erratic, as no outcrops are known from there. Most of the drill core samples in the present study are classified as arkosic arenites (Fig. 8B). Only one sample from core M52-PO-60-001 is subarkose (591 m) and one is subarkose / arkosic arenite (530 m). Five samples from the other drill cores are subarkosic in composition.

4.2.2 Vertical section of the Satakunta formation: Drill core M52-PO-60-001

The three-part character in the distribution of lithofacies in core M52-PO-60-001 is manifested in modal compositions. Quartz is abundant in the upper and especially in the lower part of the core, but clearly less abundant in the middle part (samples 114.5 to 390.3) (Fig. 9, Table 2). Quartz is least abundant in sample 390.3 (25%), composed of Sr lithofacies rich in biotite. Below 390 m the amount of quartz increases in a sawtooth-like manner. Plagioclase is more common than K-feldspar between 270 and 390 m. It increases from the top of the drill

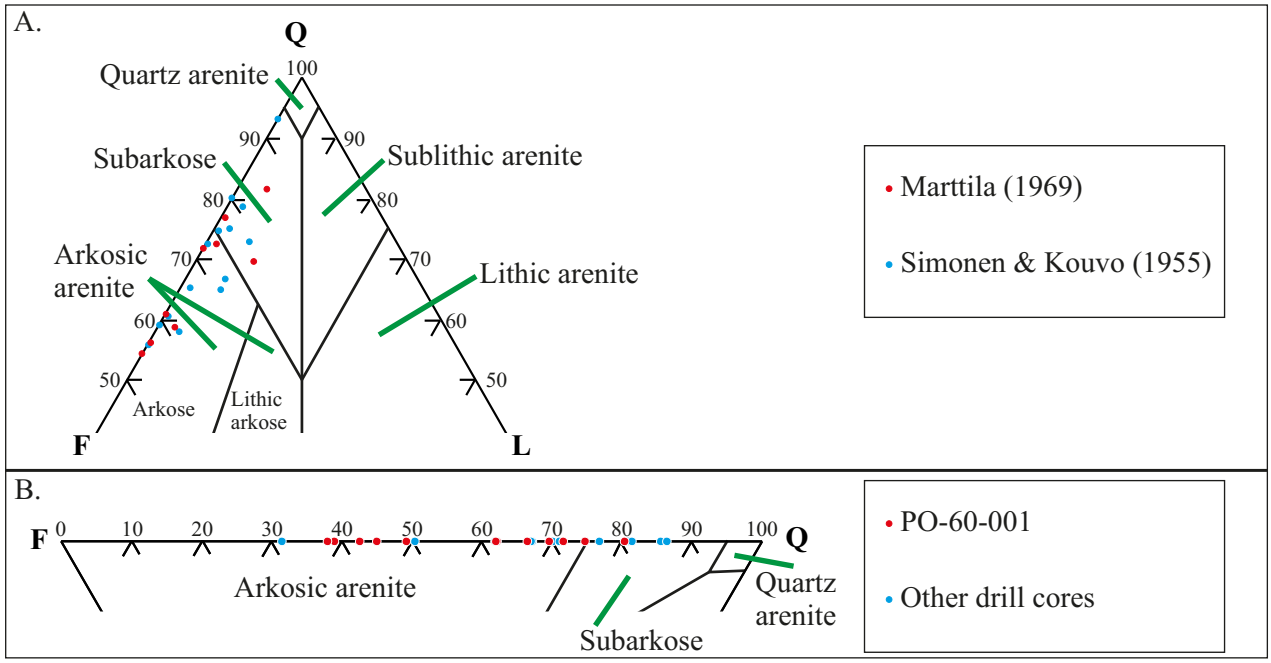

Fig. 8. The Satakunta formation is composed of arkosic arenite and subarkose. **(A)** Results from old petrographic studies on outcrop samples. **(B)** The modal composition of drill core samples determined using a Mineral Liberation Analyzer (MLA). Lithic clasts cannot be distinguished from mineral grains by MLA, but because their frequency is low, the analysed ratio Q/(Q+F) on the QF side approximates the composition in a QFL plot.

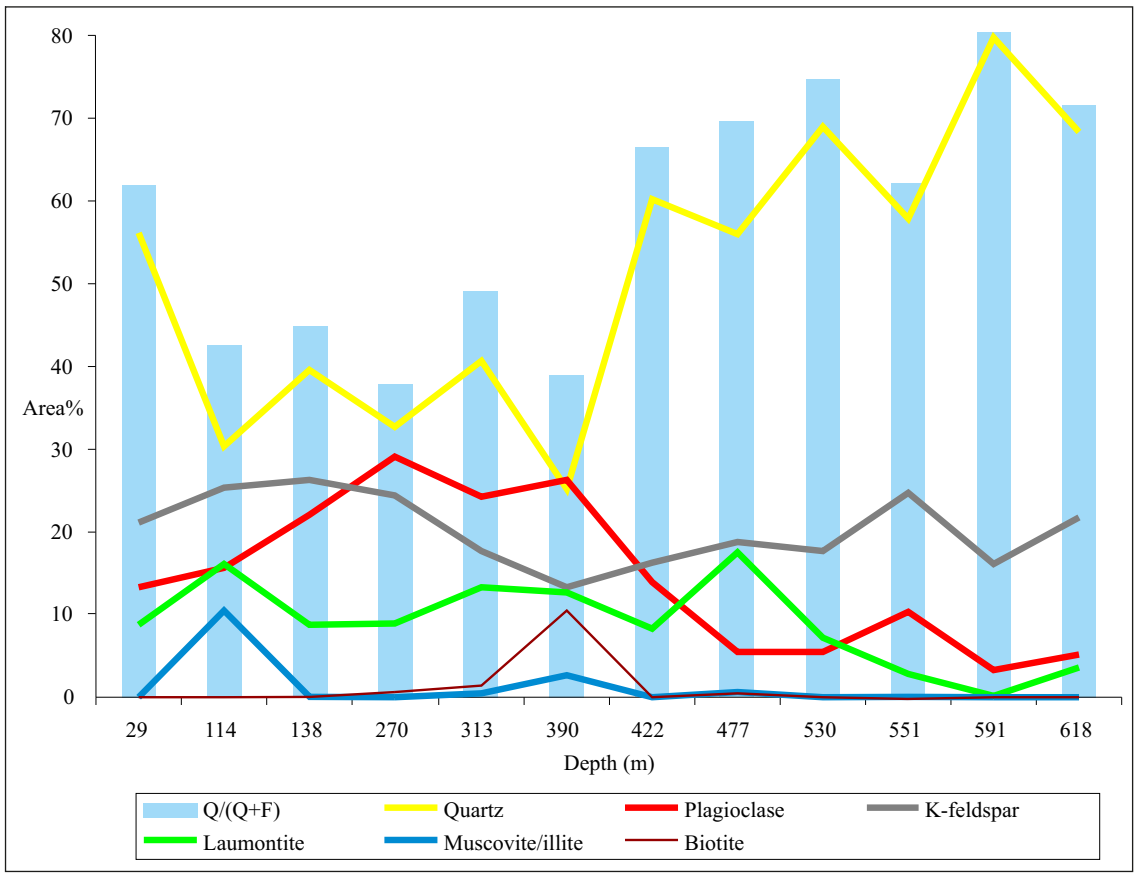

Fig. 9. Rock-forming minerals in core M52-PO-60-001. The columns indicate the ratio of quartz to the combined area of quartz and feldspars. Q = quartz, F = feldspars.

Table 2. The modal composition (%area) of samples from core M52-PO-60-001.

Phase / depth (m)	**29**	**114.5**	**138.7**	**269.7**	**313.4**	**390.3**	**422.2**	**477**	**529.7**	**551**	**591.2**	**617.6**
Quartz	56.14	30.47	39.60	32.73	40.67	25.29	60.21	56.07	69.01	58.00	79.77	68.37
Plagioclase	13.28	15.75	22.11	29.06	24.27	26.34	14.02	5.59	5.48	10.44	3.30	5.29
K-feldspar	21.09	25.36	26.32	24.45	17.68	13.32	16.28	18.84	17.80	24.80	16.11	21.75
Laumontite	8.80	16.11	8.85	8.98	13.40	12.78	8.35	17.54	7.31	2.82	0.19	3.67
Muscovite	0.08	0.92		0.48	0.45	2.25	0.16	0.43	0.14	3.72	0.34	0.45
Muscovite/illite	0.02	10.58		0.03	0.61	2.67	0.03	0.72	0.02		0.05	0.08
Biotite	0.05	0.05		0.65	1.50	10.58	0.05	0.50	0.02		0.03	0.13
Chlorite			2.23	0.32	0.70	0.41				0.05		
Almandine	0.08	0.10		0.42	0.05	0.08	0.16	0.07				
Epidote	0.15	0.15	0.19	0.67	0.18	0.61	0.18	0.13	0.10	0.07	0.06	0.08
Titanite	0.18	0.15	0.62	1.30	0.24	0.38	0.49	0.05	0.02	0.05	0.03	0.13
Tourmaline	0.02	0.26		0.02	0.02	0.02		0.02				
Zircon			0.03	0.02		0.05						0.02
Calcite	0.02			0.13	0.02	4.87			0.11			
Apatite	0.03	0.02	0.05	0.03	0.21	0.15	0.03				0.10	0.02
Allanite	0.02			0.33		0.02	0.02					
Fe oxide				0.25	0.02	0.03	0.02					
Fe hydroxide	0.03			0.10	0.02	0.05						
Other	0.02	0.07		0.02		0.11		0.05		0.04	0.02	0.03
Total	100.01	99.99	100.00	99.99	100.04	100.01	100.00	100.01	100.01	99.99	100.00	100.02

core down to 270 m, with a maximum of 29%. Below 390 m, plagioclase is scarce. Potassium feldspar is quite evenly distributed, ranging from 13 to 26%.

It must be emphasized that none of the samples from core M52-PO-60-001 necessarily come near the Svecofennian basement, as the thickness of the formation is unknown. Fresh detrital feldspar at the lowermost part of core M52-PO-60-001 shows that the subarkose at 591 m below the arkosic arenites does not indicate a systematic change to a more quartz-rich composition below arkoses. In addition, due to the abundant cementing quartz, the primary composition in the lower part may have been more immature than expressed by the mode. The sampling may also slightly bias the modal compositions, as parts that appeared rich in quartz were preferred.

Laumontite (as cement) amounts to over 7% down to 530 m. The maximum (18%) is reached at 477 m, and below 530 m laumontite is accessory. Biotite is accessory, except in one sample (11%). The amount of muscovite/illite is 11% at 114 m. It is richer in Mg but poorer in K than muscovite.

4.2.3 Lateral compositional variation in the Satakunta formation

The southwestern margin of the formation is compositionally more mature than the northeastern and central parts. All the subarkoses among the drill core samples come from the southwestern margin, and only one sample from the southwestern margin is not subarkose (Fig. 10). At the southwestern margin, quartz and muscovite are abundant, but plagioclase is nearly absent (Table 3). Abundant plagioclase and mineralogical heterogeneity are typical for the central part and northeastern margin of the formation. These spatial compositional characteristics are also apparent in the results of Marttila (1969) (Fig. 10). Exceptions are sample 1141-85-1-16.7 and Marttila's (1969) sample from Harjavalta, both poor in plagioclase. However, the latter is not in accordance with the drill core sample or with the sample from Harjavalta in Simonen and Kouvo (1955).

Quartz amounts to over 60% only in the sequence from the southwestern margin and in sample 1134-87-009-35.2. The samples with ≤ 0.02% plagioclase contain 10–17% muscovite; in other samples, muscovite amounts to 1–8%. Plagioclase (33%) is more abundant than K-feldspar (12%) only in sample 1143-85-001-13.9. Plagioclase (19%) is almost as common as K-feldspar (21%) in sample 1134-83-002-4.9. The amount of K-feldspar varies between 12–25% with no clear spatial trend. Detrital biotite is most common in the samples HARJAVALTA-003-3 (22%) and 1143-85-001-14 (7%) from the northeastern margin sequence. Laumontite is common only in core 1143-85-001 from the northeastern margin and in core M52-PO-60-001. It is absent at the southwestern margin of the formation. Sample 1143-85-001-13.9 from the northeastern margin is especially versatile in composition, as the modes of plagioclase, laumontite, chlorite, epidote, titanite, tourmaline, garnet, zircon, apatite, allanite and ilmenite are the highest in it.

4.2.4 Accessory minerals

MLA point counting indicates that muscovite is the most abundant accessory mineral in drill core M52-PO-60-001. A sample from 390 m contains 5% calcite, but it is absent from samples below 530 m. Chlorite amounts to 2% in a sample from 115 m. All samples contain titanite and epidote. Allanite, almandine, apatite, tourmaline and zircon are rare (Table 2).

In the other drill cores, accessories can be classified into three groups based on their amount: tourmaline and chlorite are the most common, followed by epidote, apatite, titanite and almandine. Ilmenite, zircon, rutile, allanite, monazite and calcite are rare. Calcite is present (0.13%) only in sample HARJAVALTA-R-003-3.0 (Table 3). The detrital heavy minerals are described in Chapter 6.

Table 3. The modal composition (%area) of samples from other drill cores.

Phase / sample	AMH-85-005-13.5	1141-89-003-35.5	1141-89-006-16.6	1141-89-002-47.2	1141-85-002-10.2	1141-89-001-14	1141-85-001-16.7	1143-85-001-13.9	HAR.-003-3	1143-85-002-22.6	1134-83-002-4.9	1134-87-009-35.2
Quartz	68.79	72.60	68.30	61.02	74.04	71.48	53.22	20.63	34.05	58.04	41.83	62.05
Plagioclase	0.02				0.02		0.84	32.63	7.91	9.63	19.89	4.92
K-feldspar	20.72	16.50	16.05	24.79	11.56	12.02	21.80	12.39	13.04	18.88	21.19	25.30
Laumontite								14.68	0.07	0.02	0.03	
Muscovite	10.10	10.09	15.35	14.07	13.83	16.23	16.79	0.96	6.61	1.60	7.59	5.00
Muscovite/illite	0.30	0.03	0.02	0.02	0.07		6.33	1.66	15.10	8.91	4.17	2.20
Biotite		0.48	0.08	0.02	0.07	0.12	0.15	6.75	21.74	1.82	3.58	0.29
Chlorite								1.71	0.11		0.67	0.02
Almandine						0.02		0.77	0.07	0.12	0.15	
Epidote								1.14	0.22	0.02	0.02	0.02
Titanite								1.12	0.06			
Tourmaline				0.02			0.03	1.58	0.15	0.55	0.41	0.03
Zircon	0.02		0.02		0.02		0.03	0.11	0.02		0.07	
Rutile	0.02	0.08	0.05	0.02			0.03			0.02		
Calcite									0.13			
Apatite		0.12	0.03	0.03	0.32	0.03		0.41	0.07	0.13	0.15	0.03
Allanite								0.20				
Monazite	0.02	0.02		0.02	0.02	0.02			0.02		0.02	
Fe oxide						0.02		0.24	0.02		0.02	
Fe hydroxide	0.02	0.02						2.75	0.51	0.18	0.05	0.07
Ilmenite		0.02				0.03		0.23	0.04	0.02	0.05	0.03
Other		0.05	0.10		0.07		0.77	0.03	0.06	0.07	0.13	0.03
Total	100.01	100.01	100.00	100.01	100.02	99.97	99.99	99.99	100.00	100.01	100.02	99.99

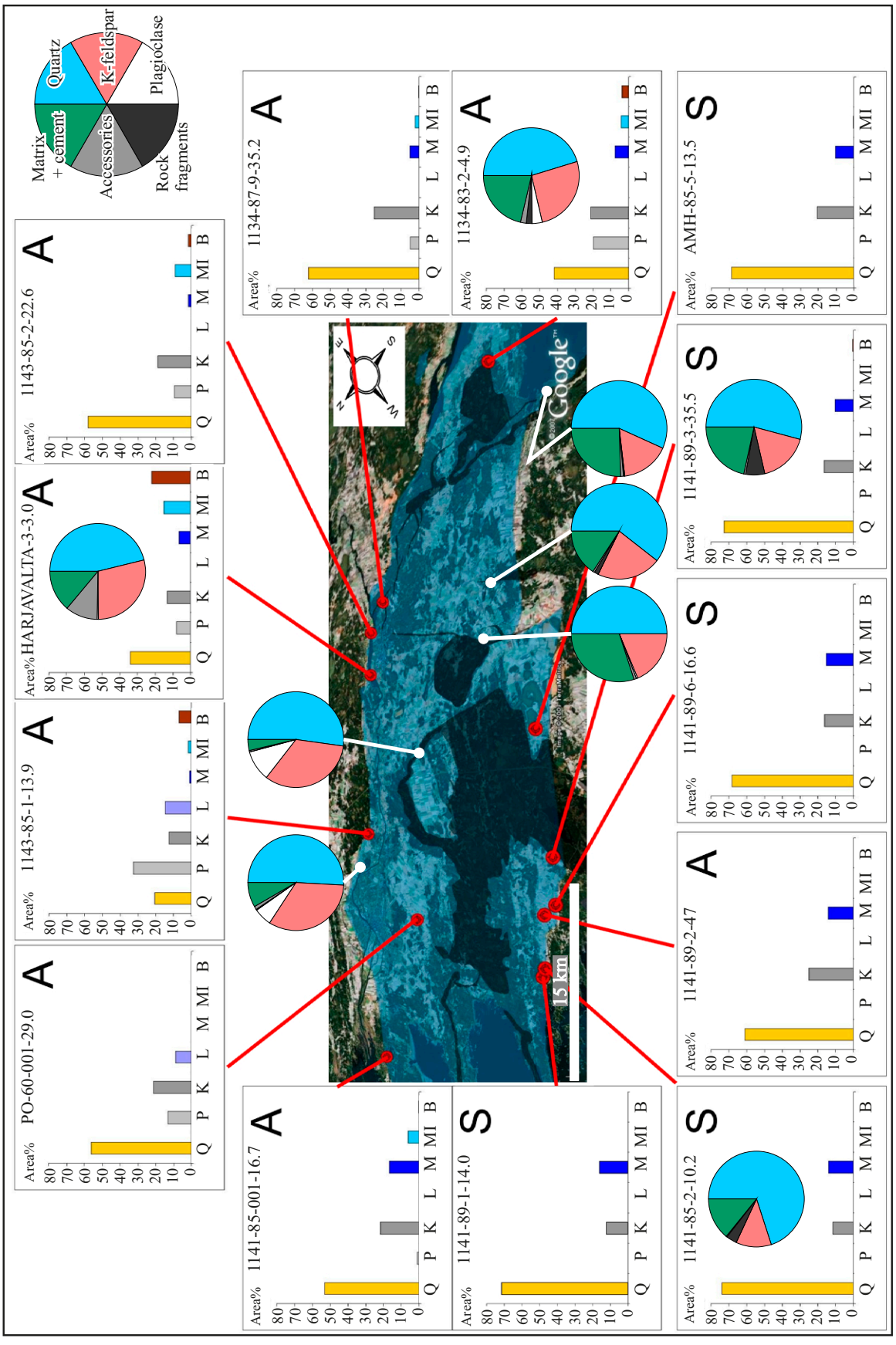

Fig. 10. Modes of the drill core samples analysed by MLA. Q = quartz, P = plagioclase, K = potassium feldspar, L = laumontite, M = muscovite, MI = muscovite/illite, B = biotite, A = arkosic arenite, S = subarkose. Pie diagrams refer to outcrop samples (Marttila 1969), some of which come from the same outcrops as a drill core sample. Lithological units are from the Geological Map of Finland 1:100 000 (GTK). Blue shading = sandstone, dark grey shading = diabase.

4.3 Other petrographic features

4.3.1 Lithic clasts

Lithic clasts observed by Simonen and Kouvo (1955) and Marttila (1969) – microcline granite and rounded quartzite – are consistent with a Svecofennian source. Only Laitakari (1925) has reported a clast of rapakivi granite. According to him, all features typical of rapakivi granite were seen in a clast in a conglomerate from Reposaari, but neither the sample nor a photograph of it are available.

Three distinguished lithic clasts were found from the drill cores in the present study. In addition, mudstone clasts, interpreted as intraclasts and unlithified at the time of deposition, are common. Granite clasts are abundant in core 1133-89-001. A fine-grained granitoid with granophyric texture was observed in core 1141-89-002, and two sandstone clasts were observed in core 1141-89-006 (Fig. 11). Both clasts of sandstone are reddish and well rounded. Quartz grains have the grain size of medium sand. Only a few strongly altered grains refer to the presence of feldspar.

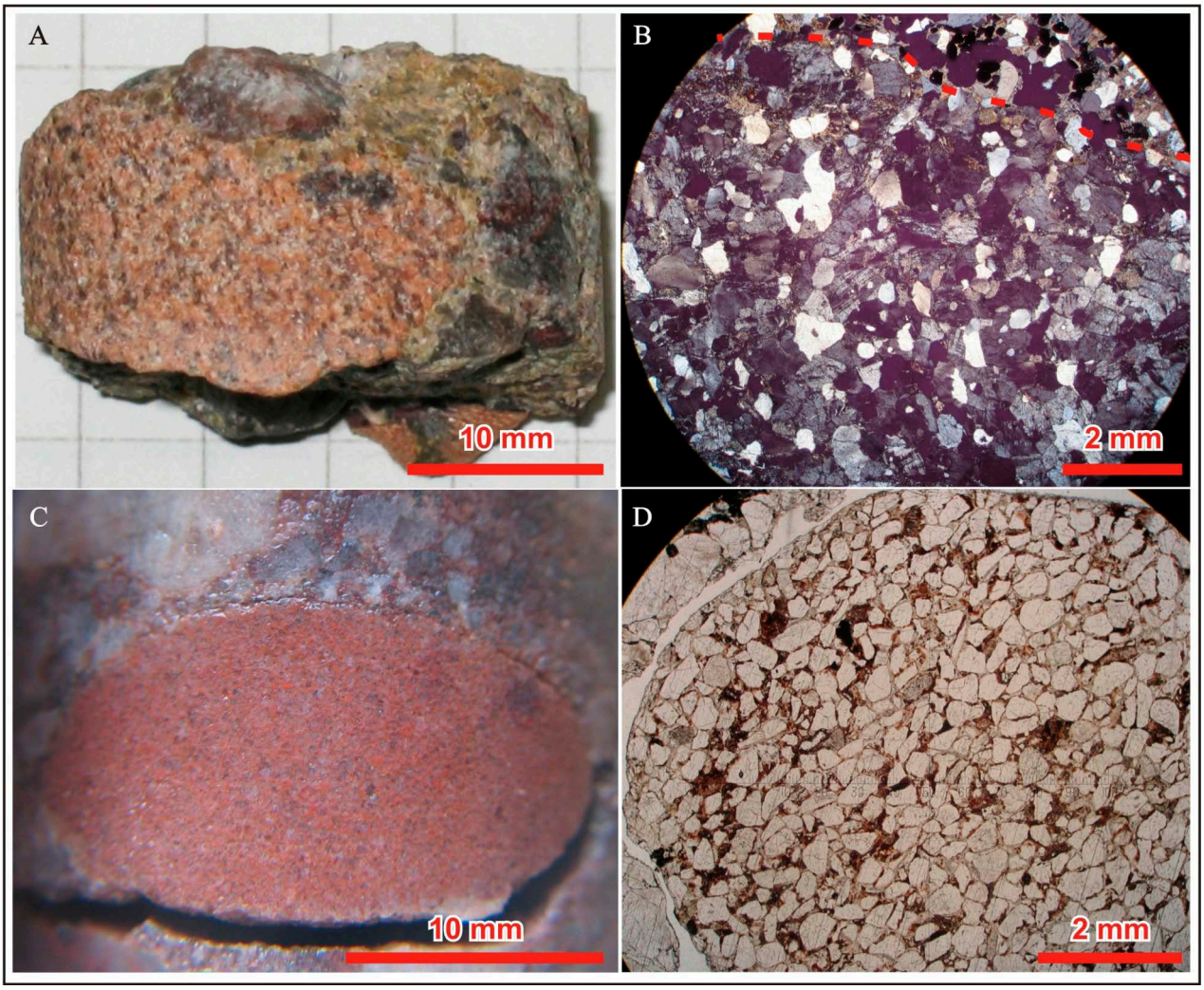

Fig. 11. Lithic clasts in the Satakunta formation. **(A)** Fine-grained granitoid with a granophyric texture. 1141-89-002. Depth 33.2 m. **(B)** Granitoid (below the red line) in XPL. **(C)** Sandstone. 1141-89-006, depth 26.9 m. **(D)** Sandstone in PPL. Photo: Jussi Pokki, GTK.

4.3.2 Diagenetic and other post-depositional features

The sandstone in the Satakunta formation is well lithified and compact. No empty pore space is visible under an optical microscope and the grains are tightly interlocked. The interrelationship of mineral grains in a sample at 313.4 m from core M52-PO-60-001 can be seen in a chart composed by XBSE analysis with MLA (Fig. 12). Quartz (40.7%) appears as unevenly distributed accumulations of grains. The dissolving of SiO_2 has left detrital grains corroded in places (Fig. 13A). In the lower part of core M52-PO-60-001, quartz overgrowth

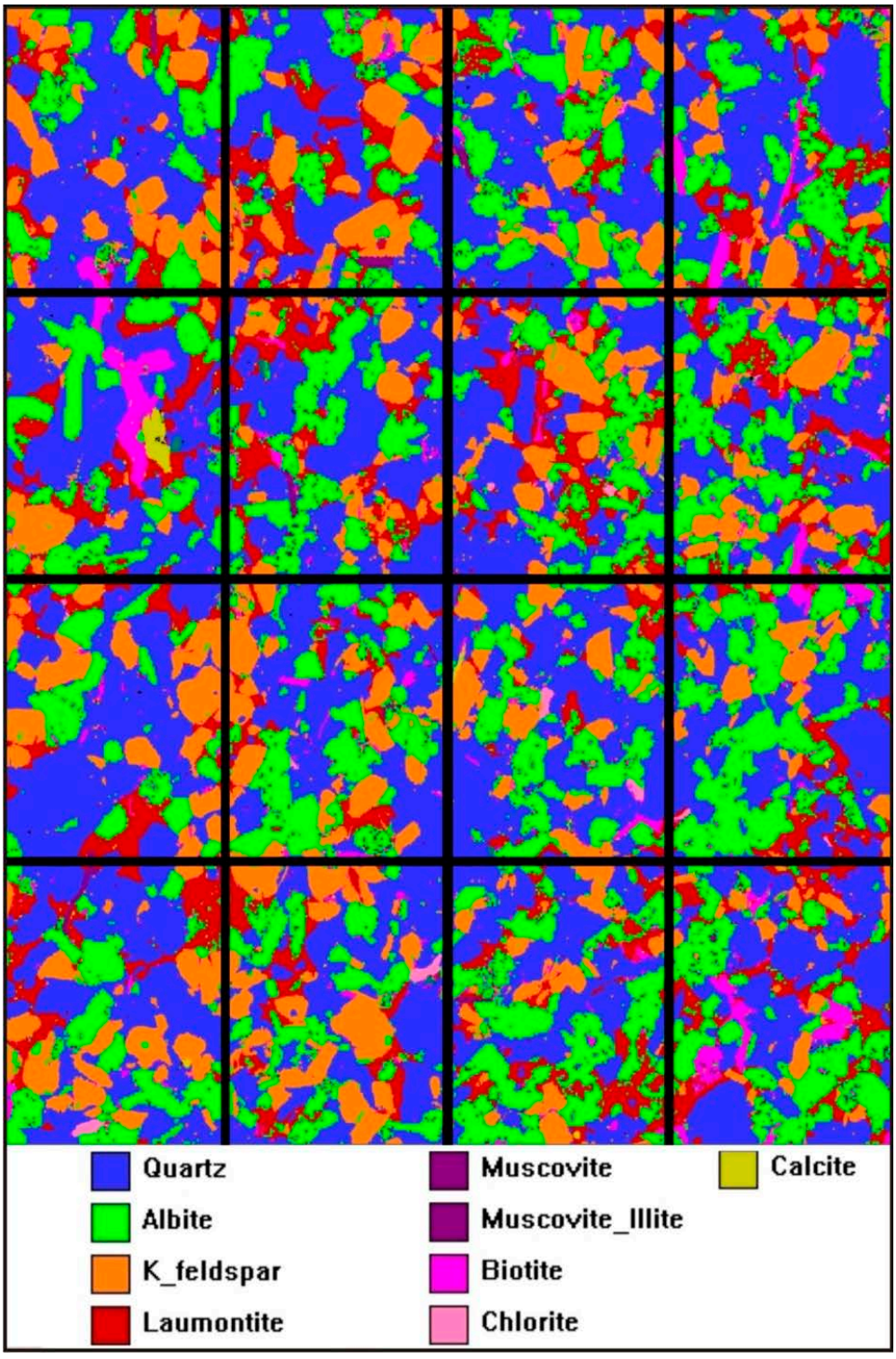

Fig. 12. MLA chart showing the interrelationship of mineral grains. Explanation in the text. M52-PO-60-001. Depth 313.4 m.

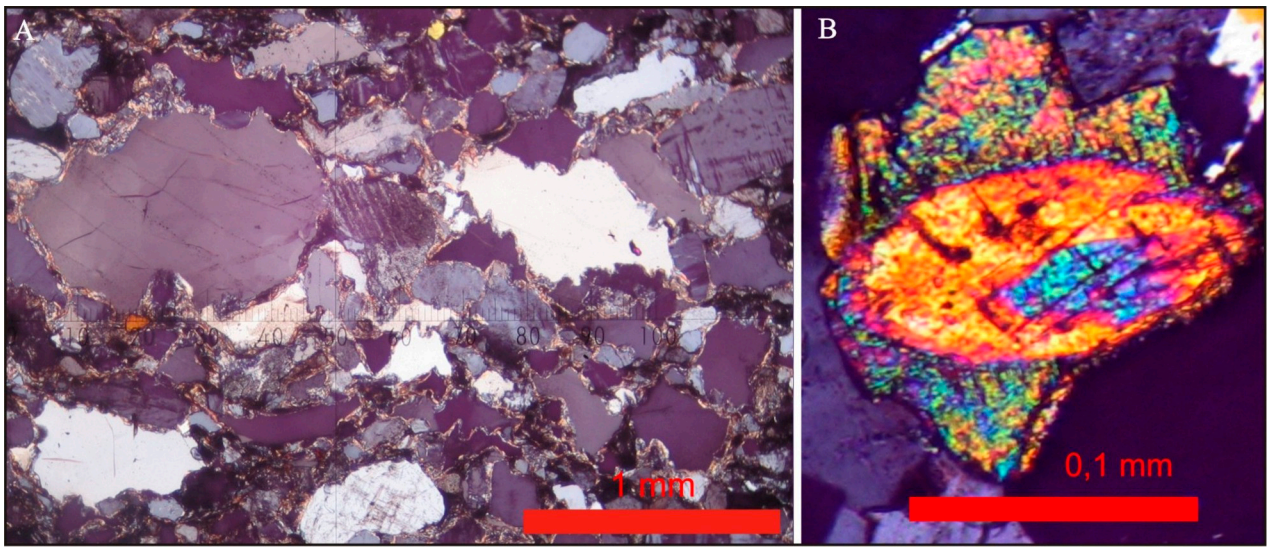

Fig. 13. **(A)** Grains with strongly corroded margins. M52-PO-60-001. Depth 513.2 m. **(B)** Overgrowth of detrital monazite. M52-PO-60-001. Depth 162.9 m. Photo: Jussi Pokki, GTK.

is very common and secondary quartz can fill interstices with no primary quartz grains around. A network of quartz with simultaneous extinction implies recrystallization. Granoblastic quartz has been observed, but it is rare. Overgrowth of accessory minerals is common (Fig. 13B).

K-feldspar (17.9%) appears as individual clastic grains that are more evenly distributed than other grains (Fig. 12). Some of them show albitized parts at the margins. Plagioclase grains are smaller than K-feldspars and they show more inclusions of accessory minerals than other minerals do. The plagioclase is albite in composition. Clearly authigenic plagioclase was not observed. Authigenic laumontite cement fills the angular interstices of other grains.

Quartz, hematite, laumontite and calcite are the cementing minerals in the sandstone. Most of the hematite is clearly older than the laumontite cement, because hematite grains appear at the margins of detrital grains and their frequency decreases into the laumontite cement (Fig. 14C). In places, hematite forms network-like textures (Fig. 14B). The light-coloured "reduced" spots do not contain hematite, but hematite is common around them.

Laumontite (Fig. 15) and carbonate are found only as cement. In many places, laumontite replaces other grains, e.g., plagioclase. The average composition of eight laumontite electron microprobe analyses was 52.3% SiO_2, 21.1% Al_2O_3 and 11.4% CaO. The youngest cementing phase consists of carbonate, as carbonate replaces laumontite in core M52-PO-60-001 (368.1 m). In that sample, carbonate replaces many detrital grains that still faintly show their original margins. In core M52-PO-60-001 as a whole, carbonate is much less abundant than laumontite, even though carbonate is more common in places than laumontite. Carbonate cement is rarely observed in outcrop samples, probably due to easy weathering.

Muscovite is more common in the weathered drill cores than in the fresh ones. It appears as small flakes between detrital grains and forms a metamorphic matrix (Simonen & Kouvo 1955, Marttila 1969). The metamorphism is the result of deep burial or the thermal effect of the intruding diabase dykes and sills. The matrix may at least in part be detrital in origin, but it seems plausible that a major part is an authigenic result of feldspar alteration.

Kohonen et al. (1993) reported glauconite from Makholma, the far northwestern part of the Satakunta formation. Instead of being diagenetic, glauconite may form by replacing calcite during subaerial exposure (Catuneanu 2006). In Makholma, most of the glauconite appears within a few millimetres from the surface, as in a crust (Fig. 16), suggesting formation during subaerial exposure. Pajunen and Wenneström (2010) have observed prehnite crystallized in faults in the sandstone.

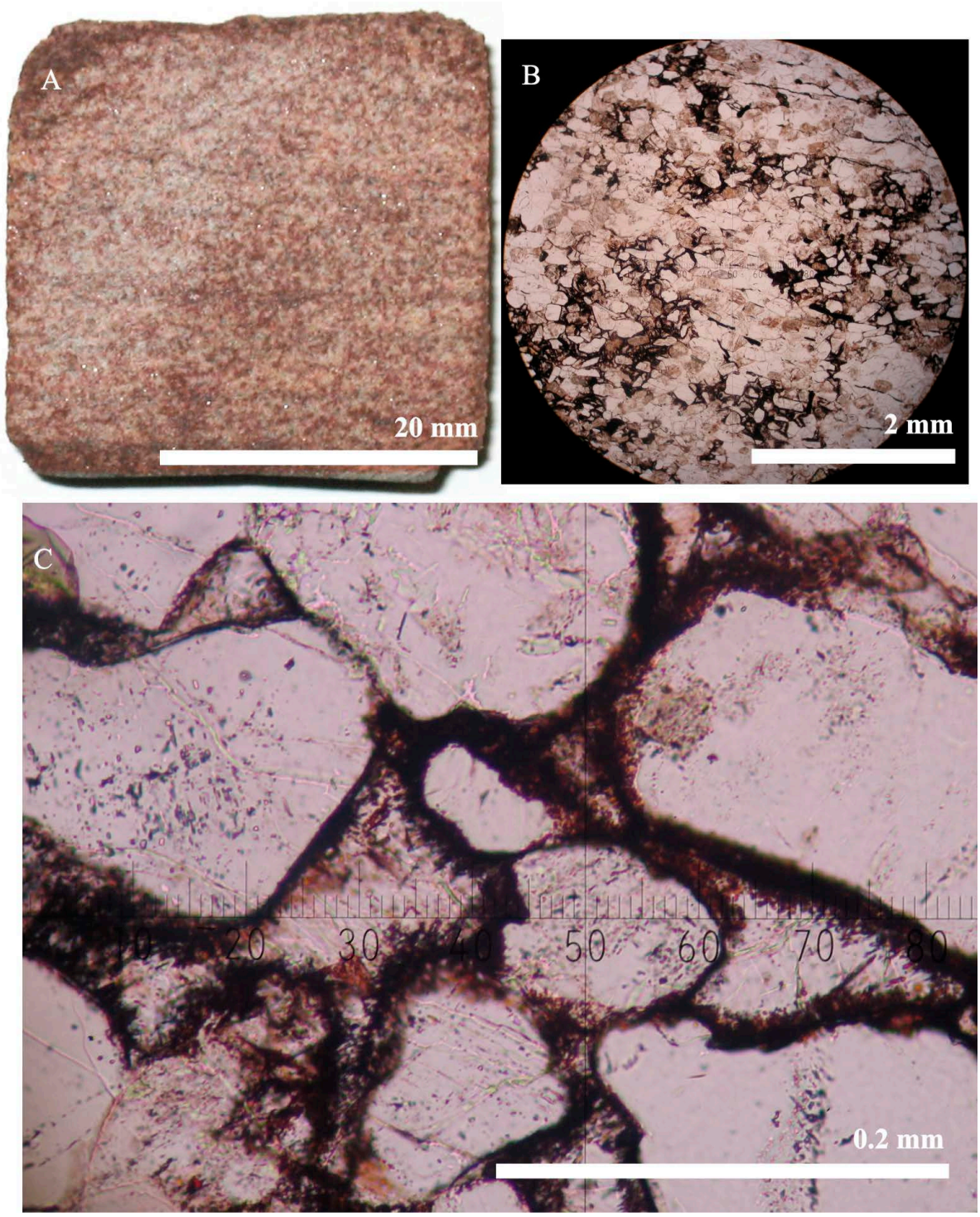

Fig. 14. M52-PO-60-001. Depth 162.8 m. Different magnifications of the same sample. **(A)** Abundant red and white spots in a hand sample. **(B)** Hematite forms a network-like texture. **(C)** Most of the hematite grains appear at the margins of detrital grains and their frequency decreases into the laumontite cement. Photo: Jussi Pokki, GTK.

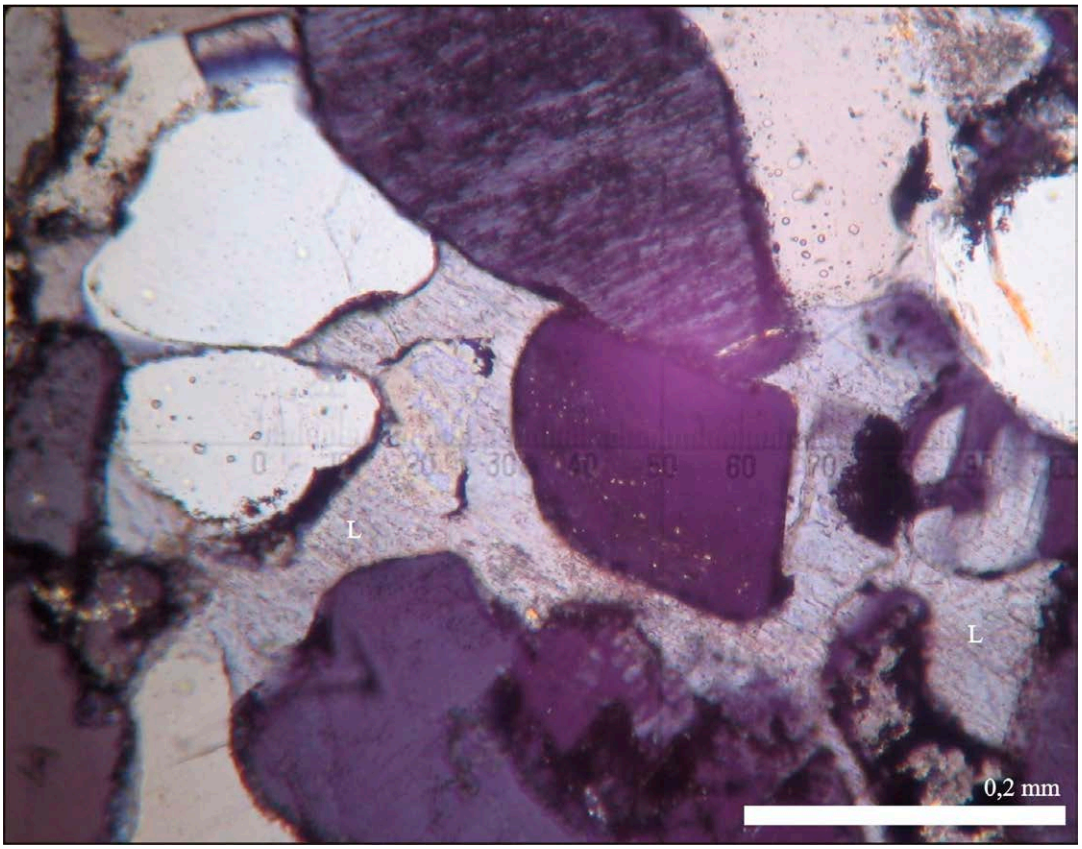

Fig. 15. Laumontite (L) filling the interstices of other grains, showing low relief and strong cleavage. Laumontite replaces a detrital grain right to the extinguished quartz at the centre. M52-PO-60-001. Depth 72 m. Photo: Jussi Pokki, GTK.

Fig. 16. Glauconite in the surface of slightly conglomeratic sandstone from the Satakunta formation, Makholma, may have been formed by the replacement of calcite during subaerial exposure. Photo: Jussi Pokki, GTK.

4.4 Summary

The main minerals provide little information concerning the provenance of the detritus. The amount of quartz indicates a more mature composition in the SW and in lower parts of core M52-PO-60-001. Based on the mineral composition, no clear indication of a quartz arenitic platform cover as a major source was found in the drill core material investigated. The few lithic clasts indicate a granitic source and the quartz arenite clasts may be intraformational or represent recycled previous cover. No mafic volcanic clasts were observed.

Abundant detrital biotite in some samples may reflect Svecofennian schist as one major source component. The observed diagenetic to low-grade metamorphic features question the usefulness of the K-feldspar/plagioclase ratio in provenance studies. In addition to direct observations of replacement, the Ca of the abundant laumontite and calcite cement may be derived from plagioclase alteration during the diagenesis. Nevertheless, Simonen and Kouvo (1955) determined the crystallographic symmetry of 35 K-feldspar grains from four samples. All of the grains were microcline, which implies a Svecofennian source, because the K-feldspar in the Laitila rapakivi granite is predominantly orthoclase. Marttila (1969) did not observe orthoclase, either.

5 CHEMICAL COMPOSITION

5.1 Method

The whole-rock geochemical composition of 32 samples was analyzed at the Geolaboratory of GTK in Espoo. In addition to XRF (code +175X) and ICP-MS (308M), the analyses include carbon using a carbon analyser (+811L), carbon in carbonate using a Leco analyser (816L), H_2O-/H_2O+ using a water analyser (815L) and Fe^{2+} (301T).

5.2 Main components

5.2.1 General features

The samples from the southwestern margin of the Satakunta formation form a coherent group in the main component diagrams (SW in Fig. 17): SiO_2 is high and all other main components are consequently low. Samples from the northeastern margin sequence and from core M52-PO-60-001 are compositionally more heterogeneous.

Six samples from core M52-PO-60-001 show SiO_2 levels at least as high as the samples from the southwestern margin sequence, but the samples from the SW are poorer in Ca and Na and contain more total Fe and K. Two samples from the northeastern margin sequence are also SiO_2-rich, but are enriched in Mg and Na compared to the samples from the SW margin. One sample (1141-85-001-16.7) from the northeastern margin is anomalous with very low amounts of Na and total Fe.

In core M52-PO-60-001, five samples contain less SiO_2 than feldspars (Fig. 17). This is due to abundant mica and/or clay minerals, and at 390.3 m also laumontite. Al and Fe are most abundant in the red mudstone, and only the two samples from 65.2 m contain more potassium and one sample from NE margin sequence contains more Mg. Calcium is second highest in abundance in the grey mudstone and only the red mudstone contains more Fe.

The densely plotting samples with high silica in K_2O-SiO_2 reflect the most typical composition of arkosic arenites: c. 70% quartz, c. 20% K-feldspar and c. 10% plagioclase. The different proportions of plagioclase and quartz control the Na contents, whereas the amounts of laumontite and oligoclase dominate the Ca. The variable abundance of biotite and clay minerals most affects the trends in Mg and Fe.

Simonen and Kouvo (1955) noted that not only was the Fe^{3+}/Fe^{2+} ratio higher in red mudstone compared to the greyish green type, but Fe_{tot} was also higher. Results from core M52-PO-60-001 also show higher Fe_{tot} in both the red sandstone and red mudstone compared to their grey

equivalents (Table 4). The Fe^{3+}/Fe^{2+} ratio is more than double in comparison to the grey types. Of the grey types, even the sandstone shows Fe^{3+}/Fe^{2+} >1, but in grey mudstone the ratios is under one. High Fe^{2+}/Fe_{tot} in general can also be a result of abundant detrital biotite, which is probably the case in the three anomalous samples that have not been framed by the dashed line in Fig. 21A.

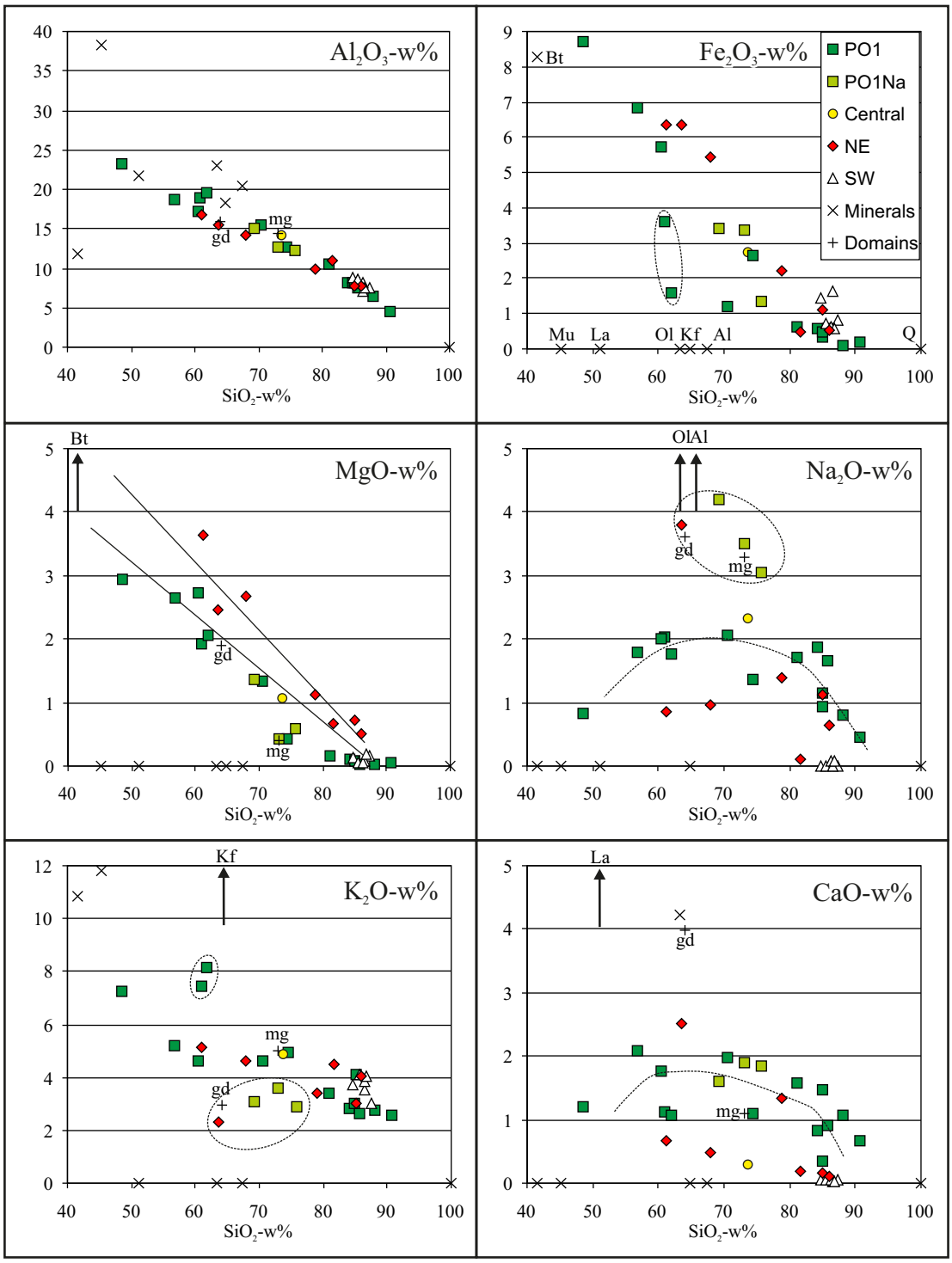

Fig. 17. Composition of the Satakunta formation according to the main geochemical components. The composition of rock-forming minerals (Barthelmy 1997) and average composition in two provenance components (Rasilainen et al. 2008) are indicated. Q = quartz, Kf = potassium feldspar, Al = albite, Ol = oligoclase, La = laumontite, Mu = muscovite, Bt = biotite, mg = microcline granite (map unit 14 in Rasilainen et al. 2008), gd = granodiorite (map unit 15SB).

Table 4. Molecular portions of Fe^{3+} and Fe^{2+} in four samples from core M52-PO-60-001. s = sandstone, ms = mudstone, m = mass, M = molar mass.
*)$n(Fe^{2+}+Fe^{3+})=2n(Fe_2O_3)=2(m(Fe_2O_3)/M(Fe_2O_3))$
**)$n(Fe^{2+})=m(FeO)/M(FeO)$
***)$n(Fe^{3+})= n(Fe^{2+}+Fe^{3+})-n(Fe^{2+})$

Depth (m)	Type	$m(Fe_2O_3)$	*)$n(Fe^{2+}+Fe^{3+})$	m(FeO)	**)$n(Fe^{2+})$	***)$n(Fe^{3+})$	$n(Fe^{3+})/n(Fe^{2+})$
65	red ss	3.62	0.045	0.20	0.003	0.043	15.3
65	grey ss	1.59	0.020	0.20	0.003	0.017	6.2
476	red ms	8.70	0.109	0.39	0.005	0.104	19.1
176	grey ms	6.81	0.085	3.37	0.047	0.038	0.8

5.2.2 Trends with depth in M52-PO-60-001

Based on the main geochemical components, core M52-PO-60-001 can be divided into three parts (Fig. 18). High SiO_2 is typical of the upper and lower parts, whereas the middle part is more complex. In the lower part, the concentrations of oxides other than SiO_2 are low. Potassium does not follow a clear trend in the core. Concentrations of Al, Fe and Mg are the highest in the middle part of the drill core. Sodium and calcium follow a similar trend to these, and the former shows a positive correlation with plagioclase, and the latter with the amount of laumontite.

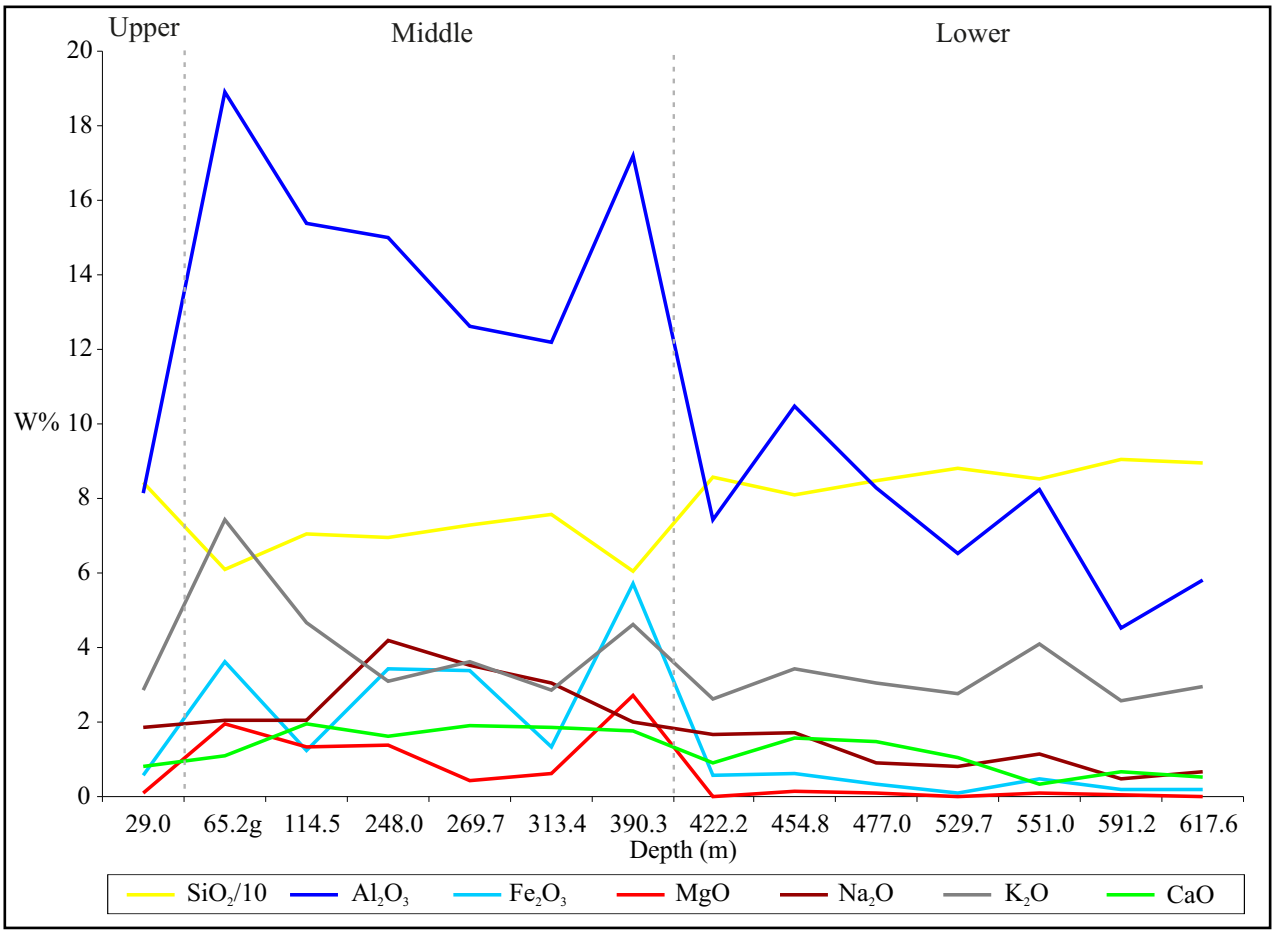

Fig. 18. Weight% of oxides in core M52-PO-60-001 as a function of depth. Dashed lines indicate the tripartite division of the drill core. g = grey.

5.3 Source component indications

The Th/Sc ratio indicates that the overall provenance is felsic in nature (Fig. 19A). Th/Sc is above the value of the granodioritic provenance component (Rasilainen et al. 2008) in all samples.

The Chemical Index of Alteration (CIA) depicts the amount of alteration in feldspars and is calculated by the formula CIA = $100(Al_2O_3/(Al_2O_3+CaO^*+Na_2O+K_2O)$ (Nebitt & Young 1982). In this equation, the oxides are expressed in moles and CaO* represents CaO in silicate minerals. Al, Ca, Na and K in detrital minerals other than feldspars and those elements in authigenetic minerals are a source of error in the CIA.

The CIA follows the lowermost upward trend with decreasing SiO_2 in core M52-PO-60-001, and the trend of the northeastern margin sequence is somewhat higher (Fig. 19C). The four anomalous samples show a CIA close to the provenance components, suggesting very little alteration. The southwestern margin of the formation is the most weathered, and fine-grained sediments from the same source would consequently plot outside the diagram.

K/Ba in the southwestern margin of the formation complies with provenance dominated by 1.84–1.82 Ga microcline granites, whereas the provenance of the northeastern margin is increasingly dominated by 1.89–1.87 Ga granodiorites in central Finland (Fig. 19B). As K/Ba can also be increased by weathering, the low K/Ba in the north-

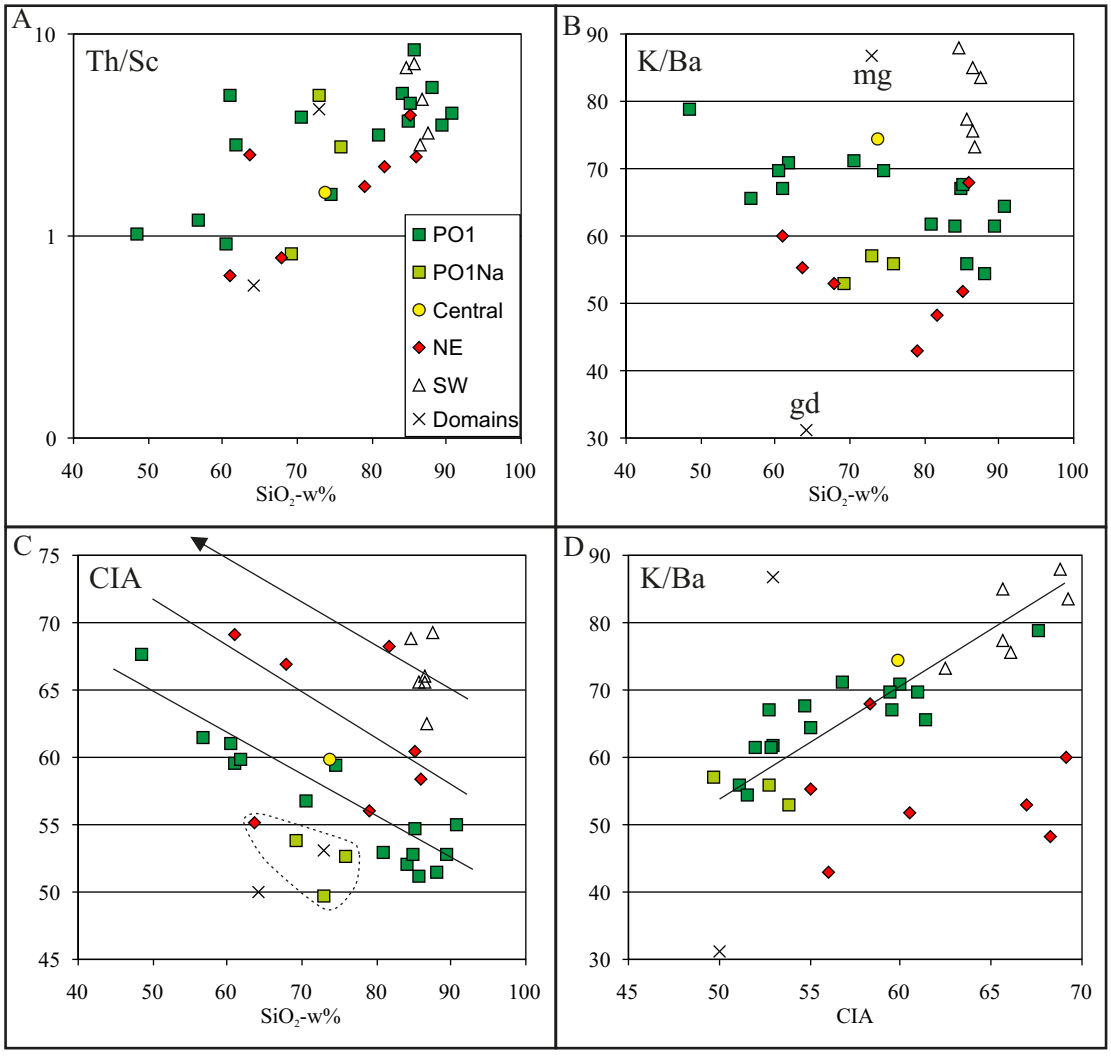

Fig. 19. **(A)** The source of the Satakunta formation is felsic throughout with a high Th/Sc ratio. **(B)** K/Ba typical of microcline granites dominates the southwestern margin sequence and that of granodiorites of central Finland dominates the northeastern margin sequence. **(C, D)** The source of the southwestern margin sequence is the most weathered. Average compositions of the two provenance components (Rasilainen et al. 2008) are indicated. mg = microcline granite (map unit 14), gd = granodiorite (map unit 15SB).

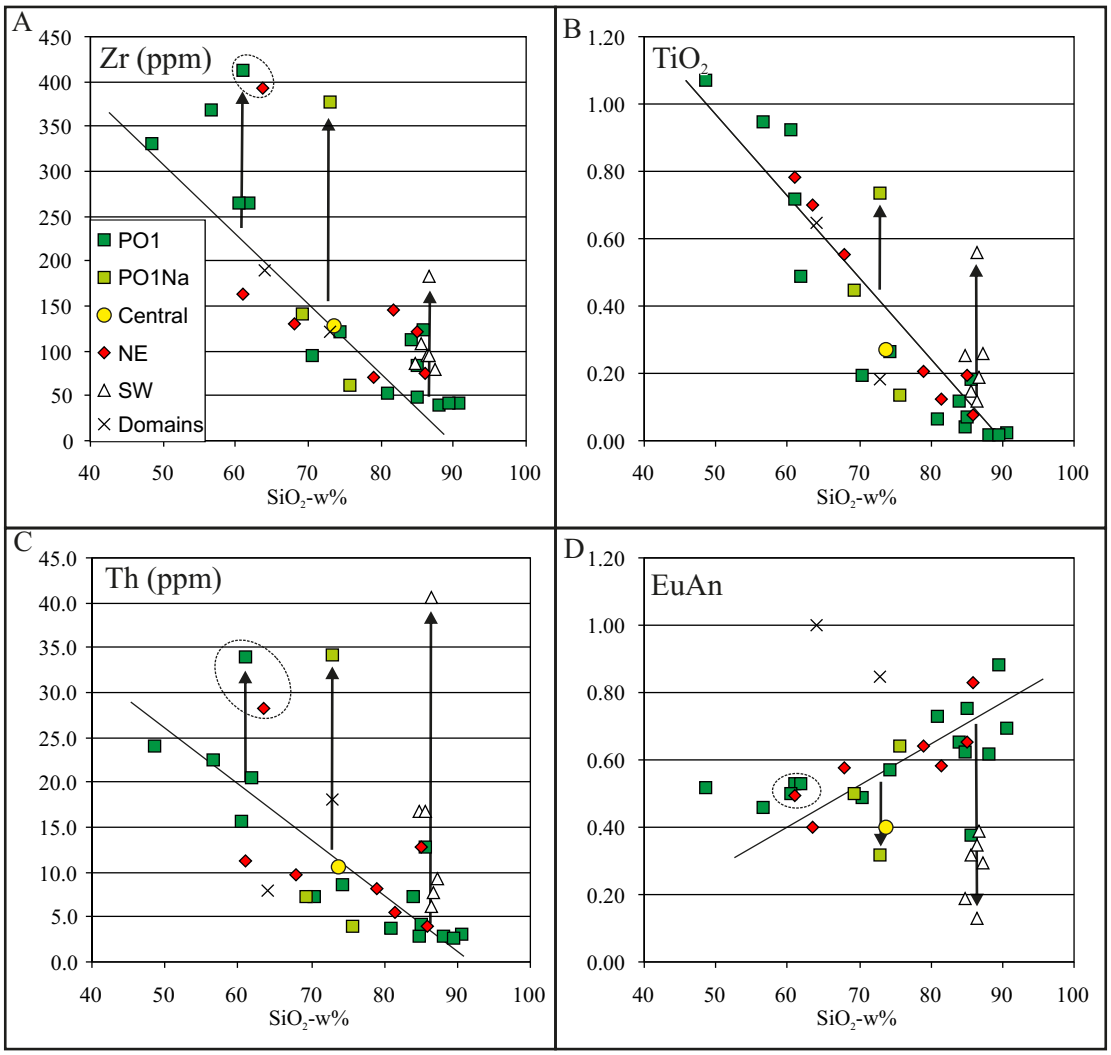

Fig. 20. Heavy mineral enrichment is most obvious at the southwestern margin of the Satakunta formation.

eastern margin sequence might distinguish it as being less weathered than the southwestern margin sequence, and four samples from the northeastern margin sequence in fact show a lower CIA than the southwestern margin sequence (Fig. 19D).

Samples from the southwestern margin sequence systematically show heavy mineral enrichment evident in concentrations of Zr, Ti (rutile, titanite) and Th (monazite, allanite). Of these samples, 1141-89-3-35 is the most anomalous in all diagrams in Fig. 20. Sample M52-PO-60-001-269 is also anomalous in all these diagrams, and its MLA analysis indicates elevated titanite and allanite. Samples M52-PO-60-001-65red and 1143-85-1-13 (both circled) are anomalous in Zr and Th, but the Eu anomaly is not below the trend in Fig. 20D, contrary to what could be expected, as the Eu anomaly below the trend is mainly caused by the deep negative Eu anomaly in monazite. Plagioclase may not have a significant role in elevating the Eu anomaly of these two samples, because the Eu anomaly is not above the trend in the samples richest in plagioclase of all the samples.

5.4 Summary

Chemical compositions verify the maturity (high SiO_2 and CIA) and recycled nature (heavy mineral enrichment) of the samples from the SW margin of the Satakunta formation. All the major elements, perhaps excluding SiO_2, show considerable mobility after deposition, and the results are not therefore useful for detailed speculations on provenance. However, all the features indicate a

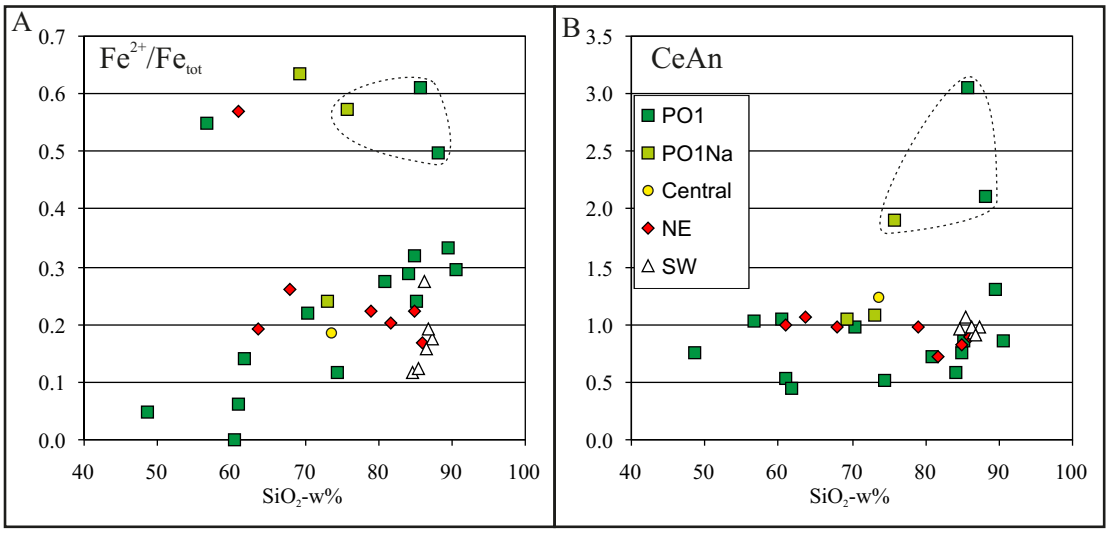

Fig. 21. Basin stage evolution is apparent as a cerium anomaly in the three samples from core M52-PO-60-001. The cerium anomaly is associated with high Fe^{2+}/Fe_{tot}, but the latter can also be a result of abundant detrital biotite.

predominantly felsic source area. Elevated Mg and Fe in the northeastern margin sequence might suggest the presence of a mafic component, but this can also be explained by detrital biotite derived from mica schists.

The red colouring may be the result of a complex, multistage redox process in the course of diagenesis and very low-grade metamorphism. Oxidizing conditions probably already prevailed during deposition, but most of the present hematite pigment formed later in epigenetic processes. At the basin burial stage, the diagenetic processes go fully in action with the circulation of fluids. This is also recorded by other elements sensitive to oxidation/reduction in core M52-PO-60-001 – including the mobilization of REEs, which is apparent in the cerium anomaly (samples framed by the dashed line in Fig. 21B) associated with high Fe^{2+}/Fe_{tot}.

6 DETRITAL HEAVY MINERALS: A REVIEW AND NEW RESULTS

Laitakari (1932) was the first to study heavy minerals in the Satakunta formation. He reported magnetite, ilmenite, garnet, monazite, zircon and topaz, but no apatite, in samples from Yläne. As topaz is quite common in some variants of the Laitila rapakivi granite, he considered the observation to imply a rapakivi source. Simonen and Kouvo (1955) were the first to conclude that Svecofennian rocks are the main source of the Satakunta formation. Detrital garnet and sillimanite from Harjavalta are evidence of a metamorphic Svecofennian source. Simonen and Kouvo (1955) observed no topaz in the sandstone, but apatite was common. Marttila (1969) finally concluded that the topaz reported by Laitakari (1932) was, in fact, apatite.

The most comprehensive study on heavy minerals in the Satakunta formation has been carried out by Marttila (1969). He identified the heavy minerals by the immersion method, the X-ray powder method and in thin sections. He concluded that nothing favours a rapakivi source, however it cannot be excluded. He also presented extensive data on length and width measurements of detrital zircons in the sandstone and noted that most of them have not been derived from any variant of rapakivi granites.

Results from Marttila's (1969) heavy mineral studies and proposed source rocks are summarized in Table 5. The most significant observations in the data are that garnet (the Svecofennian component) is present in all his samples and topaz (the rapakivi component) is absent. Marttila (1969) proposed that the detrital garnets might originate from garnet-cordierite gneiss, which also contains sillimanite, or from microcline granite and schists. Hornblende and diopside may come from diopside gneisses and amphibolites in southwestern Finland. Tourmaline is accessory in mica schist, phyllite and granite, and is common in pegmatites in southwestern Finland. Li-tourmaline comes

Table 5. Summary of the previous detrital heavy mineral studies on the Satakunta formation. Potential source rocks for each mineral are indicated in the lower part of the table. Numbers indicate verbal descriptions of abundance. XX = abundant, X = not rare, x = rare (applicable for Marttila (1969) only). A – Laitakari (1932), B – Simonen and Kouvo (1955), C – Marttila (1969), D – Ilmari Haapala, personal communication with Marttila.

		Magnetite	Hematite	Ilmenite	Garnet	Biotite	Chlorite	Epidote	Hornblende	Actinolite	Diopside	Muscovite	Tourmaline	Li-tourmaline	Titanite	Apatite	Monazite	Xenotime	Limonite	Anatase	Brookite	Rutile	Sillimanite	Pyrite	Galena	Sphalerite	Chalcopyrite	Zircon	Thomsenolite	Topaz	Fluorite	Fayalite
A	Yläne (red)	x		x	x																							x		x		
A	Yläne (light)	x		x	x												x											x		x		
B	Harjavalta	x			x	x	x	x					x		x	x							x									
B	Leistilänjärvi	x				x			x				x		x	x												x				
C	Murronmäki	2	X	x	XX	XX		XX		1		XX	10		x	XX	x					XX		X				X				
C	Kiperjärvi	2			XX	X	X		x		x		10			XX	x		X					X			X					
C	Kiukainen	100	X	x	XX	X	X	X	x		x		10		x		x	1				XX			2				X				
C	Panelia	2			X	X	X		x				10			XX																
C	Leistilänjärvi		X		X	X		x				XX	10	15		XX																
C	Harjavalta	100	XX		XX	XX	X	X				XX			x	XX					2	x	XX	X								
C	Naskalinkallio	2	X		X	X	X	x			x		10		x			x	1					XX	X								
C	Sassilanjuopa		X		X	X	X	x			x	X	10					XX		X		x		XX	X			X	X				
C	Ulvila	2	X		X	X		x				X	10				XX	x		X				XX	X				X				
C	Alteration products																																
C	Autigenic																																
C	Sulphide deposit																																
C	Contact m.morph.																																
C	Low grade m.morph.																																
C	High grade m.morph.																																
C	Pegmatites																																
C	Mafic magmatic																																
C	Felsic magmatic																																
C	Laitila rapakivi																																
A	Vehmaa rapakivi																																
D	Tarkki rapakivi																																
D	Väkkärä rapakivi																																
D	Eurajoki dyke																																

Table 6. Definitions of the heavy mineral fractions analysed by MLA.

CAR	Includes grains excluded from the ground samples by CARPCO magnetic separator. Prior to this, only Leistilänjärvi sample had undergone shaking table.
2.7–3.3	Includes minerals with specific gravity 2.7–3.3 (other than those excluded by CARPCO) This fraction was not separated in the Leistilänjärvi sample.
3.3M	Includes the most magnetic fraction with specific gravity >3.3
3.3–4.0	Includes the least magnetic fraction with specific gravity between 3.3 and 4.0

from pegmatites, sphalerite and chalcopyrite from sulphide deposits. Magnetite, ilmenite, biotite, muscovite, titanite, apatite, monazite and zircon are common in the Svecofennian basement as well as in rapakivi granite variants.

In the present study, detrital heavy minerals were identified by MLA from particular heavy mineral fractions (Table 6) from the two samples prepared for detrital zircon age determination. These samples come from the Leistilänjärvi outcrop and from the depth 614.0–615.2 m of core M52-PO-60-001. The results were recalculated to exclude quartz, feldspars and laumontite, as the separation into classes by specific gravity was not complete.

Magnetite, zircon and apatite, as well as almandine, are more common in the outcrop sample than in the drill core sample. The opposite prevails for titanite, epidote, muscovite, and also grossular and biotite (Fig. 22, Table 7). In the fractions CAR, magnetite constitutes most of the grains in the outcrop sample, whereas muscovite, epidote and biotite are the most common minerals in the drill core sample. In the fractions 3.3M, magnetite, epidote and almandine prevail in the outcrop sample, and epidote and grossular in the drill core sample. In fractions 3.3–4, zircon and apatite are prominent in the outcrop sample, and titanite and zircon in the drill-core sample. The absence of topaz in both samples is to be noted.

The presence of allanite, bastnasite and chromite should be double-checked by microanalysis. Due to the small amounts and/or need for additional identification, Fig. 22 excludes hornblende, tritomite, xenotime and calcite from the drill core sample and hornblende, clinopyroxene, huttonite and cerphosphorhuttonite from the Leistilänjärvi sample.

Barite in the drill core sample is a new mineral identified in the Satakunta formation. This was also confirmed by SEM at the University of Oslo. Barite is most typically found as concretionary masses and veins in shale, limestone and sandstone (Nesse 2000).

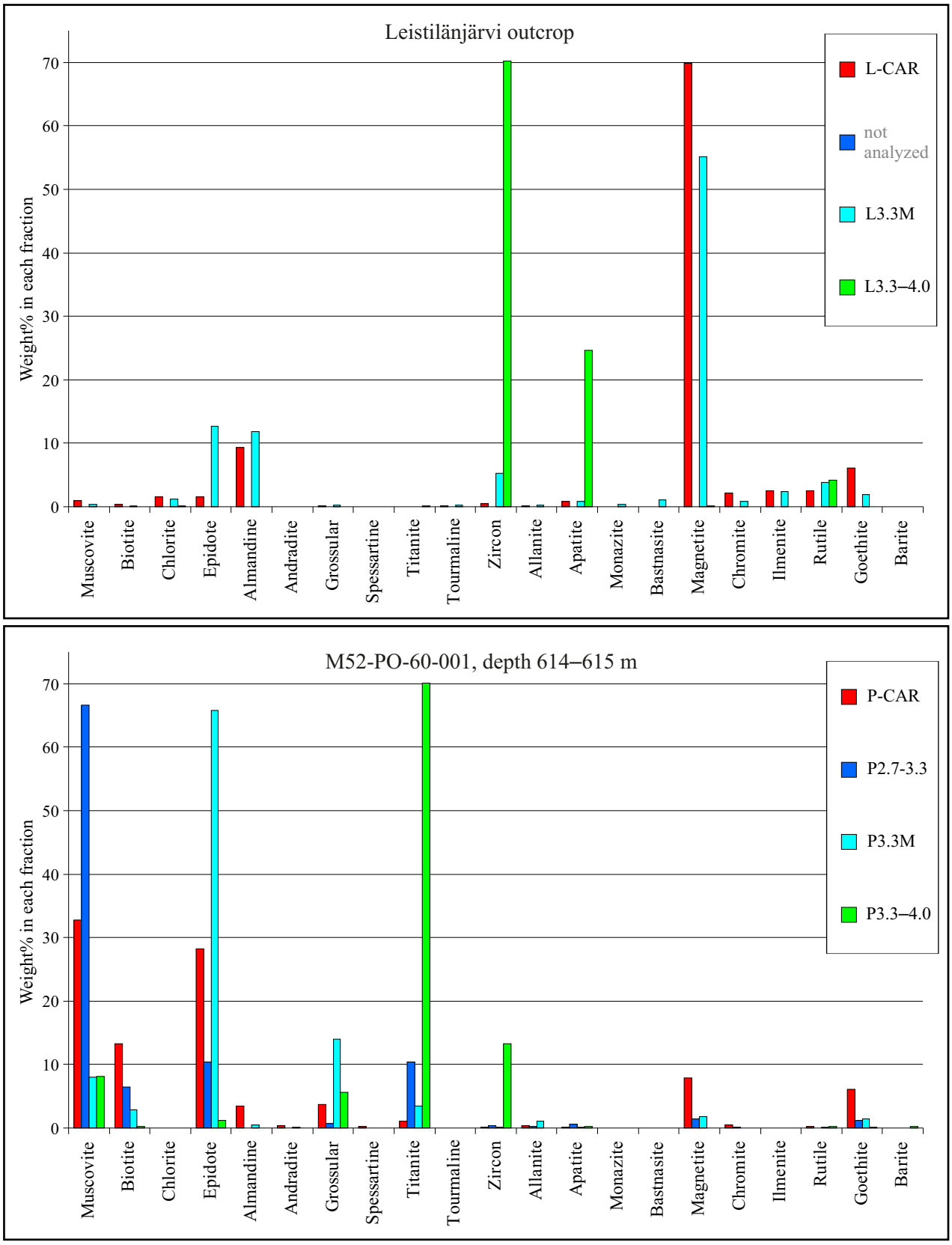

Fig. 22. Heavy minerals from different fractions of two samples analysed by MLA.

Table 7. Results from heavy mineral analysis by MLA.

Mineral	615m P-CAR wt(%)	615m P2.7–3.3 wt(%)	615m P3.3M wt(%)	615m P3.3–4 wt(%)	LEIS L-CAR wt(%)	LEIS L3.3M wt(%)	LEIS L3.3–4 wt(%)
Muscovite	32.83	66.65	8.01	8.17	1.00	0.32	0.03
Biotite	13.24	6.41	2.85	0.19	0.40	0.06	0.01
Chlorite		0.03	0.00		1.59	1.17	0.15
Hornblende	0.09		0.04		0.03	0.07	
Clinoyroxenes						0.02	0.01
Epidote	28.28	10.46	65.75	1.22	1.51	12.67	0.02
Almandine	3.50	0.05	0.52		9.33	11.86	0.01
Andradite	0.40		0.13				
Grossular	3.73	0.67	13.98	5.58	0.06	0.27	0.02
Spessartine	0.23				0.02	0.03	
Titanite	1.08	10.36	3.41	70.10		0.02	0.14
Tourmaline	0.04	0.04			0.10	0.24	0.03
Zircon	0.08	0.38	0.12	13.30	0.51	5.30	70.21
Allanite	0.38	0.19	1.12	0.04	0.06	0.19	
Tritomite			0.11	0.04			
Apatite	0.16	0.63	0.06	0.29	0.79	0.85	24.58
Monazite					0.01	0.37	0.04
Bastnasite					0.02	1.13	0.04
Xenotime				0.04			
Calcite		0.06		0.05			
Magnetite	7.89	1.45	1.76	0.05	69.89	55.09	0.17
Chromite	0.44	0.10	0.06	0.04	2.12	0.79	0.04
Ilmenite	0.04				2.54	2.39	
Rutile	0.20	0.05	0.08	0.19	2.52	3.83	4.14
Goethite	6.13	1.25	1.43	0.12	6.05	1.94	0.05
Barite		0.05		0.24			
Huttonite		0.08				0.29	0.01
Cerphosphorhuttonit						0.45	0.11
Unclassified	1.26	1.07	0.56	0.35	1.43	0.64	0.19
Total	100.00	100.00	100.00	100.00	100.00	100.00	100.00

7 NEW AGE RESULTS FROM DETRITAL ZIRCONS

Vaasjoki and Sakko (1987) analyzed four zircon and two monazite fractions for U-Pb isotopes from Kiperjärvenoja close to the Laitila rapakivi granite batholith (Fig. 3). The age of two nearly concordant monazite fractions is 1821 ± 10 Ma. The $^{207}Pb/^{206}Pb$ ages of the four discordant zircon fractions are between 1903 and 1817 Ma. Hence, the bulk of the detrital zircons cannot be derived from the Laitila rapakivi; however, the presence of an infrequent age population would remain undiscovered. Based on Wasserburg model ages, the [main] source of three of the zircon fractions could be syntectonic Svecofennian granitoids and the [main] source of one fraction could be trondhjemites at Kalanti (Vaasjoki & Sakko 1987).

In the present study, detrital zircon ages were determined in two samples at the centre of the basin, one from the deepest and one from the highest

accessible stratigraphic level. The former sample was taken from 615.2–614.0 mbgl from core M52-PO-60-001. The mass of the arkosic sample (grain size from medium to coarse sand), from which zircons were extracted, was 1.1 kg, as only one half of the core with a diameter of 31 mm was used. The latter sample was obtained from an outcrop at Leistilänjärvi (Fig. 3). Diabase occurs close to the sampling site, at a distance of several tens of metres. The mass of the pink-coloured arkosic sample with well-sorted detritus (grain size: fine sand) was about 10 kg. Even though the drill core sample was rather small, different zircon age groups were still well represented in it, as the deposition of the 120-cm-long sequence probably also took a longer time.

The pre-processing of the samples at the Geological Survey of Finland included crushing, separation with a shaking table (only for the outcrop sample) and CARPCO magnetic separation. The concentrates were handled with a heavy liquid (specific gravity 3.3), Franz magnetic separation and another heavy liquid separation (specific gravity 4.05). In preparing the mounts, random sampling, in which all grains had an equal probability of being chosen, was used to determine the overall age distribution of zircons. They were scattered on a sample plate in equal portions and an equal number of grains was chosen from each portion. The sample glass plate was randomly moved under a microscope and the grain closest to the cross-hair was chosen each time. Non-random sampling was used in search of minor age populations. This was carried out after random sampling by choosing grains with some distinguishing feature in appearance, usually exceptionally well preserved crystal surfaces, because these were regarded as relevant candidates for rapakivi zircons.

Age determinations were carried out at the LA-MC-ICP/MS laboratory of the Department of Geosciences, University of Oslo, in January–February 2008. The majority of the mounted grains were unsuitable for age determination due to being metamictic or cracked and were not analysed. In addition, grains with $^{206}Pb/^{204}Pb < 2000$ and non-Archaean grains with a central discordance over 10.0% were discarded. This, unfortunately, also greatly reduced the randomness of the randomly selected grains. Only 29% and 22% of the mounted randomly selected grains from the outcrop and the drill core sample, respectively, were incorporated in the final results (Table 8).

Simultaneous multinomial confidence limits were calculated for each 100 My bin according to the approach of Goodman (1965) by using a Microsoft Excel adaptation of a computer program originally written by May and Johnson (2005). For this, the random and non-random fractions were combined, because increasing the number of grains represented by each bin was thought to be preferable to using only randomly selected grains (the latter might not represent the age distribution in the samples, because of the reduction in randomness described above). Multinomial confidence limits enclose the true but always unknown abundance pattern with a certain degree of probability. They are also an alternative definition for the detection limit for empty bins and show the maximum size of a single age population that may have remained undetected with a certain probability after n analysis. The 95% detection limits are 0.13 in the drill core sample and 0.10 in the outcrop sample.

All detrital zircon ages comply with an exclusively Svecofennian provenance. No rapakivi zircons were detected, and the two Archaean zircons among the non-randomly selected grains have most likely been derived from Svecofennian metasedimentary rocks or are inherited cores of zircons from Svecofennian magmatic rocks. The scarcity of >1.96 Ga ages imply that Svecofennian magmatic rocks dominate over Svecofennian meta-

Table 8. Number of mounted grains and those incorporated in the final results.

	Mounted (n)	Final results (n)	Final results (%)	95% detection limit
Leistilänjärvi	**258**	**79**	**31**	**0.10**
random	168	48	**29**	
non-random	90	31	**34**	
M52-PO-60-001	**319**	**59**	**18**	**0.13**
random	207	46	**22**	
non-random	112	13	**12**	

sedimentary rocks, especially in the younger sample. Metasedimentary rocks may be a more important, yet a minor component in the older sample.

In both samples, randomly selected grains peak at 1.88 Ga (solid black curve in Fig. 23) and 1.83–1.81 Ga late orogenic granites are another important age group. In the outcrop sample, the late orogenic granites form a bulge in the age distribution pattern of the randomly selected zircons, and the highest peak in the pattern of the non-randomly selected zircons. In addition, randomly selected zircons from Leistilänjärvi show four ages >2.0 Ga, and non-randomly selected zircons from the drill core sample bulge at 1.92 Ga. The probability

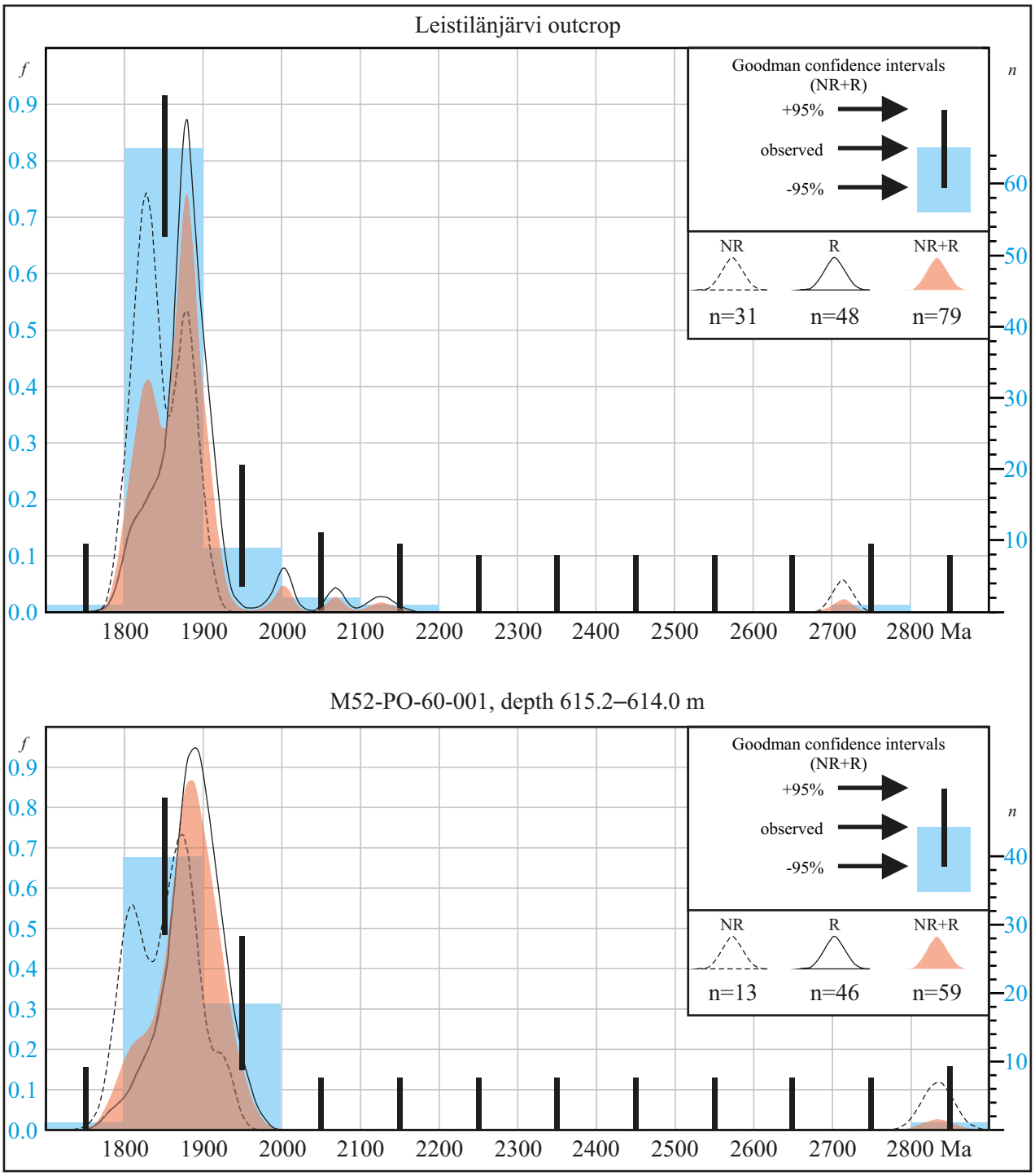

Fig. 23. Probability density plots (curves) and histograms (blue columns) showing the age distribution of detrital zircons. Both samples show maxima at 1.88 Ga and smaller maxima at 1.83 or 1.81 Ga. Black bars enclose the true frequencies of each bin with 95% probability. There is a 95% probability that no empty bin should contain a histogram column showing frequencies higher than 0.10 in the outcrop sample and 0.13 in the drill core sample, respectively. The scales on the left and right apply to the histogram only. NR = non-random. R = random.

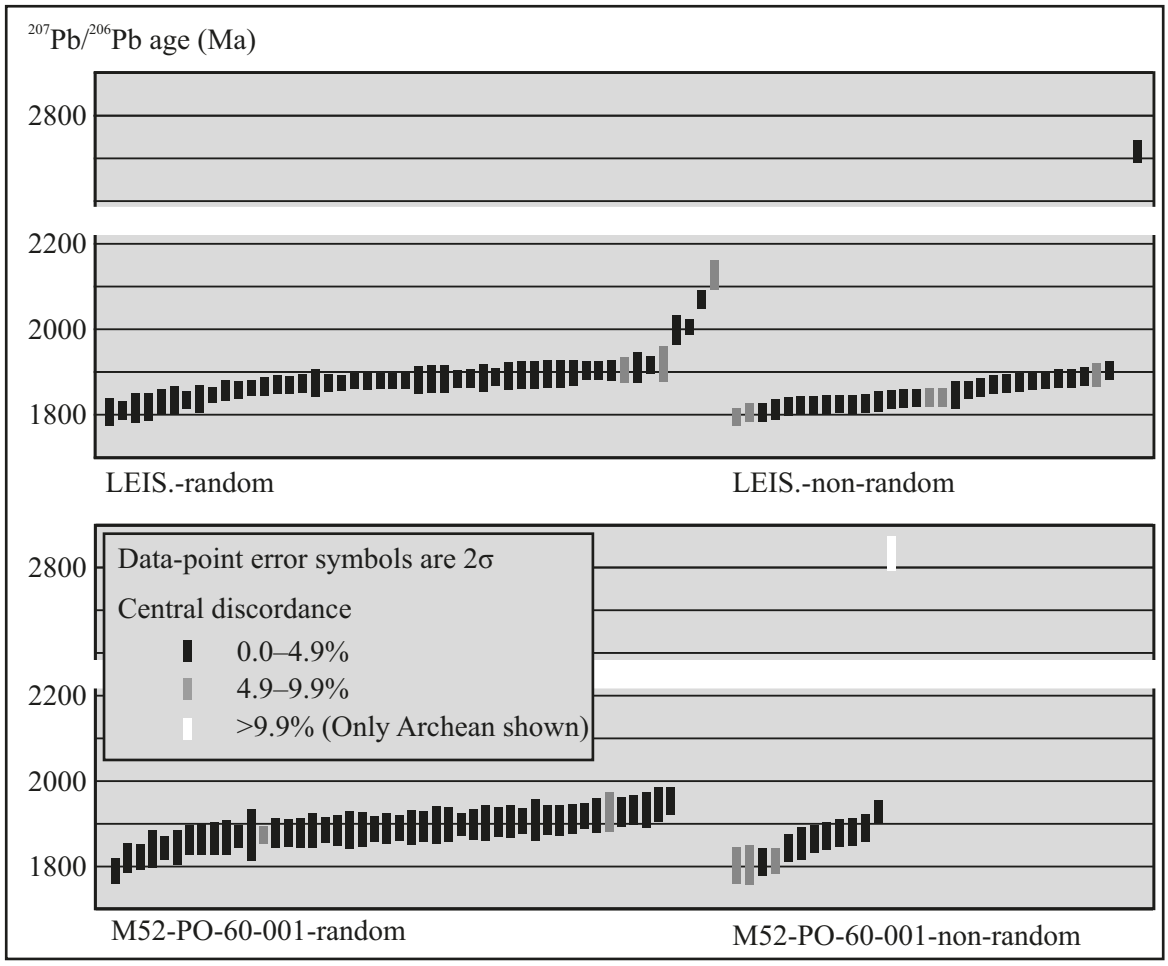

Fig. 24. $^{207}Pb/^{206}Pb$ ages of the randomly and non-randomly selected detrital zircons in the samples. 2σ error margins and classification according to central discordance have been indicated.

density diagrams of the two samples should not be directly compared because of the small and different numbers of grains analysed, and because of the systematic differences in error marginals, which are apparent in Fig. 24.

Isotopic data from the age determinations are presented in App. 5 and selected BSE images in App. 6.

8 DISCUSSION

The current dimensions of the Satakunta formation are rather well depicted. The main mineral composition, primary structures and other depositional features on outcrops have also been studied in some detail by previous authors. Here, the discussion focuses on open questions such as (1) the subdivision of the formation, (2) the timing, provenance and extent of the original basin and (3) possible tectonic relationships with the anorogenic rapakivi magmatism.

8.1 Subdivision of the Satakunta formation

One of our objectives was to consider the basis for further subdivision of the Satakunta formation. Features such as compositional maturity, differences compared to typical rift-fill arkoses, possibly

indicating stable cratonic conditions, and the presence of pre-rift strata were scrutinized. Detailed stratigraphic modelling of the sandstone turned out to be a challenging task. Compared to the extent and thickness of the formation, both deep drillings and outcrops are few. The flat topography combined with almost horizontal strata offer limited opportunities for stratigraphic type sections. The lithological observations were arranged as three main lithological assemblages (cf. Fig. 26): (1) short drill cores at the SW margin of the basin, (2) the 'type section' drill core M52-PO-60-001 with nearly 600 metres of sandstone, and (3) the Lammaistenkoski section at the NE margin of the basin in Harjavalta. All the assemblages are quite dissimilar and we were ultimately unable to correlate the observed lithofacies associations from the type section core with other drill cores and outcrop sections.

Core M52-PO-60-001, the 591-m-thick type section of the Satakunta formation, shows that the most voluminous component of the formation is medium-grained arkosic arenite in composition. The overall lithological diversity and the overall grain-size variation in core M52-PO-60-001 is strikingly low. No deepwater fine sediments or typical shallow marine shelf-type assemblages or voluminous interbeds of mudstone are present. Rifting, tectonic subsidence and relative uplift of the rift shoulders normally cause upwards-coarsening progradational sedimentary cyclicity, and result in increased immature detritus being deposited in the basin. A gradual upwards change to a more immature composition in the core at c. 400 m could be explained by the onset of a new rifting stage, but the grain size was found to be fining rather than coarsening upwards. No clear unconformities or major erosional features were observed. Nevertheless, parallel minor unconformities of the sequence are easily overlooked in a thin drill core.

Abundant cross-bedding, common thin mudstone interbeds and 'mud chips' (intraformational rip-up clasts) in core M52-PO-60-001 are consistent with the poorly channelled fluvial or partly coastal depositional environment suggested by Kohonen et al. (1993). Considering the 'type section' core (M52-PO-60-001) as a whole, it is quite clear that the observed features are more typical of a poorly channelled fluvial plain than a rapidly subsiding narrow rift basin. In fact, no features, such as prograding fans with upward-coarsening cyclicity, internal erosional features or volcanic and lake deposit interbeds, expected for a typical rift fill sequence, are present in this 591-m-thick type section.

A notable feature of the Satakunta formation is that neither the outcrops nor the drill cores from the SW margin sequence resemble the rather monotonous sandstone lithofacies assemblage of the 'type section' core (M52-PO-60-001). The outcrops of the Satakunta formation are characterized by coarse-grained conglomeratic rocks near the margins of the formation, especially in the NE (Harjavalta), whereas medium- to coarse-grained sandstones are typical of the central area outcrops. The short drill cores at the SW margin of the formation consist of subarkoses and associated conglomeratic subarkoses and conglomerates.

The conglomerates at the SW margin are enriched in quartz and show a more weathered source compared to the arkosic arenites of the 'type section' core (M52-PO-60-001). The assemblage is clearly a potential candidate for pre-rift deposits preceding the main rifting stage. The coarse clastics show some upwards-fining cyclicity, plausibly reflecting the autocyclic fluvial process (transition from main channel facies to transverse bar sand dune facies). In addition, both the few palaeocurrent observations (Kohonen et al. 1993) and the spatial grain-size distribution may indicate detritus transportation perpendicular to the margins of the present basin structure. This pattern would not support the origin as a downfaulted pre-rift sequence. Our conclusion is that the maturity of the conglomerates in the SW may be best explained by previous (pre-rift) craton cover quartz arenites or chemically weathered palaeosols as a significant source component.

There is no direct evidence of superposition of the 591 m 'type section' and the other observed assemblages ([1] quartz-rich conglomerates in SW and [2] outcrops + Harjavalta). The most potential places to meet the stratigraphically lowermost parts of the Satakunta formation are the deepest portion of the drill core reaching 620 m below the ground surface (M52-PO-60-001) and the three drill cores reaching the Svecofennian basement at the southwestern margin of the formation. Reliable bedding plane observations are scarce, but a five-degree northeasterly dip is generally prevailing. Taking this as a starting point and by assuming that the basement–sandstone contact at the southwestern margin of the basin marks the tilted base of the original depository, the quartz-rich,

coarse clastics at the southwestern margin could represent the lowermost and oldest observed units of the formation. Similar deposits could be expected below the section represented by drill core M52-PO-60-001.

The Harjavalta lithofacies assemblages and primary features can be found in Kohonen et al. (1993). The section, with immature conglomeratic arkoses and characteristic mudstone interbeds, is very different from the 'type section'. The Harjavalta lithofacies assemblage most plausibly represents the uppermost part of the present Satakunta formation, and it has been interpreted as a prograding, upwards-coarsening rift-fill system with proximal parts of the depositional system in the SE (cf. Kohonen et al. 1993).

A basin-wide stratigraphy cannot be determined for the Satakunta formation. As a summary, it can be stated that all the observed sedimentological features are compatible with an overall fluvial depositional scheme and that the observed variations do not allow sophisticated depositional reconstructions or detailed basin modelling.

8.2 Provenance

The major focus of our study was the provenance and especially the possible presence of a rapakivi component in the detritus. According to the geological map, the other obvious source rocks candidates include various Svecofennian metamorphic and igneous rocks, mafic volcanics associated with the rapakivi-age mafic Häme dyke swarm and previous sedimentary cover.

The detrital zircon age data imply an exclusively Svecofennian provenance for the Satakunta formation. The dominance of the Svecofennian component is expected, because the formation is framed by the Svecofennian basement along most of its perimeter. Based on the number of analysed zircons, there is statistically a 95% probability that the frequencies of rapakivi zircons in the drill core and outcrop samples are not higher than 0.13 and 0.10, respectively. These detection limits remained unsatisfactorily high because the number of grains analysed was not statistically adequate due to the large number of zircons that were unsuitable for age determination.

The dated samples do not represent all basin-wide units and it is not therefore possible to definitely conclude that the Satakunta formation contains no detritus from rapakivi granites. The detrital zircon age data could be complemented by analysing new samples from different depths in core M52-PO-60-001 and from outcrops preferably from the NE margin, representing – according to our understanding – the latest stage of deposition in the formation.

The coverage of the heavy mineral data is better than the dated detrital zircons. Both the reviewed previous data and our results exclude rapakivi as a major source. No topaz or other minerals indicative of rapakivi granites was found in the heavy mineral fractions of the two samples analysed by MLA. Finally, we conclude that nothing in the new or reviewed information points to rapakivi provenance.

Currently, the only suggestion in favour of a rapakivi source has been presented by Äikäs (1977). The study of one arkosic arenite sample from Tahkoluoto (NW part of the formation), comparing the inclusions in detrital quartz grains with inclusions in other nearby lithological units, led him to the conclusion that some quartz grains in the sandstone are possibly derived from rapakivi granites.

The amount of previous, recycled cover in the detritus, the amount of weathering in the source area and indications of a major mafic volcanic component are the other aspects of a provenance study. The two sandstone clasts in core 1141-89-006 demonstrate the presence of previous cover in the provenance. Their possible intraclast origin cannot be ruled out, but these clasts are very well rounded and they differ in composition from typical sandstones of the formation. A sedimentary source is also implied by the very well rounded, plausibly multicycle, quartz grains at the lower part of core M52-PO-60-001 and by the well-rounded quartz pebbles in the subarkosic sandy matrix in the southwestern margin sequence.

The provenance of sand class detritus is not easy to resolve; quartz and feldspars are seldom very informative and the lithic clasts are restricted to very fine-grained and resistant rock types. In addition, fine-grained detritus resulting from chemical weathering is sorted out and transported to distal parts of the basin. The overall quartz enrichment

may indicate either a multicycle origin or weathered source, and the amount of feldspars is often affected by post-depositional changes. In summary, it appears that the overall scarcity of lithic clasts composed of sedimentary rocks, the absence of rounded second generation overgrowths and other signs of a multicycle origin of detrital quartz and the presence of altered detrital zircons – not durable in long recycling processes – suggest that previous sedimentary cover rocks generally form only a minor provenance component for the Satakunta formation.

No direct evidence of volcaniclastic detritus was recognized. However, small mafic fragments are unstable in diagenetic processes and are seldom preserved at sand size. The presence of laumontite could potentially indicate the presence of a source with volcanic rocks (Merino et al. 1997), and mafic volcanic rocks corresponding to the Häme dyke swarm could potentially even be a major source component. However, the generally high Th/Sc ratios indicate a predominantly felsic provenance for all the samples studied, and no mafic signature – except perhaps for some samples at the NE margin – can be observed.

Simonen and Kouvo (1955) concluded that the low Al_2O_3/Na_2O shows that chemical weathering has not been strong in the Satakunta formation. However, their samples were small in number and located in the central parts of the formation, where the detritus is, indeed, the most unweathered. In the southwestern margin sequence the weathering has reached the stage of major loss of Ca and Na, and a weathered source rich in microcline granite is proposed. At the NE margin the source is less weathered, more heterogeneous and possibly granodiorite dominated.

8.3 Basin history and tectonic model

The final part of the discussion deals with the basin history and tectonic model. First, we consider the apparent provenance paradox – the total lack of rapakivi granite detritus in the Satakunta formation directly bordered by the Laitila rapakivi batholith. Second, we discuss the evolution history of the basin.

The present erosional level directly corresponds to no setup during deposition and, theoretically at least, it is possible that the Laitila batholith was never exposed to erosion at the time of deposition (Fig. 25–1). The model invokes a major faulting after the depositional stage, and the most plausible time would be the intrusion of the cross-cutting mafic dykes at c. 1270 Ma. A more probable model with a constant relative uplift of the rift margins during basin development is outlined in Fig. 25–2. In this model, the initial basin evolution is directly related to the 'rapakivi stage' some 1600–1550 Ma ago. Both models invoke a major fault between the sandstone and the rapakivi batholith. A combination of the two models with two-stage subsidence of the current Satakunta formation might also be applicable.

The starting point for the tentative basin model is the fact that the Satakunta formation as a whole, and especially the 'type section' core (M52-PO-60-001), is hardly a typical rift-fill sequence. A typical rift axial zone is characterised by intermittent lava flows and other volcanic interbeds, and by diverse sedimentary rock types from alluvial to lake deposits. The 'type section' also does not fit well with the rift margin setting with the expected coarse clastics, upwards-coarsening cycles of a regressive system and poor sorting reflecting the subsidence and rapid burial of the detritus.

We propose a basin evolution model starting at c. 1600 Ma and ending with the intrusion of the diabase dykes some 1270 Ma ago (Fig. 26). The model is an attempt to tie the observed sedimentary features to the overall tectonic evolution manifested by the intrusive ages and to offer an alternative to a simple narrow rift fill. In the model, the mature sediments of the SW margin are considered as initial deposits during the very early stage of extension and relatively isolated normal faulting. Thin previous sedimentary cover and partly weathered basement material are transported and re-deposited. The source rapidly turns to a more granitic one due to exposure and the relative uplift of the Svecofennian basement.

The monotonous succession of the 'type section' (M52-PO-60-001) is understood to be a result of a large fluvial braidplain or coastal plain representing a tectonically inactive late stage of the large extensional basin system some 1500 Ma ago. Although the grain size in a rift system is generally expected to be upwards coarsening in the marginal

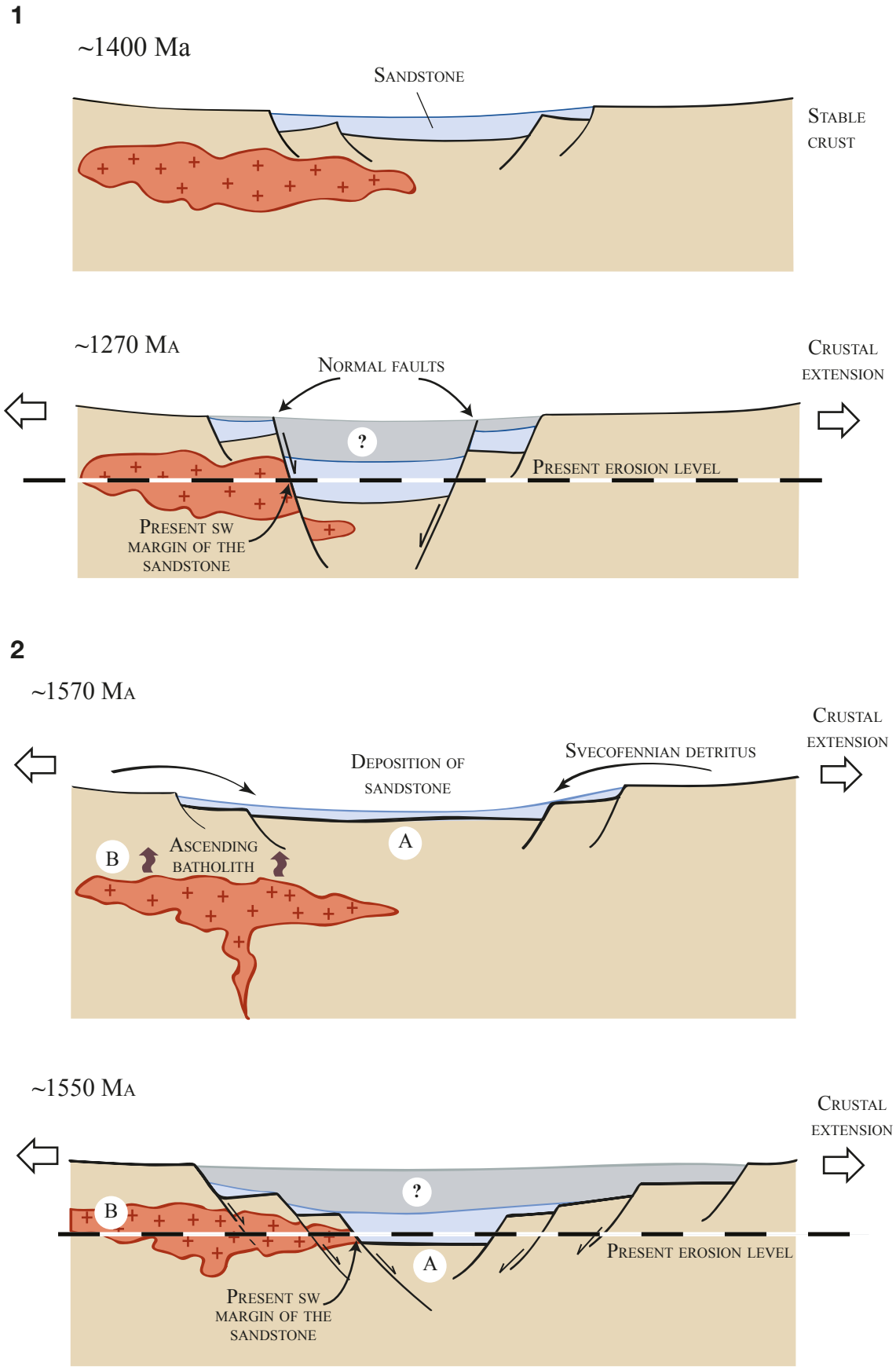

Fig. 25. Two schematic models (not to scale) explaining the current relationships at the SW margin of the Satakunta formation. (1) Simple model involving localized downfaulting during the late extension at c. 1270 Ma. (2) Model with ascending rapakivi batholith and relative subsidence of the central rift basin at c. 1550 Ma. A and B mark reference points within the Svecofennian basement.

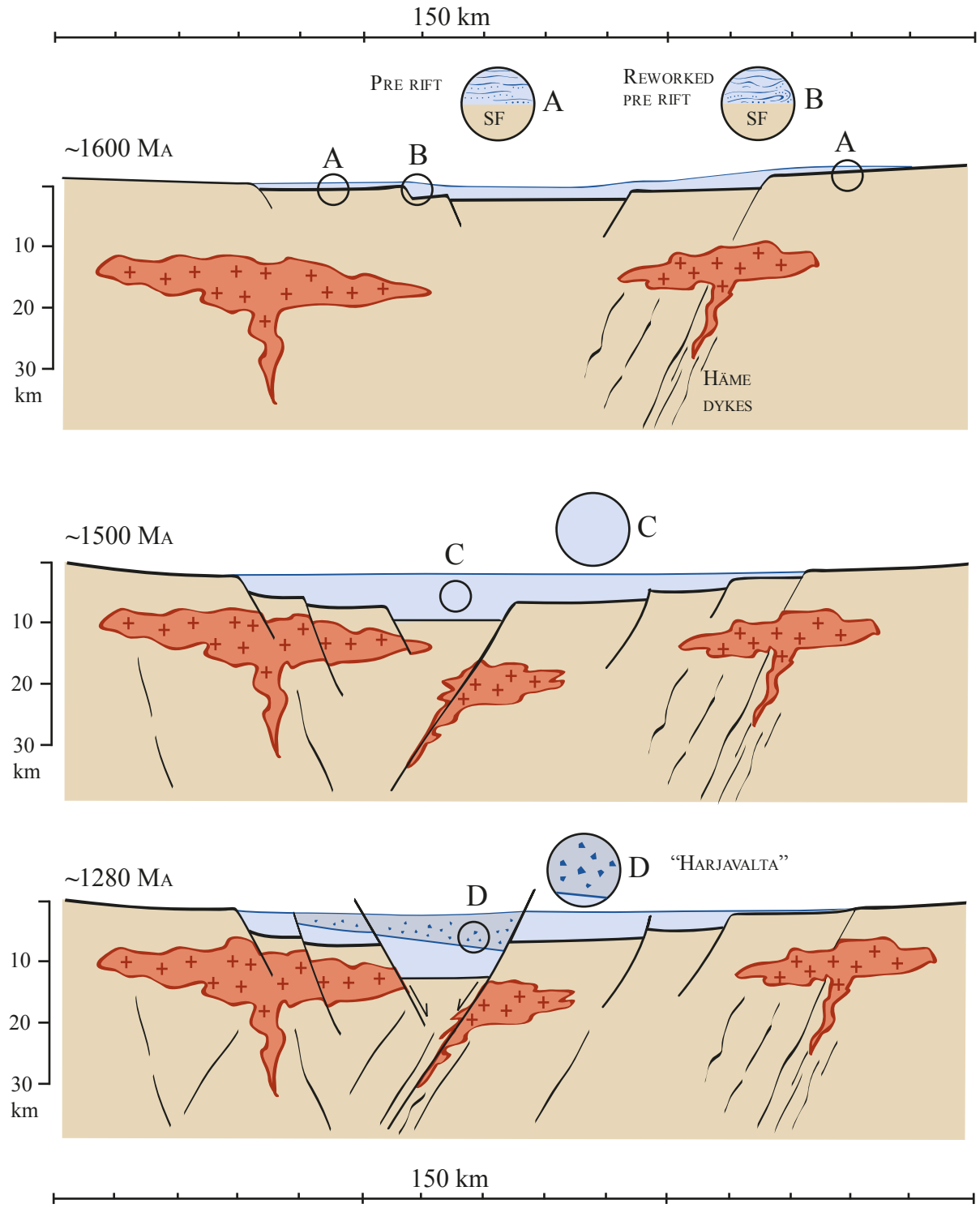

Fig. 26. A simplified evolutionary model of the Satakunta basin. Initial rifting at c. 1600 Ma is temporally and spatially connected to the zones of bimodal volcanism. The main depositional stage (c. 1500 Ma) resulted in slow subsidence of the basin. The latest depositional stage is tentatively connected to new localized rifting at c. 1280–1260 Ma. Points B, C and D refer to LA1 (SW margin of the formation), LA2 (core M52-PO-60-001) and LA3 (Harjavalta section), respectively. Point A represents the assumed pre-rift platform cover.

parts at the onset of rifting, it would be constant or upwards decreasing in non-marginal distal parts if the rate of sedimentation was lower than the rate of subsidence. In this case, the shoreline and facies would shift landwards and result in a transgressive system.

The immature, conglomeratic arkoses of the NE margin (e.g. Harjavalta section) represent the early stage of a new rifting event before the intrusion of the 1270 Ma dykes. All the features are compatible with an alluvial braidplain with heavy bedloads and rapid burial resulting in limited sorting of the sediment. This narrow rift basin may have had the SE–NW axis indicated by the unimodal NW-directed palaeocurrents in Harjavalta (Kohonen et al. 1993).

The age relationship and causal connection between the sandstone deposition and the intrusion of rapakivi granites remain unknown. For now it must be concluded that even though the preserved part of the sandstone is probably older than the exhumation of the rapakivi, the rifting, basin formation and sandstone deposition may be either older or younger than the crystallization of the Laitila rapakivi batholith.

9 SUMMARY AND CONCLUSIONS

The Satakunta formation is composed of subarkose at the southwestern margin and arkosic arenite in other parts. The sandstone is well lithified and compact with no visible pore space. Carbonate cement was locally observed and red colouring is typical for most of the sandstone. Very low-grade metamorphic laumontite and accessory barite are reported for the first time.

Three distinct lithological assemblages (LA) are characterized, but poor data coverage prevents the formal lithostratigraphic subdivision of the Satakunta formation. It is tentatively suggested that the quartz-enriched coarse clastics at the present SW margin of the formation (LA1), the homogenous sandstones in core M52-PO-60-001 (LA2; Satakunta formation type section) and the conglomeratic arkoses of the Lammaistenkoski section in Harjavalta (LA3) represent three distinct basin stages. Based on lithofacies features and composition, the assemblages are understood as reworked derivatives of remnant pre-rift sediments (LA1), as deposits of a relatively stable fluvial plain in a distal part of an extensive basin system (LA2, type section) and as proximal rift fill deposits plausibly related to the late stages of basin formation (LA3).

All the observed features and pre-existing data, including conventional zircon ages and detrital heavy mineral assemblages, indisputably indicate that the adjacent Laitila batholith or other rapakivi granites cannot have been a major source for the Satakunta formation. Our detrital zircon data with 138 analysed grains from two samples exclusively imply a Svecofennian provenance with an age peak at 1.88 Ga for the Satakunta formation. Geochemical data predominantly favour a felsic source area. The Laitila rapakivi granite batholith was plausibly exposed only after the main depositional stage.

The MLA technique is an excellent tool for petrography, quantitative analysis of the most common minerals in sandstone, and especially for the recognition of detrital heavy minerals.

The presented evolution model suggests multiphase basin development. The first basin stages are connected to progressing extension of the upper crust in relation to bimodal (rapakivi-type) magmatism and the late basin stages involve the development of a narrow rift basin following the trend of the margins of the current Satakunta formation.

ACKNOWLEDGEMENTS

This study was mainly funded by the Academy of Finland (Project 1215351; O.T. Rämö. PI). Tuula Saastamoinen (GTK) and Jukka Laukkanen (GTK) carried out the MLA analyses. Siri Simonsen (University of Oslo) was of invaluable help in performing the LA-MC-ICP/MS analysis. The support of the Geological Survey of Finland (GTK) is greatly appreciated. Laumontite was identified by Lassi

Pakkanen (GTK) by EPMA and Harri Kutvonen (GTK) is thanked for the final drawing of Figs. 25–26. Research Professor Kari Strand (Thule Institute) delivered useful comments that improved the paper.

REFERENCES

Äikäs, T. 1977. Sulkeumat Satakunnan hiekkakivimuodostuman detritaalisen kvartsin alkuperäkivilajien määrittämisessä. Unpublished master's thesis (additional subject), University of Helsinki, Department of Geology and Mineralogy. 29 p. (in Finnish)

Amantov, A., Laitakari, I. & Poroshin, Ye. 1996. Jotnian and Postjotnian: sandstones and diabases in the surroundings of the Gulf of Finland. In: Koistinen, T. (ed.) Explanation to the map of Precambrian basement of the Gulf of Finland and surrounding area 1 : 1 million. Geological Survey of Finland, Special Paper 21, 99–113. Available at: http://arkisto.gtk.fi/sp/sp21/sp_021_pages_099_113.pdf

Barthelmy, D. 1997. Mineralogy Database. [WWW document]. [referred 17.09.2007]. Available at: http://webmineral.com

Bedrock of Finland - DigiKP. Digital map database [Electronic resource]. Espoo: Geological Survey of Finland [referred 15.06.2013]. Version 1.0.

Catuneanu, O. 2006. Principles of Sequence Stratigraphy. San Diego: Elsevier. 375 p.

Elo, S. 1976. An interpretation of a recently measured gravity profile across the Jotnian sandstone formation in southwestern Finland. Geological Survey of Finland, archive report Q20/21/1976/1. 11 p. Available at: http://arkisto.gsf.fi/q20/Q20_21_1976_1.pdf

Elo, S. 1982. Satakunnan kallioperää koskevista gravimetrisista tutkimuksista. Geological Survey of Finland, archive report Q20/21/1982/1. 17 p. Available at: http://arkisto.gsf.fi/q20/Q20_21_1982_1.pdf

Elo, S. & Pirttijärvi, M. 2010. Satakunnan painovoimatutkimukset. Summary: Gravity investigations in Satakunta. In: Korhonen, R. (ed.) Geotietoa Satakunnasta : GeoPori-, GeoSatakunta- ja InnoGeo-projektien loppuraportti. Geological Survey of Finland, Report of Investigation 183, 65–104. (Electronic publication). Available at: http://arkisto.gtk.fi/tr/tr183/tr183_pages_65_104.pdf

Eskola, P. 1907. Satakunnan hiekkakiven geologiasta. Satakunta, Kotiseutututkimuksia I, 39–45.

Eskola, P. 1925. Ala-Satakunnan kallioperusta. Satakunta, Kotiseutututkimuksia V, 297–334.

Folk, R. L. 1954. The distinction between grain size and mineral composition in sedimentary-rock nomenclature. Journal of Geology 62, 344–359.

Goodman, L. 1965. On simultaneous confidence intervals for multinomial proportions. Technometrics 7, 247–254.

Haapala, I. 1977. Petrography and geochemistry of the Eurajoki stock: a rapakivi-granite complex with greisen-type mineralization in southwestern Finland. Geological Survey of Finland, Bulletin 286. 128 p., 1 app. map. Available at: http://arkisto.gtk.fi/bul/bt_286.pdf

Hämäläinen, A. 1985. Satakunnan jotunialueen geologisen karttakuvan historiallinen kehitys sekä uuteen tutkimusaineistoon perustuva kallioperäkarttaluonnos. Unpublished master´s thesis, University of Helsinki, Department of Geology. 104 p., 10 apps. (in Finnish)

Kohonen, J., Pihlaja, P., Kujala, H. & Marmo, J. 1993. Sedimentation of the Jotnian Satakunta sandstone, western Finland. Geological Survey of Finland, Bulletin 369. 35 p. Available at: http://arkisto.gtk.fi/bul/bt_369.pdf

Kohonen, J. & Rämö, O. T. 2005. Sedimentary rocks, diabases, and late cratonic evolution. In: Lehtinen, M., Nurmi, P. A. & Rämö, O. T. (eds) Precambrian Geology of Finland – Key to the Evolution of the Fennoscandian Shield. Amsterdam: Elsevier B.V., 563–603.

Koistinen, T., Stephens, M., Bogatchev, V., Nordgullen, O., Wennerström, M. & Korhonen, J. 2001. Geological map of the Fennoscandian shield, scale 1:2 000 000. Geological Survey of Finland, Geological Survey of Norway, Geological Survey of Sweden, Ministry of Natural Resources of Russia.

Korhonen, J. V., Aaro, S., All, T., Elo, S., Haller, L. Å., Kääriäinen, J., Kulinich, A., Skilbrei, J. R., Solheim, D., Säävuori, H., Vaher, R., Zhdanova, L. & Koistinen, T. 2002. Bouguer Anomaly Map of the Fennoscandian Shield 1: 2 000 000. Geological Survey of Finland, Geological Survey of Norway, Geological Survey of Sweden, Ministry of Natural Resources of Russian Federation.

Korja, A., Korja, T., Luosto, U. & Heikkinen, P. 1993. Seismic and geoelectric evidence for collisional and extensional events in the Fennoscandian Shield – implications for Precambrian crustal evolution. Tectonophysics 219, 129–152.

Lahtinen, R., Korja, A. & Nironen, M. 2005. Paleoproterozoic tectonic evolution. In: Lehtinen, M., Nurmi, P. A. & Rämö, O. T. (eds) Precambrian Geology of Finland – Key to the Evolution of the Fennoskandian Shield. Amsterdam: Elsevier B.V., 481–532.

Laitakari, A. 1925. Über das jotnische Gebiet von Satakunta. Fennia 45 (8). 43 p.

Laitakari, A. 1932. Suomen kivien raskaista mineraaleista II. Teknillinen aikakauslehti, 408–413.

Laurén, L. 1970. An interpretation of the negative gravity anomalies associated with the rapakivi granites and the Jotnian sandstone in southern Finland. Geologiska Föreningens I Stockholm Förhandlingar 93, 21–34.

Marttila, E. 1969. Satakunnan hiekkakiven sedimentaatio-olosuhteista. Unpublished licentiate thesis, University of Turku, Department of Geology. 157 p. (in Finnish)

May, W. L. & Johnson, W. D. 2005. Constructing two-sided simultaneous confidence intervals for multinomial proportions for small counts in a large number of cells. Journal of Statistical Software 5, Issue 6. 23 p.

Merino, E., Girard, J-P., May, M. & Ranganathan, V. 1997. Diagenetic mineralogy, geochemistry, and dynamics of mesozoic arkoses, Hartford rift basin, Connecticut, U.S.A.. Journal of Sedimentary Research 67 (1), 212–224.

Miall, A. D. 1977. A Review of the braided river depositional environment. Earth-Science Reviews 13, 1–62.

Nesbitt, H. W. & Young, G. M. 1982. Early Proterozoic climates and plate motions inferred from major element chemistry of lutites. Nature 199, 715–717.

Nesse, W. 2000. Introduction to mineralogy. Oxford

University Press. 442 p.

Pajunen, M. & Wennerström, M. 2010. Satakunnan hiekkakiven hauraiden rakenteiden kehityksestä. Summary: Development of brittle structures in the Satakunta sandstone. In: Korhonen, R. (ed.) Geotietoa Satakunnasta : GeoPori-, GeoSatakunta- ja InnoGeo-projektien loppuraportti. Geological Survey of Finland, Report of Investigation 183, 11–63. (Electronic publication). Available at: http://arkisto.gtk.fi/tr/tr183/tr183_pages_11_63.pdf

Pihlaja, P. 1987. Porin seudun subjotuniset diabaasit. Summary: The Subjotnian diabases of the Pori region, southwestern Finland. In: Aro, K. & Laitakari, I. (eds) Suomen diabaasit ja muut mafiset juonikivilajit. Summary: Diabases and other mafic dyke rocks in Finland. Geological Survey of Finland, Report of Investigation 76, 133–150. Available at: http://arkisto.gtk.fi/tr/tr76/tr76_pages_133_150.pdf

Pokki, J. 2007. Mesoproterotsooisen Satakunnan hiekkakiven koostumus ja raekokoanalyysi. Unpublished master's thesis, University of Helsinki, Department of geology and mineralogy. 107 p., 4 apps. (in Finnish). Available at: http://arkisto.gsf.fi/opinnaytteet/pokki_2007.pdf

Pokki, J., Kohonen, J., Rämö, O. T. & Andersen, T. 2013. The Suursaari conglomerate (SE Fennoscandian shield; Russia) – Indication of cratonic conditions and rapid reworking of quartz arenitic cover at the outset of the emplacement of the rapakivi granites at ca. 1.65 Ga. Precambrian Research 233, 132–143.

Puranen, M. 1963. A geophysical investigation of the Satakunta sandstone area in South-western Finland. Geoexploration 1, 6–15.

Rämö, O. T., Mänttäri, I., Vaasjoki, M., Upton, B. & Sviridenko, L. 2001. Age and significance of Mesoproterozoic CFB magmatism, lake Ladoga region, NW Russia. Geological Society of America, Abstracts with programs for annual meeting 33 (2001), A139.

Rämö, O. T. & Haapala, I. 2005. Rapakivi granites. In: Lehtinen, M., Nurmi, P. A. & Rämö, O. T. (eds) Precambrian Geology of Finland – Key to the Evolution of the Fennoscandian Shield. Amsterdam: Elsevier B.V., 533–562.

Rämö, O. T., Mänttäri, I., Huhma, H., Niin, M. & Pokki, J. 2007. 1635 Ma bimodal volcanism associated with the Wiborg rapakivi batholith (Suursaari, Gulf of Finland, Russia). In: Miller, J. A. & Kisters, A. F. M. (eds) 6th international Hutton Symposium. Abstract volume & program guide. Stellenbosch: Stellenbosch University, 174–175.

Rasilainen, K., Lahtinen, R. & Bornhorst, T. J. 2008. Chemical characteristics of Finnish bedrock – 1:1 000 000 scale bedrock map units. Geological Survey of Finland, Report of Investigation 171. 94 p. (Electronic publication). Available at: http://arkisto.gtk.fi/tr/tr171.pdf

Sauramo, M. 1916. Jotunisen ajan Satakunta. Satakunta, Kotiseutututkimuksia IV, 192–199.

Simonen, A. 1960. Pre-Quaternary rocks in Finland. Bulletin de la Commission Geológique de Finlande 191. 49 p. Available at: http://arkisto.gtk.fi/bul/bt_191.pdf

Simonen, A. 1980. The Precambrian in Finland. Geological Survey of Finland, Bulletin 304. 56 p. Available at: http://arkisto.gtk.fi/bul/bt_304.pdf

Simonen, A. 1987. Kaakkois-Suomen rapakivimassiivin kartta-alueiden kallioperä. Summary: Pre-Quaternary Rocks of the Map-Sheet areas of the rapakivi massif in SE Finland. Geological Map of Finland 1:100 000, Explatation to the Maps of Pre-Quaternary Rocks, Sheets 3023+3014, 3024, 3041, 3042, 3044, 3113, 3131, 3133. Geological Survey of Finland. 49 p. Available at: http://arkisto.gtk.fi/kps/kps3023+3014.pdf

Simonen, A. & Kouvo, O. 1955. Sandstones in Finland. Bulletin de la Commission Geológique de Finlande 168, 57–87. Available at: http://arkisto.gtk.fi/bul/bt168/bt_168_pages_057_087.pdf

Söderlund, U., Patchett, P., Vervoort, J. & Isachsen, C. 2004. The Lu-176 decay constant determined by Lu-Hf and U-Pb isotope systematics of Precambrian mafic intrusions. Earth and Planetary Science Letters 219 (3–4), 311–324.

Strand, K., Köykkä, J. & Kohonen, J. (eds) 2010. Guidelines and procedures for naming Precambrian geological units in Finland. 2010 Edition Stratigraphic Commission of Finland: Precambrian Sub-Commission. Geological Survey of Finland, Guide 55. 41 p. Available at: http://arkisto.gtk.fi/op/op55.pdf

Suominen, V. 1991. The chronostratigraphy of southwestern Finland with special reference to Postjotnian and Subjotnian diabases. Geological Survey of Finland, Bulletin 356. 100 p., 5 apps. Available at: http://arkisto.gtk.fi/bul/bt_356.pdf

Tynni, R. & Uutela, A. 1984. Microfossiles from the Precambrian Muhos formation in Western Finland. Geological Survey of Finland, Bulletin 330. 38 p. Available at: http://arkisto.gtk.fi/bul/bt_330.pdf

Vaasjoki, M. 1977. Rapakivi granites and other postorogenic rocks in Finland: their age and the lead isotopic composition of certain associated galena mineralizations. Geological Survey of Finland, Bulletin 294. 64 p., 2 apps. Available at: http://arkisto.gtk.fi/bul/bt_294.pdf

Vaasjoki, M. & Sakko, M. 1987. Zirkoni-indikaatio Satakunnan hiekkakiven alkuperästä. Geologi 39, 184–187.

APPENDICES

Appendix 1. Type samples of the lithofacies in the drill cores, Satakunta formation.

Appendix 2. Samples from core M52-PO-60-001, Satakunta formation.

Appendix 3. Samples from other drill cores, Satakunta formation.

Appendix 4. Whole-rock geochemical data, Satakunta formation.

Appendix 5. U-Pb isotopic data, Satakunta formation.

Appendix 6. BSE images of detrital zircons, Satakunta formation.

Appendix 7. Published zircon ages in SW Finland.

Appendix 1. Type samples of the lithofacies in drill cores from the Satakunta formation. **(A)** Mudstone (Fm). M52-PO-60-001. Depth 494 m. **(B)** Mudstone (Fl). M52-PO-60-001. 348 m. **(C)** Sandy mudstone. HARJAVALTA-R-001. 20.7 m. **(D)** Muddy sandstone. HARJAVALTA-R-001. 2.2 m. **(E)** Muddy sandstone (Sl). M52-PO-60-001. 262 m. **(F)** Muddy sandstone (Sr). M52-PO-60-001. 390 m. **(G)** Sandstone. K52-1141-89-002. 42.0 m. **(H)** Sandstone (St1). M52-PO-60-001. 551 m. **(I)** Sandstone (St2). M52-PO-60-001. 138 m. **(J)** Slightly conglomeratic sandstone. K52-1141-89-006. 16.2 m. **(K)** Conglomeratic sandstone. K52-1141-89-002. 41.6 m. **(L)** Sandy conglomerate. K52-1141-89-002. 42.2 m. **(M)** Conglomerate. K52-1141-89-002. 49.7 m. Photo: Jussi Pokki, GTK.

Appendix 2. Samples from drill core M52-PO-60-001. All images are at the same scale. The whole-rock geochemistry from the red (sample PO-60-65-H) and grey (PO-60-65-P) parts of sample 65.2 were analysed separately. Of the samples 390.3 and 617.2, only the left-hand piece and the coarse part on the right, respectively, were selected for whole-rock geochemical analysis. Photo: Jussi Pokki, GTK.

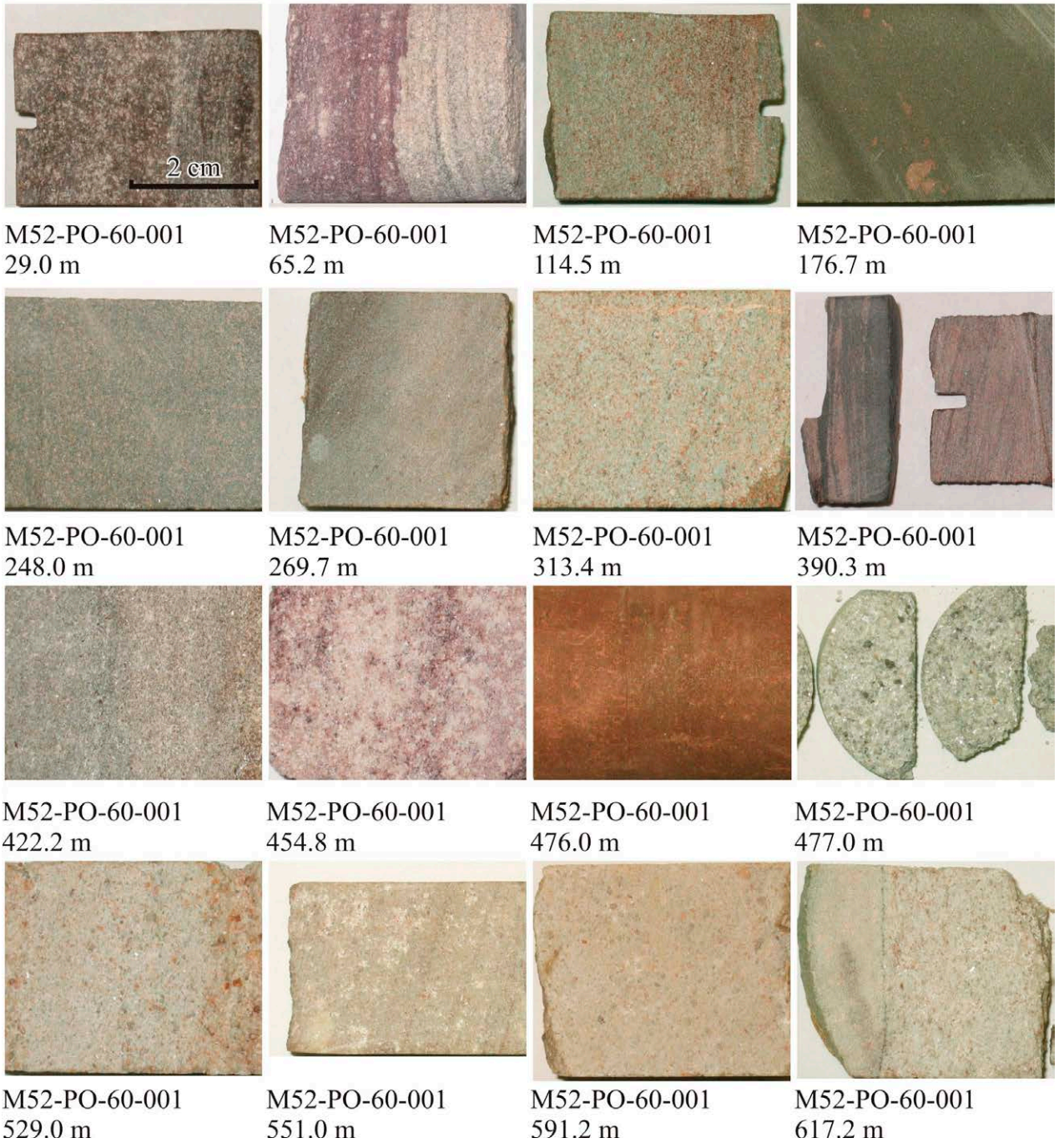

Appendix 3. Samples from other drill cores from the Satakunta formation. All images are at the same scale. Photo: Jussi Pokki, GTK.

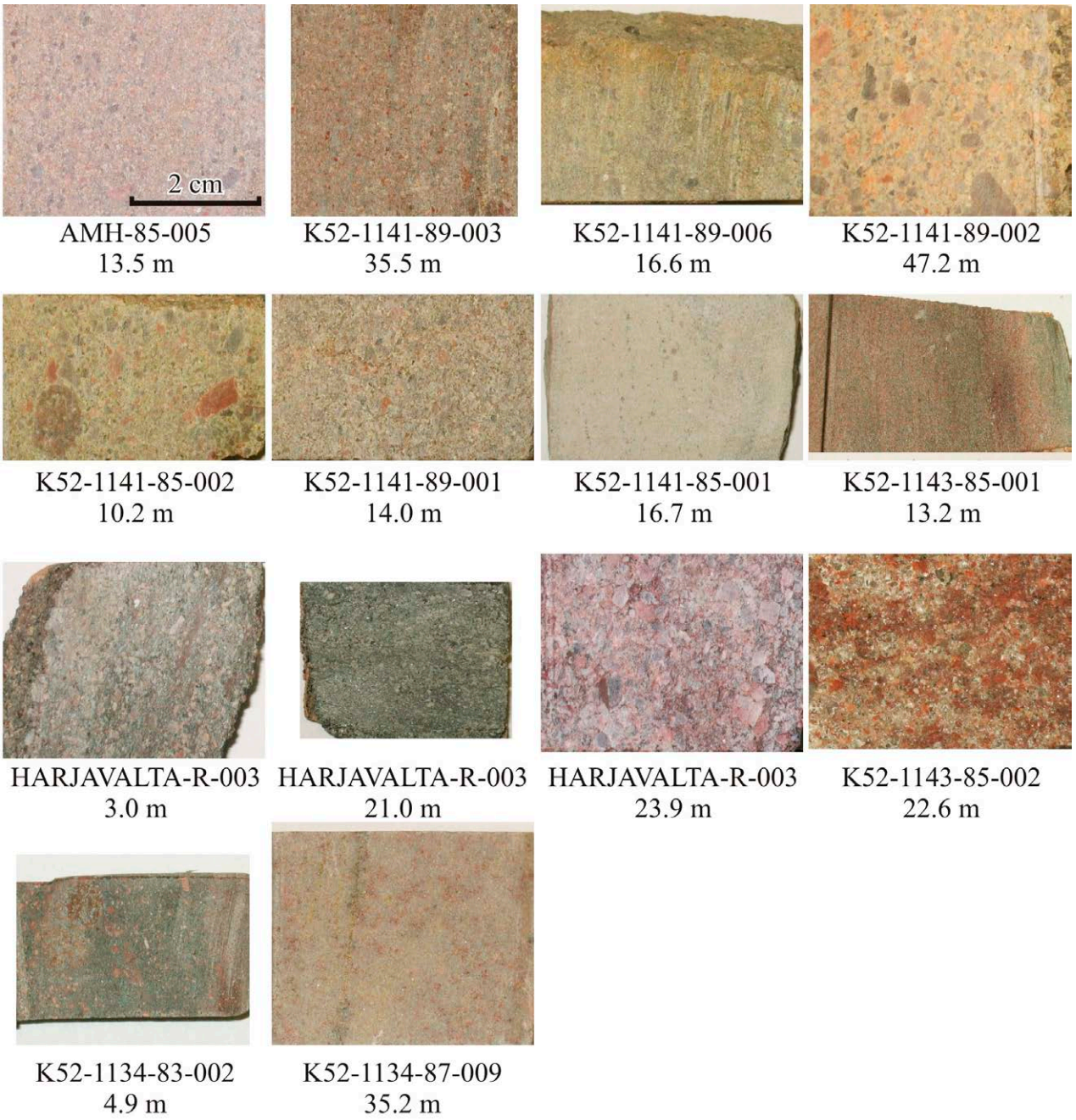

Appendix 4. Whole-rock geochemical data, Satakunta formation.

Sample	Lithofacies (rock type)	40	43	Na_2O % + 175X	MgO % + 175X	Al_2O_3 % + 175X	SiO_2 % + 175X	P_2O_5 % + 175X	K_2O % + 175X	CaO % + 175X	TiO_2 % + 175X	MnO % + 175X	Fe_2O_3 % + 175X	S % + 175X	Cl % + 175X	Cr % + 175X	Ni % + 175X	Cu % + 175X	Zn % + 175X	Ga % + 175X	As % + 175X	Sr % + 175X	Mo % + 175X	Sn % + 175X	Sb % + 175X	Ba % + 175X	Pb % + 175X	Bi % + 175X	FeO % 301T
PO-60-29	SS (arkose)	yes	yes	1.86	0.098	8.13	84.1	0.027	2.84	0.832	0.119	0.011	0.581	<0.006	<0.006	<0.003	0.01	<0.002	<0.002	<0.002	<0.003	0.009	<0.001	<0.002	<0.01	0.038	<0.003	<0.003	0.15
PO-60-65-H	SS	no	yes	2.04	1.93	18.9	60.9	0.222	7.42	1.11	0.717	0.077	3.62	<0.006	<0.006	0.004	<0.002	<0.002	0.008	0.004	<0.003	0.021	<0.001	<0.002	<0.01	0.092	0.006	<0.003	0.20
PO-60-65-P	SS	no	yes	1.76	2.07	19.6	61.9	0.208	8.13	1.07	0.490	0.058	1.59	<0.006	0.007	0.006	<0.002	<0.002	0.008	0.003	<0.003	0.021	<0.001	<0.002	<0.01	0.095	0.005	<0.003	0.20
PO-60-114	SS	no	yes	2.06	1.35	15.4	70.5	0.085	4.65	1.97	0.192	0.044	1.22	<0.006	0.007	<0.003	<0.002	<0.002	0.005	0.003	<0.003	0.016	<0.001	<0.002	<0.01	0.054	0.004	<0.003	0.24
PO-60-176	M	yes	yes	1.79	2.65	18.8	56.7	0.173	5.19	2.10	0.946	0.099	6.81	<0.006	0.011	0.008	0.00	0.002	0.015	0.004	<0.003	0.020	<0.001	<0.002	<0.01	0.066	0.004	<0.003	3.37
PO-60-247	MS	yes	yes	4.21	1.37	15.0	69.3	0.091	3.08	1.60	0.448	0.064	3.43	<0.006	0.013	0.004	<0.002	<0.002	0.006	0.003	<0.003	0.018	<0.001	<0.002	<0.01	0.048	0.003	<0.003	1.96
PO-60-269	S	no	yes	3.51	0.433	12.6	73.0	0.106	3.60	1.89	0.736	0.038	3.38	<0.006	0.017	0.004	<0.002	<0.002	0.004	<0.002	<0.003	0.018	<0.001	<0.002	<0.01	0.052	0.004	<0.003	0.73
PO-60-313	S	yes	yes	3.04	0.599	12.2	75.8	0.200	2.88	1.86	0.137	0.036	1.33	<0.006	0.023	<0.003	<0.002	<0.002	0.003	<0.002	<0.003	0.017	<0.001	<0.002	<0.01	0.043	<0.003	<0.003	0.69
PO-60-390	MS	no	yes	2.01	2.72	17.2	60.5	0.143	4.64	1.77	0.924	0.080	5.72	<0.006	0.034	0.011	0.004	<0.002	0.014	0.004	<0.003	0.019	<0.001	<0.002	<0.01	0.055	0.004	<0.003	
PO-60-422	S	yes	yes	1.65	<0.0332	7.42	85.7	0.020	2.63	0.905	0.182	0.015	0.56	<0.006	0.013	<0.003	<0.002	<0.002	<0.002	<0.002	<0.003	0.010	<0.001	<0.002	<0.01	0.039	<0.003	<0.003	0.31
PO-60-454	S	yes	yes	1.72	0.163	10.5	81.0	0.037	3.42	1.59	0.062	0.012	0.616	<0.006	0.014	<0.003	<0.002	<0.002	0.002	<0.002	<0.003	0.016	<0.001	<0.002	<0.01	0.046	<0.003	<0.003	0.15
PO-60-476	M	yes	yes	0.84	2.94	23.2	48.5	0.120	7.25	1.21	1.07	0.142	8.70	<0.006	0.048	0.010	0.00	<0.002	0.018	0.005	<0.003	0.016	<0.001	<0.002	<0.01	0.077	0.007	<0.003	0.39
PO-60-477(Wi)	S	no	yes	0.927	0.079	8.27	84.9	0.022	3.03	1.47	0.041	0.011	0.347	<0.006	0.009	<0.003	<0.002	<0.002	<0.002	<0.002	<0.003	0.014	<0.001	<0.002	<0.01	0.038	<0.003	<0.003	0.10
PO-60-477(Fe)	S	yes	no																										
PO-60-506	Crushed SS+M [=weathered?]	yes	yes	1.37	0.434	12.7	74.4	0.341	4.95	1.09	0.264	0.076	2.63	<0.006	0.018	<0.003	<0.002	<0.002	0.005	0.002	<0.003	0.012	<0.001	<0.002	<0.01	0.059	0.006	<0.003	0.28
PO-60-529	S	yes	yes	0.793	<0.0332	6.54	88.1	0.015	2.74	1.07	0.018	<0.0077	0.114	<0.006	0.023	<0.003	<0.002	<0.002	<0.002	<0.002	<0.003	0.009	<0.001	<0.002	<0.01	0.042	<0.003	<0.003	0.05
PO-60-551	S	yes	yes	1.14	0.091	8.24	85.1	0.028	4.10	0.335	0.072	0.020	0.475	<0.006	0.032	<0.003	<0.002	<0.002	0.002	<0.002	<0.003	0.009	<0.001	<0.002	<0.01	0.050	0.004	<0.003	0.10
PO-60-591	S	yes	yes	0.458	0.047	4.52	90.7	0.429	2.59	0.662	0.023	0.019	0.197	<0.006	0.019	<0.003	<0.002	<0.002	<0.002	<0.002	<0.003	0.006	<0.001	<0.002	<0.01	0.033	<0.003	<0.003	0.05
PO-60-617	S	no	yes	0.657	<0.0332	5.81	89.4	0.017	2.96	0.526	0.020	<0.0077	0.189	<0.006	0.013	<0.003	0.00	<0.002	<0.002	<0.002	<0.003	0.008	<0.001	<0.002	<0.01	0.040	<0.003	<0.003	0.06
1134-83-2-4	SCS (arkose)	no	yes	2.32	1.06	14.1	73.6	0.068	4.86	0.299	0.268	0.048	2.75	<0.006	0.007	<0.003	<0.002	<0.002	0.005	0.002	<0.003	0.025	<0.001	<0.002	<0.01	0.054	<0.003	<0.003	0.46
1134-87-9-35	SS (arkose)	yes	yes	0.651	0.514	7.76	86.0	0.024	4.04	0.100	0.078	0.012	0.512	<0.006	<0.006	<0.003	<0.002	<0.002	0.003	<0.002	<0.003	0.007	<0.001	<0.002	<0.01	0.049	<0.003	<0.003	0.08
1141-85-1-16(Wi)	SS (arkose)	no	yes	0.117	0.669	11.0	81.6	0.022	4.48	0.178	0.126	0.021	0.483	<0.006	0.006	<0.003	<0.002	<0.002	0.003	<0.002	<0.003	0.007	<0.001	<0.002	<0.01	0.077	<0.003	<0.003	0.09
1141-85-1-16(Fe)	SS (arkose)	yes	no																										
1141-85-2-10	SCS (subarkose)	yes	yes	<0.0674	0.162	7.45	87.4	0.032	3.04	0.056	0.262	0.015	0.832	0.0367	<0.006	<0.003	<0.002	<0.002	0.003	<0.002	<0.003	0.003	<0.001	<0.002	<0.01	0.030	<0.003	<0.003	0.13
1141-89-1-13	SCS (subarkose)	yes	yes	<0.0674	0.141	8.88	84.7	0.028	3.71	0.045	0.254	0.023	1.43	<0.006	0.006	<0.003	<0.002	<0.002	<0.002	<0.002	<0.003	0.003	<0.001	<0.002	<0.01	0.035	<0.003	<0.003	0.15
1141-89-2-47	CS (arkose)	no	yes	<0.0674	0.067	8.60	85.6	0.025	4.14	0.052	0.147	0.022	0.701	<0.006	0.008	<0.003	0.00	<0.002	0.002	<0.002	<0.003	0.004	<0.001	<0.002	<0.01	0.044	<0.003	<0.003	0.08
1141-89-3-35	SCS (subarkose)	yes	yes	<0.0674	0.087	7.16	86.5	0.035	3.54	0.030	0.561	0.012	1.64	<0.006	0.008	<0.003	<0.002	<0.002	0.003	<0.002	<0.003	0.003	<0.001	<0.002	<0.01	0.035	0.003	<0.003	0.23
1141-89-6-16(Wi)	SCS (subarkose)	no	yes	0.083	0.059	8.21	86.4	0.021	3.83	0.043	0.116	0.017	0.615	<0.006	0.009	<0.003	<0.002	<0.002	<0.002	<0.002	<0.003	0.004	<0.001	<0.002	<0.01	0.042	<0.003	<0.003	0.15
1141-89-6-16(Fe)	SCS (subarkose)	yes	no																										
1143-85-2-22	SCS (arkose)	no	yes	1.11	0.731	7.82	85.0	0.060	3.01	0.167	0.193	0.020	1.13	<0.006	<0.006	<0.003	<0.002	<0.002	0.003	<0.002	<0.003	0.008	<0.001	<0.002	<0.01	0.048	<0.003	<0.003	0.23
1143-85-1-13	MS (arkose)	no	yes	3.81	2.46	15.5	63.6	0.235	2.33	2.51	0.697	0.103	6.36	<0.006	0.006	0.007	0.00	<0.002	0.010	0.002	<0.003	0.016	<0.001	<0.002	<0.01	0.035	0.004	<0.003	1.09
AMH-85-5-13	CS (subarkose)	yes	yes	0.084	0.185	7.54	86.7	0.031	4.06	0.020	0.190	<0.0077	0.578	<0.006	0.006	<0.003	0.00	<0.002	0.002	<0.002	<0.003	0.005	<0.001	<0.002	<0.01	0.046	<0.003	<0.003	0.10
HV-3-2	MS (arkose)	no	yes	0.954	2.68	14.2	68.0	0.121	4.63	0.484	0.554	0.054	5.42	<0.006	0.009	0.010	0.00	<0.002	0.010	0.003	<0.003	0.009	<0.001	<0.002	<0.01	0.073	0.004	<0.003	1.28
HV-3-20	SS	no	yes	0.866	3.64	16.8	61.1	0.167	5.11	0.671	0.784	0.078	6.33	<0.006	0.011	0.015	0.01	<0.002	0.014	0.003	<0.003	0.010	<0.001	<0.002	<0.01	0.071	0.009	<0.003	3.24
HV-3-23(Wi)	SS	no	yes	1.40	1.11	9.99	78.9	0.092	3.38	1.33	0.204	0.026	2.20	<0.006	0.006	0.004	<0.002	<0.002	0.004	<0.002	<0.003	0.012	<0.001	<0.002	<0.01	0.066	0.004	<0.003	0.44
HV-3-23(Fe)	SS	yes	no																										

40 = grinding in Fe pan
43 = grinding in Widia pan (source of contamination of W and Co)

Appendix 4. Cont.

Sample	Lithofacies (rock type)	40	43	Ce mg/kg 308M	Co mg/kg 308M	Dy mg/kg 308M	Er mg/kg 308M	Eu mg/kg 308M	Gd mg/kg 308M	Hf mg/kg 308M	Ho mg/kg 308M	La mg/kg 308M	Lu mg/kg 308M	Nb mg/kg 308M	Nd mg/kg 308M	Pr mg/kg 308M	Rb mg/kg 308M	Sc mg/kg 308M	Sm mg/kg 308M	Ta mg/kg 308M	Tb mg/kg 308M	Th mg/kg 308M	Tm mg/kg 308M	U mg/kg 308M	V mg/kg 308M	W mg/kg 308M	Y mg/kg 308M	Yb mg/kg 308M	Zr mg/kg 308M
PO-60-29	SS (arkose)	yes	yes	21.1	1.98	1.76	0.86	0.47	2.16	2.90	0.30	17.8	0.14	2.84	13.0	3.87	98.6	1.41	2.20	0.32	0.33	7.21	0.15	1.99	7.91	1.75	7.47	0.90	112
PO-60-65-H	SS	no	yes	82.5		5.69	2.55	1.69	8.97	10.5	0.98	76.7	0.37	13.0	62.0	17.3	285	6.86	10.2	1.60	1.19	33.9	0.37	6.26	31.2		26.7	2.73	413
PO-60-65-P	SS	no	yes	50.5		4.48	1.92	1.63	8.33	6.96	0.74	43.9	0.25	10.5	62.9	16.7	313	7.31	10.1	1.19	1.01	20.6	0.28	4.74	52.0		21.2	2.04	264
PO-60-114	SS	no	yes	36.9		2.55	1.32	0.59	3.57	2.65	0.47	17.4	0.14	3.57	17.4	4.56	176	1.87	3.70	0.38	0.49	7.31	0.18	4.75	91.6		12.6	1.05	95.7
PO-60-176	M	yes	yes	132	18.6	7.84	4.76	1.52	9.97	9.64	1.64	61.3	0.68	24.8	54.5	14.7	309	18.6	10.1	2.09	1.42	22.4	0.69	9.43	157	3.37	43.4	4.62	369
PO-60-247	MS	yes	yes	70.9	9.74	4.21	1.82	1.04	6.36	3.65	0.73	31.4	0.23	13.6	31.2	8.01	159	9.02	6.25	1.20	0.82	7.38	0.29	5.37	79.8	2.79	21.8	1.68	141
PO-60-269	S	no	yes	236		8.24	3.70	1.57	13.4	9.44	1.43	103	0.49	14.2	90.2	25.9	128	6.94	16.1	1.97	1.85	34.3	0.49	7.72	46.0		38.2	3.23	378
PO-60-313	S	yes	yes	55.6	3.80	1.46	0.73	0.52	2.56	1.57	0.29	14.2	<0.1	2.16	13.8	3.24	106	1.40	2.39	0.22	0.32	3.88	0.11	1.83	13.1	2.59	8.26	0.65	60.7
PO-60-390	MS	no	yes	107		6.74	3.66	1.38	8.26	7.00	1.26	48.3	0.49	21.4	43.8	11.9	253	17.2	8.42	1.85	1.24	15.6	0.53	7.30	103		35.1	3.53	265
PO-60-422	S	yes	yes	152	0.97	4.09	1.92	0.74	6.03	3.02	0.79	22.2	0.21	4.65	24.7	6.30	82.6	1.53	5.91	0.66	0.87	12.7	0.22	2.40	19.8	1.12	27.6	1.60	124
PO-60-454	S	yes	yes	11.9	2.76	0.94	0.45	0.30	1.21	1.38	0.16	8.19	<0.1	1.58	6.49	1.78	121	1.16	1.27	<0.2	0.16	3.70	<0.1	1.89	8.49	0.58	4.55	0.44	52.4
PO-60-476	M	yes	yes	103	23.8	7.76	4.51	1.64	9.01	8.70	1.51	66.2	0.72	28.2	54.0	15.3	382	23.8	10.0	2.38	1.43	24.1	0.71	8.96	66.3	3.15	40.9	4.78	330
PO-60-477(Wi)	S	no	yes	14.0		0.85	0.38	0.28	1.32	1.27	0.17	8.98	<0.1	0.99	7.47	2.07	107	0.76	1.40	<0.2	0.17	2.79	<0.1	1.04	3.19		4.36	0.44	48.1
PO-60-477(Fe)	S	yes	no	15.0	1.80	0.92	0.42	0.28	1.27	1.42	0.15	8.67	<0.1	1.03	7.66	2.07	102	0.69	1.34	<0.2	0.18	3.11	<0.1	1.26	3.05	2.98	4.46	0.46	53.2
PO-60-506	Crushed SS+M [=weathered?]	yes	yes	24.5	6.40	2.52	1.42	0.69	3.55	3.20	0.49	23.3	0.21	6.26	21.1	5.39	169	5.29	3.76	0.62	0.47	8.59	0.2	3.62	12.7	3.51	13.3	1.39	122
PO-60-529	S	yes	yes	27.2	0.63	0.6	0.23	0.20	1.03	1.06	0.11	6.36	<0.1	0.70	5.42	1.39	86.1	0.52	0.95	<0.2	0.12	2.83	<0.1	1.17	12.2	1.01	3.02	0.28	40.4
PO-60-551	S	yes	yes	19.1	1.35	1.22	0.71	0.43	1.71	2.17	0.23	10.3	<0.1	1.91	9.66	2.63	143	0.93	1.75	0.22	0.24	4.23	<0.1	1.24	2.61	0.63	6.44	0.59	84.5
PO-60-591	S	yes	yes	15.9	0.76	0.79	0.39	0.34	1.60	1.24	0.16	8.93	<0.1	0.59	8.22	2.06	91.0	0.76	1.39	<0.2	0.19	3.05	<0.1	1.77	2.83	1.14	5.00	0.39	42.1
PO-60-617	S	no	yes	11.6		0.52	0.29	0.21	0.68	1.21	0.11	4.40	<0.1	0.55	4.07	0.97	104	0.71	0.75	<0.2	0.11	2.54	<0.1	0.89	3.22		2.80	0.26	41.0
1134-83-2-4	SCS (arkose)	no	yes	32.0		2.72	1.67	0.32	2.46	3.60	0.56	12.2	0.23	9.05	11.4	2.98	196	6.52	2.37	0.86	0.44	10.6	0.24	2.50	12.0		15.0	1.68	129
1134-87-9-35	SS (arkose)	yes	yes	10.0	2.26	0.74	0.45	0.28	1.10	1.85	0.16	5.31	<0.1	1.76	4.98	1.30	150	1.62	0.96	<0.2	0.14	4.04	<0.1	0.90	5.15	3.97	4.47	0.46	75.8
1141-85-1-16(Wi)	SS (arkose)	no	yes	37.3		1.49	0.83	0.48	2.31	3.55	0.27	25.6	0.12	2.50	19.6	5.47	124	2.53	2.62	0.41	0.29	5.55	0.12	2.23	18.3		7.39	0.81	146
1141-85-1-16(Fe)	SS (arkose)	yes	no	36.9	2.61	1.47	0.83	0.50	2.48	4.84	0.29	25.6	0.14	2.42	19.8	5.51	133	2.38	2.98	0.28	0.30	7.05	0.14	2.39	10.9	1.29	7.34	0.82	182
1141-85-2-10	SCS (subarkose)	yes	yes	32.1	2.32	1.62	0.89	0.22	2.04	2.28	0.32	16.2	0.13	4.72	12.6	3.48	106	2.89	2.46	0.49	0.34	9.35	0.13	13.2	19.1	1.71	8.94	0.89	78.9
1141-89-1-13	SCS (subarkose)	yes	yes	84.2	2.14	3.33	1.51	0.44	5.74	2.60	0.56	40.1	0.22	6.62	41.3	10.8	140	2.44	8.07	1.65	0.74	16.7	0.22	2.44	15.9	2.01	15.8	1.52	86.5
1141-89-2-47	CS (arkose)	no	yes	37.5		2.66	1.25	0.30	2.91	3.33	0.47	16.9	0.21	4.28	15.0	4.01	149	2.38	2.84	0.82	0.48	16.8	0.20	2.18	3.42		13.0	1.27	109
1141-89-3-35	SCS (subarkose)	yes	yes	137	2.21	4.82	1.68	0.46	9.66	5.01	0.69	70.3	0.26	9.36	62.1	16.7	123	2.43	11.5	1.74	1.14	40.6	0.25	6.67	4.70	3.67	19.9	1.71	183
1141-89-6-16(Wi)	SCS (subarkose)	no	yes	16.7		1.65	0.91	0.20	1.77	2.78	0.33	8.01	0.14	2.74	7.27	2.02	130	2.23	1.70	0.33	0.29	6.28	0.14	2.42	13.0		9.31	0.99	94.2
1141-89-6-16(Fe)	SCS (subarkose)	yes	no	19.8	3.49	1.78	1.02	0.17	1.79	3.11	0.38	10.5	0.19	4.72	8.71	2.23	133	2.78	1.80	0.50	0.31	6.70	0.16	3.03	13.8	2.15	9.82	1.08	107
1143-85-2-22	SCS (arkose)	no	yes	26.5		2.54	1.52	0.55	2.56	3.38	0.49	15.4	0.22	3.27	14.4	3.72	67.9	3.26	2.56	0.37	0.40	12.8	0.23	1.76	16.1		13.3	1.41	122
1143-85-1-13	MS (arkose)	no	yes	142		7.55	3.65	1.49	10.8	10.1	1.34	61.0	0.49	13.0	63.3	16.6	94.4	11.2	11.5	1.45	1.52	28.2	0.51	6.57	102		36.3	3.23	393
AMH-85-5-13	CS (subarkose)	yes	yes	40.4	2.08	1.65	0.93	0.37	2.54	2.37	0.32	21.0	0.14	2.38	19.8	5.24	131	1.60	3.11	0.37	0.33	7.64	0.16	1.66	3.20	2.73	8.85	0.97	93.9
HV-3-2	MS (arkose)	no	yes	63.3		3.54	1.87	0.98	5.25	3.62	0.66	30.5	0.30	11.1	28.7	7.49	178	12.4	5.08	0.95	0.67	9.64	0.28	4.18	69.7		19.0	1.86	131
HV-3-20	SS	no	yes	65.9		4.45	2.37	0.92	5.70	4.76	0.87	31.4	0.36	13.8	29.9	7.75	206	17.7	5.60	1.27	0.83	11.3	0.34	5.32	92.6		23.7	2.26	164
HV-3-23(Wi)	SS	no	yes	42.4		3.38	1.86	0.80	3.44	2.06	0.66	20.5	0.24	3.39	19.4	5.09	87.8	4.65	4.06	0.32	0.61	8.15	0.28	1.88	25.5		18.7	1.67	71.1
HV-3-23(Fe)	SS	yes	no	43.3	4.04	3.40	1.70	0.81	4.70	2.01	0.62	20.0	0.24	2.88	22.1	5.50	81.8	4.27	4.21	0.24	0.66	7.72	0.24	1.98	29.7	2.36	17.7	1.49	70.4

40 = grinding in Fe pan
43 = grinding in Widia pan (source of contamination of W and Co)

Appendix 4. Cont.

Sample	Lithofacies (rock type)	40	43	C % + 811L	H_2O % 815L	C (in non-carbonate) % 816L	C (in carbonate) % 816L
PO-60-29	SS (arkose)	yes	yes	0.09	1.10	0.05	0.04
PO-60-65-H	SS	no	yes	0.04	3.25	-	-
PO-60-65-P	SS	no	yes	0.05	2.94	-	-
PO-60-114	SS	no	yes	0.05	3.28	0.02	0.03
PO-60-176	M	yes	yes	0.10	4.73	0.04	0.06
PO-60-247	MS	yes	yes	0.06	2.63	0.02	0.04
PO-60-269	S	no	yes	0.09	1.52	0.04	0.05
PO-60-313	S	yes	yes	0.06	2.55	0.03	0.03
PO-60-390	MS	no	yes	0.13	4.37	0.05	0.08
PO-60-422	S	yes	yes	0.07	1.39	0.04	0.03
PO-60-454	S	yes	yes	0.04	2.18	-	-
PO-60-476	M	yes	yes	0.04	5.24	-	-
PO-60-477(Wi)	S	no	yes	0.04	1.82	-	-
PO-60-477(Fe)	S	yes	no			-	-
PO-60-506	Crushed SS+M [=weathered?]	yes	yes	0.08	1.69	0.03	0.04
PO-60-529	S	yes	yes	0.04	1.56	-	-
PO-60-551	S	yes	yes	0.05	0.68	0.03	0.02
PO-60-591	S	yes	yes	0.05	0.36	0.04	0.01
PO-60-617	S	no	yes	0.04	0.72	-	-
1134-83-2-4	SCS (arkose)	no	yes	0.05	1.74	-	-
1134-87-9-35	SS (arkose)	yes	yes	0.04	0.79	-	-
1141-85-1-16(Wi)	SS (arkose)	no	yes	0.17	1.87	0.09	0.08
1141-85-1-16(Fe)	SS (arkose)	yes	no			-	-
1141-85-2-10	SCS (subarkose)	yes	yes	0.04	0.99	-	-
1141-89-1-13	SCS (subarkose)	yes	yes	0.04	1.12	-	-
1141-89-2-47	CS (arkose)	no	yes	0.04	0.94	-	-
1141-89-3-35	SCS (subarkose)	yes	yes	0.05	0.78	0.02	0.03
1141-89-6-16(Wi)	SCS (subarkose)	no	yes	0.07	0.93	0.03	0.04
1141-89-6-16(Fe)	SCS (subarkose)	yes	no			-	-
1143-85-2-22	SCS (arkose)	no	yes	0.07	1.08	0.01	0.06
1143-85-1-13	MS (arkose)	no	yes	0.11	3.49	0.04	0.07
AMH-85-5-13	CS (subarkose)	yes	yes	0.04	0.73	-	-
HV-3-2	MS (arkose)	no	yes	0.13	2.81	0.05	0.08
HV-3-20	SS	no	yes	0.49	4.42	0.37	0.12
HV-3-23(Wi)	SS	no	yes	0.20	1.67	0.07	0.14
HV-3-23(Fe)	SS	yes	no			-	-

40 = grinding in Fe pan
43 = grinding in Widia pan (source of contamination of W and Co)

Appendix 5. U-Pb isotopic data, Satakunta formation.

Sample	U (ppm)	^{206}Pb (ppm)	^{206}Pb/ ^{204}Pb	^{206}Pb/ ^{238}U*	±σ (%)	^{207}Pb/ ^{235}U*	±σ (%)	^{207}Pb/ ^{206}Pb*	±σ (%)	ρ[a]	Disc.[b] (%)	Min rim (%)	^{206}Pb/ ^{238}U (Ma)	±σ (Ma)	^{207}Pb/ ^{235}U (Ma)	±σ (Ma)	^{207}Pb/ ^{206}Pb (Ma)	±σ (Ma)
M52-PO-60-001, Satakunta, Finland. Coordinates in ETRS89-TM35FIN: P = 6823667, I = 220208.																		
nonrandomly selected detrital zircons (n=13)																		
PO-42	582	108	32516	0.3381	0.62	5.148	9.0	0.1102	0.1	0.92	5	.	1878	30	1844	15	1803	17
PO-32	689	128	39174	0.3389	0.65	5.168	7.8	0.1103	0.1	0.92	5.1	.	1881	31	1847	13	1805	23
PO-20	643	120	60949	0.3392	0.62	5.186	9.0	0.1106	0.1	0.95	4.9	.	1883	30	1850	15	1810	16
PO-31	717	134	45743	0.3404	0.62	5.215	8.8	0.1109	0.1	0.89	5	.	1888	30	1855	14	1814	15
PO-03	291	53	23119	0.3338	0.61	5.192	9.4	0.1127	0.1	0.92	0.9	.	1857	29	1851	15	1844	16
PO-66	230	41	10404	0.3262	0.61	5.093	8.6	0.1134	0.1	0.75	-2.2	.	1820	30	1835	14	1854	19
PO-109	360	67	8919	0.3406	0.63	5.352	9.5	0.1140	0.1	0.95	1.6	.	1889	30	1877	15	1864	16
PO-38	92	17	6342	0.3343	0.62	5.280	9.2	0.1146	0.1	0.82	-0.9	.	1859	30	1866	15	1873	16
PO-104	145	26	8464	0.3301	0.61	5.228	9.2	0.1150	0.1	0.88	-2.6	.	1839	29	1857	15	1880	16
PO-75	96	18	11104	0.3450	0.65	5.473	9.9	0.1151	0.1	0.85	1.8	.	1911	31	1896	16	1881	16
PO-02	185	35	13966	0.3394	0.62	5.410	9.5	0.1156	0.1	0.78	-0.4	.	1884	30	1886	15	1890	16
PO-65	333	63	3703	0.3433	0.67	5.578	11.4	0.1181	0.1	0.84	-1.7	.	1903	32	1913	18	1927	14
PO-14	84	25	16343	0.5122	1.27	13.354	50.9	0.2008	0.3	0.93	-12.6	.	2666	54	2705	36	2833	20
randomly selected detrital zircons (n=46)																		
PO-189	370	66	25625	0.3305	0.61	4.994	8.9	0.1094	0.1	0.92	3.5	.	1841	30	1818	15	1790	15
PO-180	281	51	8729	0.3268	0.44	5.019	4.1	0.1113	0.1	0.72	0.1	.	1823	21	1823	7	1821	17
PO-217	66	12	7545	0.3203	0.56	4.922	8.3	0.1114	0.1	0.71	-1.8	.	1791	27	1806	14	1822	15
PO-242	283	52	25414	0.3397	1.22	5.290	13.6	0.1126	0.1	0.87	3	.	1885	59	1867	22	1842	22
PO-212	265	47	10909	0.3302	0.68	5.137	10.0	0.1128	0.1	0.93	-0.3	.	1839	33	1842	17	1844	14
PO-146	213	37	19689	0.3281	0.71	5.109	10.7	0.1129	0.1	0.90	-1	.	1829	34	1838	18	1846	20
PO-181	287	55	6696	0.3481	0.49	5.471	4.6	0.1139	0.1	0.82	4	.	1926	23	1896	7	1863	17
PO-219	117	20	5606	0.3199	0.51	5.022	8.5	0.1140	0.1	0.73	-4.6	-0.1	1789	25	1823	14	1863	18
PO-274	105	19	3312	0.3259	1.16	5.129	13.8	0.1142	0.1	0.80	-3	.	1818	56	1841	23	1867	19
PO-283	299	55	21155	0.3374	1.20	5.315	14.0	0.1142	0.1	0.94	0.4	.	1874	58	1871	22	1868	20
PO-186	188	35	45664	0.3429	0.72	5.417	11.2	0.1145	0.1	0.83	1.8	.	1901	35	1888	18	1872	13
PO-149	356	63	30722	0.3365	1.10	5.326	18.5	0.1147	0.2	0.85	-0.2	.	1870	53	1873	30	1875	30
PO-177	393	76	21352	0.3562	0.98	5.644	14.8	0.1147	0.1	0.93	5.7	.	1964	46	1923	23	1875	10
PO-171	346	66	9274	0.3451	0.48	5.470	4.7	0.1149	0.1	0.89	2	.	1911	23	1896	7	1879	17
PO-176	343	64	13468	0.3397	0.47	5.384	4.5	0.1149	0.1	0.77	0.4	.	1885	23	1882	7	1879	16
PO-266	386	72	12307	0.3454	1.25	5.477	15.1	0.1150	0.1	0.85	2.1	.	1912	60	1897	24	1879	17
PO-136	332	60	3695	0.3395	0.74	5.399	11.6	0.1153	0.1	0.79	.	.	1884	36	1885	18	1885	20
PO-191	92	17	6571	0.3381	0.61	5.378	9.6	0.1154	0.1	0.81	-0.5	.	1877	29	1881	15	1886	15

Appendix 5. Cont.

Sample	U (ppm)	^{206}Pb (ppm)	^{206}Pb/ ^{204}Pb	^{206}Pb/ ^{238}U*	±σ (%)	^{207}Pb/ ^{235}U*	±σ (%)	^{207}Pb/ ^{206}Pb*	±σ (%)	ρ[a]	Disc.[b] (%)	Min rim (%)	^{206}Pb/ ^{238}U (Ma)	±σ (Ma)	^{207}Pb/ ^{235}U (Ma)	±σ (Ma)	^{207}Pb/ ^{206}Pb (Ma)	±σ (Ma)
PO-238	239	44	20017	0.3427	0.58	5.452	9.6	0.1154	0.1	0.69	0.9	.	1900	28	1893	15	1886	18
PO-255	292	54	21187	0.3444	1.24	5.490	14.6	0.1154	0.1	0.73	1.5	.	1908	60	1899	23	1886	22
PO-282	238	44	17494	0.3434	1.28	5.464	15.1	0.1155	0.1	0.75	0.9	.	1903	61	1895	24	1887	20
PO-216	88	16	7983	0.3278	0.58	5.219	9.1	0.1155	0.1	0.86	-3.7	.	1828	28	1856	15	1888	15
PO-288	315	59	77564	0.3403	0.55	5.422	4.8	0.1156	0.1	0.85	-0.1	.	1888	27	1888	8	1889	18
PO-209	107	19	13570	0.3345	0.61	5.333	9.8	0.1156	0.1	0.72	-1.8	.	1860	30	1874	16	1890	15
PO-124	481	90	46828	0.3488	0.80	5.571	12.5	0.1158	0.1	0.95	2.3	.	1929	38	1912	19	1892	20
PO-234	260	47	13928	0.3395	1.18	5.437	14.5	0.1160	0.1	0.84	-0.5	.	1884	57	1891	23	1895	18
PO-128	231	42	10372	0.3416	0.83	5.470	13.9	0.1161	0.1	0.66	-0.2	.	1895	40	1896	22	1897	22
PO-157	236	43	4111	0.3449	0.71	5.525	10.5	0.1161	0.1	0.92	0.8	.	1910	34	1905	16	1898	20
PO-298	144	26	5732	0.3373	0.69	5.401	10.7	0.1162	0.1	0.69	-1.5	.	1873	33	1885	17	1898	13
PO-264	453	85	4665	0.3498	1.23	5.617	15.2	0.1163	0.1	0.75	2.2	.	1934	59	1919	23	1900	18
PO-123	99	18	10372	0.3373	0.66	5.410	8.9	0.1165	0.1	0.83	-2	.	1874	32	1886	14	1903	21
PO-159	127	24	4155	0.3410	0.47	5.480	4.7	0.1166	0.1	0.85	-0.8	.	1892	23	1897	7	1904	17
PO-289	300	57	7134	0.3453	0.61	5.554	5.2	0.1167	0.1	0.59	0.3	.	1912	29	1909	8	1906	19
PO-194	211	39	8830	0.3395	0.64	5.465	10.3	0.1168	0.1	0.90	-1.5	.	1884	31	1895	16	1908	15
PO-190	345	66	67372	0.3526	1.18	5.686	18.1	0.1169	0.2	0.86	2.4	.	1947	56	1929	28	1909	24
PO-307	219	41	11705	0.3441	0.58	5.544	9.5	0.1169	0.1	0.76	-0.2	.	1906	28	1907	15	1909	17
PO-310	323	61	8571	0.3414	0.54	5.502	5.2	0.1169	0.1	0.80	-1	.	1893	26	1901	8	1909	18
PO-158	346	66	5272	0.3487	1.24	5.621	15.4	0.1170	0.1	0.80	1	.	1928	59	1919	24	1911	17
PO-226	171	31	9684	0.3388	0.89	5.491	13.8	0.1175	0.1	0.84	-2.3	.	1881	43	1899	22	1919	15
PO-206	304	57	25927	0.3384	0.48	5.488	4.4	0.1177	0.1	0.74	-2.5	.	1879	23	1899	7	1921	20
PO-151	246	43	6028	0.3307	0.65	5.380	10.1	0.1181	0.2	0.89	-5.2	-1.6	1842	31	1882	16	1928	23
PO-256	428	83	33574	0.3580	1.30	5.840	16.4	0.1181	0.1	0.95	2.8	.	1973	62	1952	24	1928	17
PO-220	162	30	3394	0.3341	0.59	5.437	11.9	0.1184	0.1	0.66	-4.7	.	1858	28	1891	19	1932	17
PO-139	309	56	4809	0.3416	0.86	5.574	14.6	0.1184	0.1	0.88	-2.4	.	1894	41	1912	23	1933	21
PO-130	681	127	2790	0.3484	0.79	5.725	13.0	0.1193	0.1	0.72	-1.2	.	1927	38	1935	20	1946	20
PO-199	316	60	3008	0.3521	0.67	5.813	11.3	0.1199	0.1	0.84	-0.7	.	1944	32	1948	17	1954	16

Appendix 5. Cont.

Sample	U (ppm)	^{206}Pb (ppm)	^{206}Pb/ ^{204}Pb	^{206}Pb/ ^{238}U*	±σ (%)	^{207}Pb/ ^{235}U*	±σ (%)	^{207}Pb/ ^{206}Pb*	±σ (%)	ρ[a]	Disc.[b] (%)	Min rim (%)	^{206}Pb/ ^{238}U (Ma)	±σ (Ma)	^{207}Pb/ ^{235}U (Ma)	±σ (Ma)	^{207}Pb/ ^{206}Pb (Ma)	±σ (Ma)
LEIS Leistilänjärvi, Satakunta, Finland. Coordinates in ETRS89-TM35FIN: P = 6812348, I = 229946.																		
nonrandomly selected detrital zircons (n=31)																		
LEIS-20	732	160	45892	0.3386	0.40	5.126	7.3	0.1097	0.1	0.92	5.6	2.8	1880	19	1840	12	1794	10
LEIS-64	46	10	4323	0.3427	0.44	5.216	8.0	0.1103	0.1	0.80	6.2	2.4	1900	21	1855	13	1804	11
LEIS-68	46	10	3038	0.3207	0.40	4.880	7.3	0.1104	0.1	0.82	-0.7	.	1793	20	1799	13	1805	11
LEIS-16	348	70	10515	0.3305	0.40	5.048	7.5	0.1107	0.1	0.93	2	.	1841	19	1827	13	1811	12
LEIS-80	65	13	2688	0.3200	0.40	4.907	7.3	0.1112	0.1	0.64	-1.9	.	1790	19	1803	13	1819	11
LEIS-15	105	21	2589	0.3107	0.36	4.765	6.9	0.1112	0.1	0.91	-4.7	-2.8	1744	18	1779	12	1820	11
LEIS-46	53	11	6524	0.3241	0.40	4.974	7.4	0.1113	0.1	0.77	-0.6	.	1810	19	1815	13	1820	11
LEIS-49	181	39	13237	0.3333	0.41	5.124	7.6	0.1114	0.1	0.84	2	.	1854	20	1840	13	1823	11
LEIS-51	631	139	20783	0.3407	0.43	5.241	7.9	0.1115	0.1	0.94	4.2	1.5	1890	21	1859	13	1824	10
LEIS-75	253	53	7970	0.3226	0.41	4.960	7.4	0.1115	0.1	0.92	-1.3	.	1803	20	1812	13	1824	11
LEIS-40	84	17	7393	0.3142	0.34	4.835	6.5	0.1116	0.1	0.85	-4	-1.7	1761	17	1791	11	1825	11
LEIS-10	156	33	3094	0.3151	0.50	4.864	9.0	0.1119	0.1	0.91	-4	-1.5	1765	25	1796	16	1830	12
LEIS-48	254	55	29713	0.3320	0.41	5.140	7.6	0.1123	0.1	0.88	0.8	.	1848	20	1843	13	1836	11
LEIS-84	149	31	3256	0.3250	0.41	5.033	7.6	0.1123	0.1	0.84	-1.5	.	1814	20	1825	13	1837	11
LEIS-28	318	70	16385	0.3367	0.44	5.218	8.1	0.1123	0.1	0.97	2.1	.	1871	21	1856	13	1838	10
LEIS-23	160	31	3720	0.3015	0.34	4.673	6.2	0.1124	0.1	0.79	-8.7	-6	1699	17	1762	11	1839	11
LEIS-06	195	41	2855	0.3129	0.44	4.856	8.2	0.1125	0.1	0.94	-5.3	-3.5	1755	22	1795	14	1840	11
LEIS-32	207	38	4497	0.3215	0.65	4.997	12.1	0.1128	0.1	0.92	-3	.	1797	32	1819	21	1845	16
LEIS-31	363	79	39860	0.3345	0.44	5.240	8.1	0.1136	0.1	0.97	0.2	.	1860	21	1859	13	1857	10
LEIS-55	417	94	37891	0.3472	0.47	5.454	8.7	0.1139	0.1	0.97	3.7	0.8	1921	22	1893	14	1862	11
LEIS-73	120	26	5644	0.3332	0.43	5.251	8.1	0.1143	0.1	0.92	-1	.	1854	21	1861	13	1869	11
LEIS-30	91	19	6628	0.3309	0.41	5.227	7.9	0.1146	0.1	0.86	-1.9	.	1842	20	1857	13	1873	11
LEIS-90	203	44	64023	0.3378	0.43	5.338	8.2	0.1146	0.1	0.88	0.1	.	1876	21	1875	13	1874	11
LEIS-19	314	68	3497	0.3329	0.40	5.276	7.9	0.1150	0.1	0.88	-1.6	.	1852	19	1865	13	1879	11
LEIS-45	126	27	6925	0.3342	0.42	5.302	8.1	0.1151	0.1	0.92	-1.4	.	1859	20	1869	13	1881	10
LEIS-57	215	47	13149	0.3333	0.50	5.293	9.1	0.1152	0.1	0.97	-1.8	-0.4	1854	24	1868	15	1883	11
LEIS-89	212	46	3802	0.3364	0.44	5.344	8.3	0.1153	0.1	0.94	-0.9	.	1869	21	1876	13	1884	11
LEIS-65	109	24	3893	0.3358	0.42	5.347	8.2	0.1155	0.1	0.77	-1.4	.	1866	20	1876	13	1888	11
LEIS-07	264	50	3945	0.3159	0.37	5.037	8.1	0.1158	0.1	0.87	-7.6	-5.1	1770	18	1826	14	1893	14
LEIS-71	257	57	14443	0.3405	0.43	5.468	8.5	0.1165	0.1	0.77	-0.9	.	1889	21	1896	13	1904	11
LEIS-66	224	76	24997	0.5164	0.84	13.100	37.9	0.1867	0.2	0.88	-2.8	.	2684	36	2687	27	2714	13

Appendix 5. Cont.

Sample	U (ppm)	^{206}Pb (ppm)	^{206}Pb/ ^{204}Pb	^{206}Pb/ ^{238}U*	±σ (%)	^{207}Pb/ ^{235}U*	±σ (%)	^{207}Pb/ ^{206}Pb*	±σ (%)	ρ[a]	Disc.[b] (%)	Min rim (%)	^{206}Pb/ ^{238}U (Ma)	±σ (Ma)	^{207}Pb/ ^{235}U (Ma)	±σ (Ma)	^{207}Pb/ ^{206}Pb (Ma)	±σ (Ma)
randomly selected detrital zircons (n=48)																		
LEIS-164	139	25	27214	0.3258	0.57	4.968	8.1	0.1103	0.1	0.61	1.1	.	1818	27	1814	14	1804	16
LEIS-105	608	141	7047	0.3249	0.59	4.944	9.5	0.1105	0.1	0.95	0.3	.	1814	29	1810	16	1808	11
LEIS-244	36	6	67398	0.3156	0.54	4.834	7.9	0.1109	0.1	0.62	-2.8	.	1768	27	1791	14	1815	17
LEIS-230	336	61	39188	0.3304	0.58	5.069	8.5	0.1110	0.1	0.92	1.8	.	1840	28	1831	14	1816	16
LEIS-227	69	12	2897	0.3193	0.56	4.927	8.3	0.1118	0.1	0.89	-2.5	.	1786	27	1807	14	1829	15
LEIS-240	296	53	19531	0.3284	0.58	5.083	8.5	0.1121	0.1	0.86	.	.	1830	28	1833	14	1833	16
LEIS-209	312	59	22609	0.3385	0.66	5.235	11.9	0.1121	0.1	0.90	2.9	.	1880	32	1858	19	1834	10
LEIS-218	70	12	7398	0.3214	0.56	4.974	8.3	0.1122	0.1	0.72	-2.3	.	1796	27	1815	14	1835	16
LEIS-207	209	39	26308	0.3321	0.64	5.161	11.7	0.1127	0.1	0.85	0.3	.	1848	31	1846	19	1844	9
LEIS-109	292	58	20659	0.3333	0.41	5.216	7.9	0.1134	0.1	0.89	0.1	.	1855	20	1855	13	1855	12
LEIS-201	188	35	16152	0.3342	0.64	5.230	11.9	0.1135	0.1	0.92	0.1	.	1859	31	1857	19	1856	10
LEIS-251	97	18	6018	0.3299	0.60	5.178	11.1	0.1138	0.1	0.81	-1.4	.	1838	29	1849	18	1861	9
LEIS-102	584	126	135521	0.3327	0.43	5.233	8.1	0.1141	0.1	0.93	-1	.	1851	21	1858	13	1866	11
LEIS-114	68	14	2896	0.3242	0.42	5.106	7.9	0.1143	0.1	0.72	-3.6	.	1810	20	1837	13	1869	11
LEIS-192	175	33	16401	0.3394	0.65	5.349	12.2	0.1143	0.1	0.82	0.9	.	1884	31	1877	19	1869	10
LEIS-101	170	36	9254	0.3319	0.43	5.236	8.1	0.1145	0.1	0.82	-1.5	.	1847	21	1858	13	1872	11
LEIS-241	392	72	20779	0.3362	0.58	5.312	8.8	0.1145	0.1	0.88	-0.1	.	1868	28	1871	14	1872	16
LEIS-195	297	57	37175	0.3440	0.68	5.431	13.1	0.1145	0.1	0.89	2	.	1906	33	1890	21	1873	10
LEIS-246	195	37	7485	0.3346	0.63	5.288	11.9	0.1146	0.1	0.70	-0.9	.	1861	30	1867	19	1874	9
LEIS-249	158	30	12144	0.3293	0.61	5.212	11.5	0.1148	0.1	0.86	-2.6	.	1835	30	1854	19	1877	9
LEIS-181	255	49	20411	0.3365	0.63	5.327	12.1	0.1149	0.1	0.78	-0.5	.	1870	30	1873	19	1878	10
LEIS-204	334	65	26829	0.3461	0.66	5.480	12.2	0.1149	0.1	0.85	2.3	.	1916	32	1897	19	1878	9
LEIS-255	210	41	69003	0.3400	0.65	5.384	12.3	0.1149	0.1	0.88	0.5	.	1887	31	1882	20	1878	9
LEIS-182	229	44	17400	0.3378	0.64	5.354	12.2	0.1150	0.1	0.83	-0.2	.	1876	31	1877	19	1879	10
LEIS-235	53	10	4946	0.3265	0.58	5.183	9.5	0.1151	0.1	0.72	-3.6	.	1822	28	1850	16	1881	16
LEIS-145	168	30	9573	0.3272	0.58	5.194	8.8	0.1152	0.1	0.86	-3.5	.	1825	28	1852	14	1882	16
LEIS-159	136	25	9791	0.3348	0.59	5.324	9.1	0.1152	0.1	0.77	-1.2	.	1862	29	1873	15	1883	16
LEIS-190	306	59	18058	0.3421	0.65	5.431	12.4	0.1152	0.1	0.75	0.8	.	1897	31	1890	20	1883	10
LEIS-92	260	55	10478	0.3291	0.41	5.225	8.0	0.1152	0.1	0.83	-3.1	-0.1	1834	20	1857	13	1884	11
LEIS-117	343	65	18620	0.3426	0.62	5.454	9.4	0.1153	0.1	0.87	1	.	1899	30	1893	15	1885	16
LEIS-210	127	24	6467	0.3379	0.66	5.371	12.4	0.1154	0.1	0.86	-0.6	.	1877	32	1880	20	1886	10
LEIS-222	27	5	3706	0.3270	0.58	5.213	9.1	0.1157	0.1	0.71	-4.1	.	1824	28	1855	15	1890	16
LEIS-138	180	33	19219	0.3353	0.61	5.349	9.5	0.1157	0.1	0.90	-1.7	.	1864	29	1877	15	1891	16
LEIS-158	128	23	7732	0.3328	0.59	5.316	9.0	0.1158	0.1	0.69	-2.4	.	1852	28	1871	15	1892	16
LEIS-153	54	10	9757	0.3284	0.58	5.241	9.0	0.1158	0.1	0.71	-3.8	.	1831	28	1859	15	1893	16
LEIS-225	126	23	10850	0.3312	0.59	5.292	9.2	0.1159	0.1	0.91	-3.1	-0.1	1844	28	1868	15	1894	16

Appendix 5. Cont.

Sample	U (ppm)	^{206}Pb (ppm)	^{206}Pb/^{204}Pb	^{206}Pb/^{238}U*	±σ (%)	^{207}Pb/^{235}U*	±σ (%)	^{207}Pb/^{206}Pb*	±σ (%)	ρ[a]	Disc.[b] (%)	Min rim (%)	^{206}Pb/^{238}U (Ma)	±σ (Ma)	^{207}Pb/^{235}U (Ma)	±σ (Ma)	^{207}Pb/^{206}Pb (Ma)	±σ (Ma)
LEIS-133	205	39	15286	0.3424	0.60	5.484	9.3	0.1161	0.1	0.90	0.2	.	1898	29	1898	15	1896	15
LEIS-97	246	52	4432	0.3296	0.42	5.285	8.2	0.1164	0.1	0.90	-4	-1.7	1836	20	1867	13	1902	11
LEIS-93	137	29	9690	0.3286	0.42	5.275	8.1	0.1165	0.1	0.90	-4.4	-2	1832	20	1865	13	1903	11
LEIS-206	118	22	11112	0.3363	0.70	5.395	12.1	0.1165	0.1	0.82	-2.2	.	1869	34	1884	19	1903	12
LEIS-219	174	30	10133	0.3183	0.56	5.105	8.6	0.1165	0.1	0.83	-7.4	-3.4	1781	27	1837	14	1903	15
LEIS-212	271	51	6788	0.3386	0.61	5.452	9.4	0.1169	0.1	0.73	-1.8	.	1880	29	1893	15	1909	18
LEIS-171	146	27	5484	0.3310	0.66	5.348	13.5	0.1173	0.1	0.82	-4.5	.	1843	32	1877	22	1916	10
LEIS-151	264	46	6846	0.3182	0.54	5.142	7.1	0.1175	0.1	0.36	-8.4	-1.7	1781	27	1843	12	1918	21
LEIS-239	133	26	7351	0.3537	0.66	5.972	11.2	0.1228	0.1	0.90	-2.8	.	1952	31	1972	16	1997	17
LEIS-205	206	42	20298	0.3611	0.71	6.118	14.5	0.1232	0.1	0.87	-1.2	.	1987	34	1993	21	2003	9
LEIS-110	184	44	13986	0.3712	0.51	6.527	11.3	0.1278	0.1	0.87	-2.1	.	2035	24	2050	15	2068	11
LEIS-216	70	15	40842	0.3740	0.71	6.771	13.8	0.1322	0.1	0.73	-5	.	2048	33	2082	18	2127	17

[a] Error correlation.

[b] Degree of discordance calculated at the closest approach of the 2σ error ellipse to concordia.

Appendix 6. BSE images of detrital zircons with $^{207}Pb/^{206}Pb$ ages and 2σ error margins indicated. **(A)** Grains contributing mostly to the 1.83–1.81 Ga peak. **(B)** Grains contributing to the 1.89–1.88 Ga peak. **(C)** >1.89 Ga. **(D)** Six randomly selected grains, which were mounted almost consecutively, as an example of the large number of grains unsuitable for age determination.

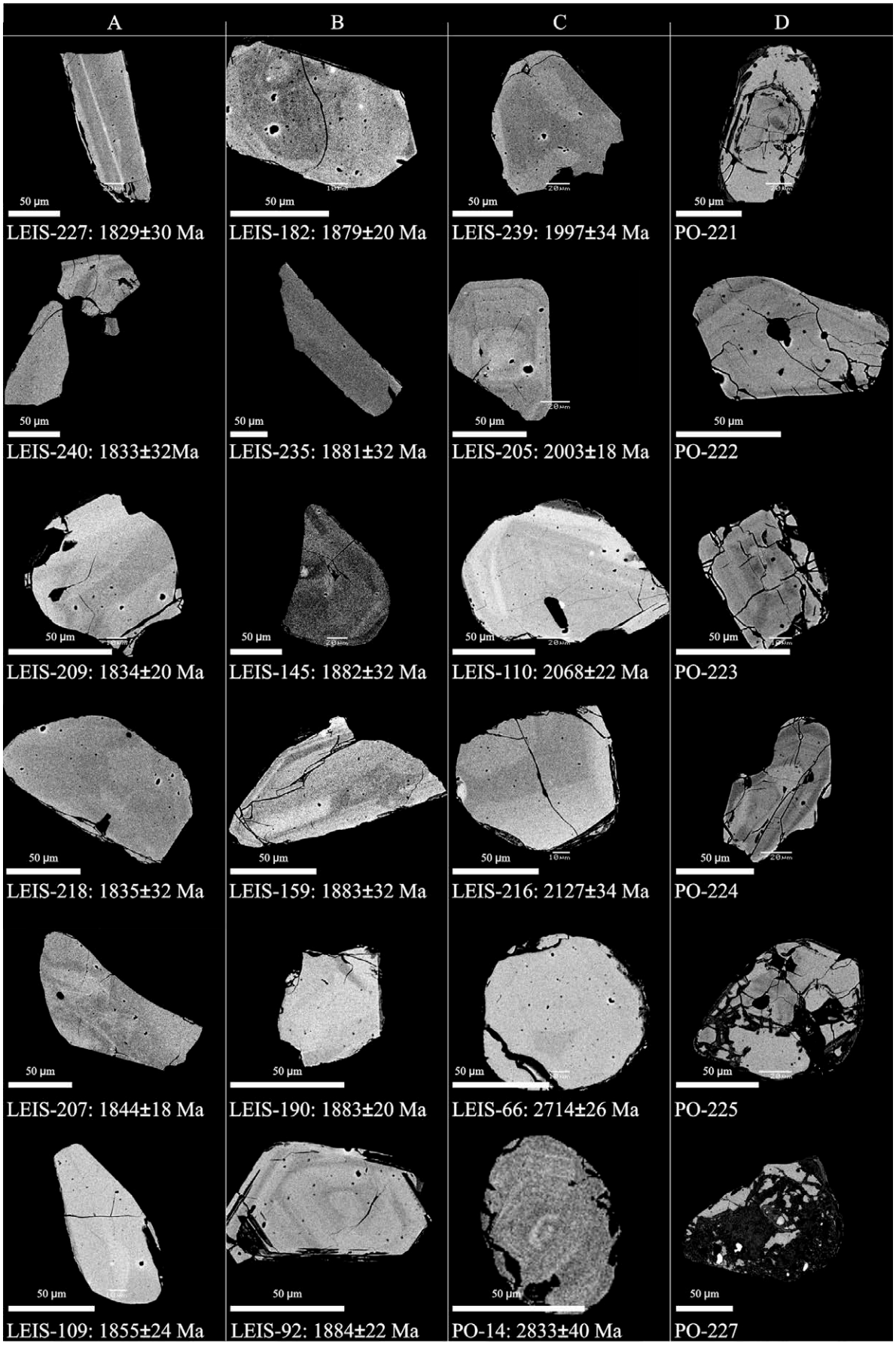

Appendix 7. Published zircon ages (2σ error margins) in southwestern Finland. Visit GTK Active Map Explorer (http://geo-maps2.gtk.fi/activemap/) for further information on the age determinations. Compilation of age data: Hannu Huhma (GTK). Geology based on the GTK bedrock map database (Bedrock of Finland – DigiKP). Contains data from the National Land Survey of Finland Topographic Database 03/2013 © NLS and HALTIK.

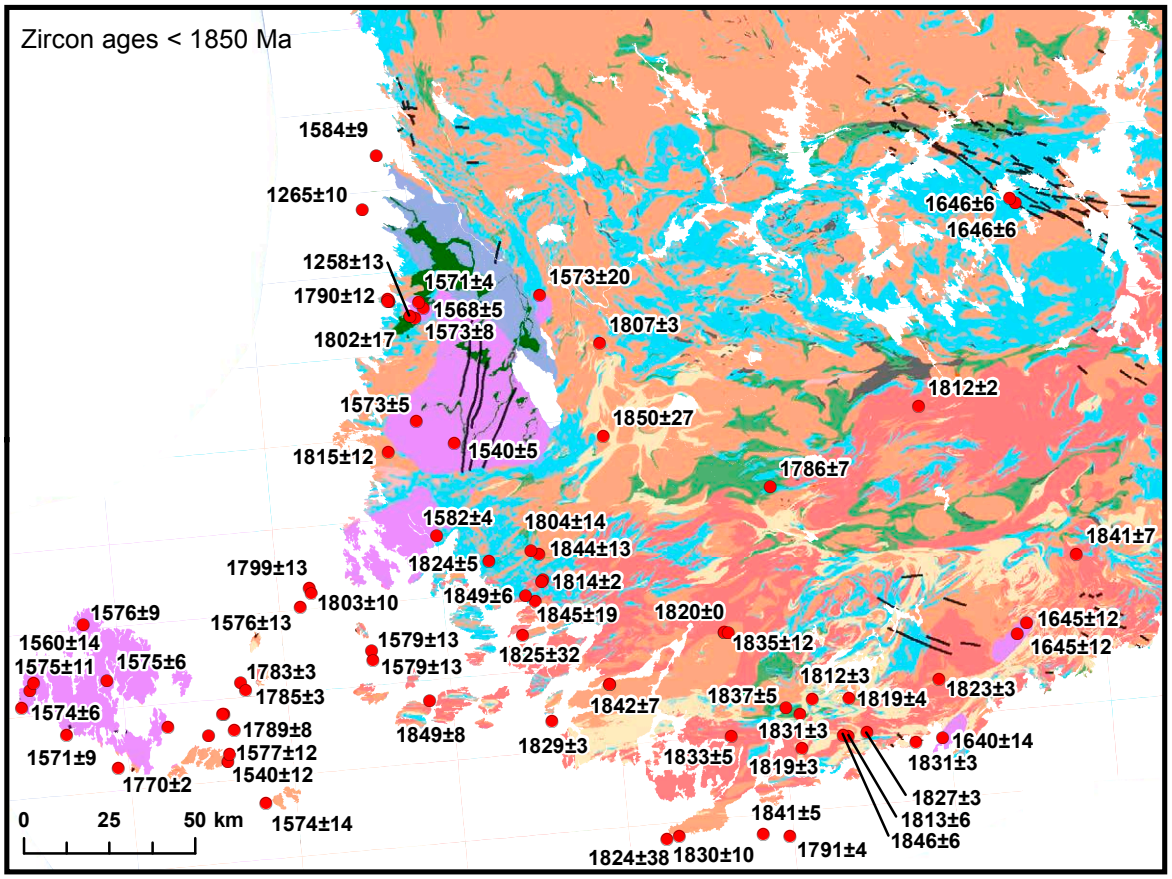

www.gtk.fi
info@gtk.fi

The Satakunta formation (traditionally referred to as the Satakunta sandstone) is a Mesoproterozoic sequence of sandstones and conglomerates in a fault-bounded basin within the Palaeoproterozoic Svecofennian Domain in SW Finland. In this report we describe its compositional variations and consider its subdivision, which could represent different basin stages of the formation. The provenance of the Satakunta formation and especially the possible presence of detritus from rapakivi granites have been studied and discussed for more than 100 years. Here, the question is addressed for the first time using single-zircon age determinations. We also propose a basin evolution model starting from c. 1600 Ma and ending at 1270 Ma.

ISBN 978-952-217-264-8 (pdf)
ISSN 0781-4240